



WPI

Bioreactor for *In Vitro* Evaluation of Tumor Cell Invasion Potential

Project ID: CFW 2102

This report represents the work of one or more WPI Undergraduate Students submitted to the faculty as evidence of completion of a degree requirement. WPI routinely publishes these reports on the web without editorial or peer review

Submitted by:

Camryn Berry

Kiersten Hoglund

Alexander Lopes

Paige O'Gorman

Professor Catherine Whittington, Ph.D., Advisor
Department of Biomedical Engineering

Table of Contents

Authorship.....	1
Acknowledgements.....	2
Abstract.....	3
Chapter 1: Introduction.....	4
Chapter 2: Literature Review.....	6
2.1 Cancerous Cells and Tumor Progression.....	6
2.1.1 Tumor Microenvironment.....	7
2.1.2 Clinical Practices.....	8
2.2 Metastatic Cancers.....	9
2.3 Tumor Modeling for Drug Discovery.....	10
2.3.1 Two-Dimensional and Three-Dimensional In Vitro Cell Culture Methods.....	12
2.3.2 Cancer Cell Lines.....	13
2.3.3 Hydrogel Scaffolds.....	14
2.3.4 Scaffold Free Methods.....	16
2.4 In Vitro Techniques for Studying Cell Migration and Invasion.....	17
2.4.1 Scratch Assay and Cell Exclusion Zone Assay.....	17
2.4.2 Boyden Chamber Assay and Transwell Migration Assay.....	18
2.4.3 3D Tumor Tissue Invasion for High-throughput High Content Phenotypic Drug Screening.....	19
2.4.4 Image Analysis.....	19
2.5 Fluid Flow in Cancer.....	20
2.5.1 Perfusion and Blood Flow.....	20
2.5.2 Interstitial Fluid Flow.....	20
2.6 Types of Bioreactor Systems.....	21
2.7 Modeling Cancerous Interstitial Fluid Flow In Vitro.....	23
2.7.1 Microfluidics.....	24
2.7.2 Shear Flow Study: Human Epithelial Ovarian Cancer.....	25
2.7.3 Continuous Interstitial Flow Study: Human Breast Carcinoma.....	25
2.8 State of the Art Devices and Methods of Invasion Analysis.....	26
2.8.1 Perfused Tumor Tissue Model for Invasion Analysis.....	26
2.8.2 Microfluidic Cell Migration Assay for Glioblastoma Patients.....	26
2.8.3 Perfusion Bioreactor System for Engineered Breast Cancer Surrogates for Preclinical Testing.....	27
Chapter 3: Project Strategy.....	28
3.1: Client Statement.....	28
3.2 Technical Design Requirements.....	29
3.3 Objectives for Invasion.....	31

3.4 Objectives for Scaffold and Membrane	33
3.5 Objectives for System Flow.....	35
3.6 Objectives for Device Fabrication	36
3.7 Objectives for Industry Use	38
3.8 Standards for Design Requirements	39
Chapter 4: Design Process	41
4.1 Needs Analysis by Pairwise Comparison	41
4.2 Overall System Design	42
4.2.1 Preliminary Designs	42
4.3 Developing Image Analysis Methodology	46
4.3.1 Image Analysis Method: MATLAB®	47
4.3.2 Image Analysis Method: CellProfiler™.....	51
4.4 Scaffold Testing.....	54
4.4.1 Requirements for Scaffolding	55
4.4.2 Scaffold Base Material Considerations	56
4.4.3 Crosslinkers.....	57
4.5 Membrane Considerations	58
4.5.1 Objectives for Membrane within the CCH Unit.....	58
4.5.2 Material Considerations for Membrane Within the CCH Unit	59
Chapter 5: Design Verification and Validation Testing	62
5.1 Design Viability Testing and Verification.....	62
5.1.1 CCH Unit and Tubing Leakage Testing	63
5.1.2 CCH Unit Material Cytotoxicity Testing	63
5.1.3 Full System Flow Verification Testing	64
5.2 Verifying Cell Quantification Method.....	65
5.3 Hydrogel Characterization Methods.....	66
5.3.1 Hydrogel Formation	66
5.3.2 Rheological Testing	67
5.3.3 Cell Viability Testing.....	69
5.3.4 Diffusivity Testing	69
5.4 Membrane Characterization Methods.....	71
5.4.1 Membrane Fluid Flow Testing	71
5.4.2 Membrane Cell Adhesion Testing.....	73
Chapter 6: Results and Discussion.....	75
6.1 Basic Design Viability Testing Results	75
6.1.1 CCH Unit and Tubing Leakage Testing.....	75
6.1.2 Full System Flow Verification Testing	75
6.2 Verifying Cell Quantification Methods	76

6.3 Hydrogel Characterization.....	78
6.3.1 Hydrogel Formation.....	78
6.3.2 Rheological Testing.....	80
6.3.3 Cell Viability Testing: Scaffold.....	82
6.3.4 Diffusivity Testing: Scaffold.....	83
6.4 Membrane Characterization.....	84
6.4.1 Membrane Fluid Flow Testing.....	84
6.4.2 Cellular Adhesion Testing.....	86
6.5 Project Impact.....	89
6.5.1 Economic Impact.....	89
6.5.2 Environmental Impact.....	89
6.5.3 Societal Impact.....	89
6.5.4 Ethical Concerns.....	90
6.5.5 Health and Safety.....	90
6.5.6 Manufacturing Concerns.....	90
6.5.7 Sustainability Impact.....	91
Chapter 7: Final Design and Project Impact.....	92
7.1 Final System Design.....	92
7.2 Industry Standards.....	93
Chapter 8: Future Work and Conclusions.....	94
8.1 Full System Implementation.....	94
8.1.1 Syringe Pump.....	94
8.1.2 CCH Unit Design.....	94
8.1.3 Full System Testing.....	95
8.2 Simulation Future Work.....	95
8.3 Image Processing Future Work.....	96
8.4 Scaffold Future Work.....	97
8.5 Membrane Future Work.....	98
8.5.1 Material Alterations and Replacements.....	98
8.5.2 Validation Methods.....	98
8.6 Conclusions.....	99
Chapter 9: Appendices.....	100
Appendix A: Solidworks Drawing Iteration 1.....	100
Appendix B: Solidworks Drawing Iteration 2.....	101
Appendix C: Solidworks Drawing Iteration 2.....	102
Appendix D: 3D Printed Iteration 1.....	103
Appendix E: 3D Printed Iteration 2.....	104
Appendix F: MATLAB® Code for Image Processing.....	105

Appendix G: CellProfiler Pipeline.....	113
Appendix H: Test Images for Cell Image Analysis.....	114
Appendix I: Rheometer Setup/Procedure.....	119
Appendix J: Rheometer Testing Results.....	122
Appendix K: Leakage Testing Procedure.....	125
Appendix L: Flow Verification Testing Procedure.....	126
Appendix M: Procedures for Scaffold Formation.....	127
Appendix N: Scaffold Diffusion Testing Procedure.....	128
Appendix O: Membrane Fluid Flow Procedure.....	129
Appendix P: Cellular Adhesion Testing.....	130
Appendix Q: Cell Seeding Procedure.....	131
References.....	133

Table of Figures

Figure 1: Stages of Tumor Progression [6].....	6
Figure 2: Interactions in the Tumor Microenvironment [7].....	7
Figure 3: Pharmaceutical Development Process.....	11
Figure 4: 2D and 3D Cell Culture Methods.....	13
Figure 5: Experimental process of a scratch assay [37].....	17
Figure 6: Experimental Process of the Cell Exclusion Zone Assay [38].....	18
Figure 7: Experimental Process of the Boyden Chamber Assay	19
Figure 8: Interstitial Flow Between Tissue Cells and Blood Vessels.....	21
Figure 9: Set-Up of Perfusion Bioreactor from 2019-2020 MQP Group.....	26
Figure 10: Conceptual Schematic of Device Design	29
Figure 11: Preliminary Design 1 (Two-Chamber).....	42
Figure 12: Preliminary Design 2 (4 Channel Flow Bioreactor).....	43
Figure 13: Preliminary Design 3 (Previous MQP Team Design).....	44
Figure 14: Conceptual Design of Bioreactor System	45
Figure 15: The User Interface of the MATLAB® Program (Developed by Previous MQP Team for Cell Counting and Invasion Distances).....	47
Figure 16: Popup Window that Allows User to Enter Specified Distance of Scale Bar (in μm) .	48
Figure 17: (A) The reference line that shows the visual distance between point one and two on a Sample Image of Panc-1 cells. (B) The results panel displaying the specific distance of the line, in μm	49
Figure 18: Sample Panc-1 cell Image output and results from using the density profile of combined images function [26]	50
Figure 19: MATLAB® Portrayal of Clustered Cell Count on Sample Image of Panc-1 cells.....	51
Figure 20: Cell Profiler Main Screen Displaying Pipeline (left) and Sample Imported Image (right)	52
Figure 21: Raw Sample Image of MDA-MB-231 cell line Displayed (Top Left), Separation Boundaries of Identified Objects (Top Right), Object Outlines Based on Pipeline Criteria (Bottom Left)	54
Figure 22: Polycarbonate Membrane Face On, Handled with Forceps	61
Figure 23: Conceptual Device Design with Dimensions (not to scale)	62
Figure 24: Setup of Individual CCH Unit Leakage Test	63
Figure 25: Empty Scaffold Chamber Flow Testing Setup Including Syringe Pump, Three Syringes, Tubing, CCH Unit, and 15mL Conical Tubes	65
Figure 26: MCR 302 WESP Rheometer Used for Testing Hydrogel Stiffness Properties.....	68
Figure 27: Glucose Diffusion through Scaffold Setup Schematic.....	70
Figure 28: Experimental Setup of Glucose Scaffold Diffusion Test on Stir Plate	71
Figure 29: Experimental Setup for Fluid Flow Experiments.....	72
Figure 30: The Membrane Clamped by Tubing Connector.....	73

Figure 31: Apparatus Used in the Cellular Adhesion Experiment to Evaluate the Flow of Cells through the Membrane	74
Figure 32: No Leakage Between Tubing Connections and CCH Unit	75
Figure 33: Percent Error Results for CellProfiler™ versus MATLAB® Cell Counts	76
Figure 34: MATLAB® cell count of Image 1 (left) and CellProfiler™ cell count of Image 1 (right)	77
Figure 35: MATLAB® cell count of Image 2 (left) and CellProfiler™ cell count of Image 2 (right)	78
Figure 36: Scaffold Formation using Gelatin and Glutaraldehyde.	79
Figure 37: Variations of Gelatin and Alginate Gels After Polymerization	80
Figure 38: Oscillatory shear testing performed on three independent samples of 8.6% gelatin, 0.19% alginate and 33 mM calcium chloride (graph is in logarithmic scale)	81
Figure 39: Non-Viable Cells Stained with Trypan Blue on Scaffold (8.6% Gelatin, 0.19% Alginate, 33mM Calcium Chloride)	83
Figure 40: Glucose Reading in Donor Chamber (mg/dL) Over 24 Hours	84
Figure 41: Image of the Contents of the Bottom Tube in Trial 2	87
Figure 42: Membrane with 3T3 Cells Adhered	88

Table of Tables

Table 1: Common Metastatic Cancers and the Locations Spread to Most Often.....	10
Table 2: Cell Line Considerations [25].....	14
Table 3: Summary of Types of Bioreactors.....	23
Table 4: Invasion Functional Requirements and Means.....	31
Table 5: Invasion Design Criteria.....	32
Table 6: Scaffold Functional Requirements and Means.....	33
Table 7: Scaffold Design Criteria.....	34
Table 8: System Flow Functional Requirements and Means.....	35
Table 9: System Flow Design Criteria.....	36
Table 10: Objectives for Device Fabrication.....	37
Table 11: Functional Requirements and Design Objectives for Device Fabrication.....	37
Table 12: Industry Use Functional Requirements and Means.....	38
Table 13: Industry Use Design Criteria.....	39
Table 14: Needs Analysis by Pairwise Comparison.....	41
Table 15: Decision Matrix with Preliminary Designs.....	46
Table 16: Needs Analysis for Scaffold Criteria.....	55
Table 17: Membrane Functional Requirements and Means.....	58
Table 18: Membrane Design Criteria.....	59
Table 19: Pairwise Comparison for Membrane Requirements.....	60
Table 20: Comparison of Membrane Materials.....	60
Table 21: Differing Glutaraldehyde Concentrations for Hydrogel Formation.....	67
Table 22: Differing CaCl ₂ Concentrations for Hydrogel Formation.....	67
Table 23: Results of output flow volume between each empty scaffold chamber in the CCH unit (last row represents mean ± standard deviation).....	76
Table 24: Scaffold Formulations Tested in Triplicate/Duplicate and the Average ± Standard Deviation.....	81
Table 25: Time Durations of Membrane Fluid Flow Experiment Trials.....	85
Table 26: Flow Rates of Membrane Fluid Flow Experiment Trials.....	86

Table of Equations

Equation 1: Darcy's Law for Fluid Flow through Porous Medium [51].....	24
Equation 2: Permeability Coefficient Calculation	24
Equation 3: Speed to Volumetric Flow Rate	36
Equation 4: Percent Error Equation	66
Equation 5: Flow Rate	85

Authorship

Section	Primary Author
Chapter 1: Introduction	Paige O’Gorman
Chapter 2: Literature Review: 2.1	Kiersten Hoglund and Camryn Berry
Chapter 2: Literature Review: 2.2	Camryn Berry
Chapter 2: Literature Review: 2.3	Camryn Berry and Alexander Lopes
Chapter 2: Literature Review: 2.4	Camryn Berry and Paige O’Gorman
Chapter 2: Literature Review: 2.5	Paige O’Gorman
Chapter 2: Literature Review: 2.6	Alexander Lopes
Chapter 2: Literature Review: 2.7	Alexander Lopes and Paige O’Gorman
Chapter 2: Literature Review: 2.8	Kiersten Hoglund
Chapter 3: Project Strategy	Everyone
Chapter 4: Design Process: 4.1	Camryn Berry
Chapter 4: Design Process: 4.2	Alexander Lopes
Chapter 4: Design Process: 4.3	Paige O’Gorman
Chapter 4: Design Process: 4.4	Paige O’Gorman
Chapter 4: Design Process: 4.5	Camryn Berry
Chapter 5: Design Verification...: 5.1	Alexander Lopes
Chapter 5: Design Verification...: 5.2	Paige O’Gorman
Chapter 5: Design Verification...: 5.3	Paige O’Gorman and Kiersten Hoglund
Chapter 5: Design Verification...: 5.4	Camryn Berry
Chapter 6: Results and Verification: 6.1	Alexander Lopes
Chapter 6: Results and Verification: 6.2	Paige O’Gorman
Chapter 6: Results and Verification: 6.3	Paige O’Gorman and Kiersten Hoglund
Chapter 6: Results and Verification: 6.4	Camryn Berry
Chapter 6: Results and Verification: 6.5	Kiersten Hoglund
Chapter 7: Final Design...: 7.1	Alexander Lopes
Chapter 7: Final Design...: 7.2	Kiersten Hoglund
Chapter 8: Future Work...: 8.1	Alexander Lopes
Chapter 8: Future Work...: 8.2	Alexander Lopes
Chapter 8: Future Work...: 8.3	Paige O’Gorman
Chapter 8: Future Work...: 8.4	Paige O’Gorman
Chapter 8: Future Work...: 8.5	Camryn Berry
Chapter 8: Future Work...: 8.6	Kiersten Hoglund

Acknowledgements

The team would like to acknowledge and thank our project advisor, Dr. Catherine Whittington for her support and guidance throughout the year. We would also like to thank the Dr. Sakthikumar Ambady for providing us with an extra cell line from his “Cellular Engineering” laboratory so that we could complete our membrane diffusion testing. Further, the team would like to acknowledge Laboratory Manager, Lisa Wall, and Robert Kirch for helping the team get settled in the laboratory space, order needed products, and 3D print our device. Additionally, the team would like to thank Athenia Jones and Brian Ruliffson, PhD students in the Whittington Laboratory, for assisting with experimental testing of scaffold materials. Lastly, we would like to thank Worcester Polytechnic Institute for providing us with the funding, resources, and opportunity to perform our research this year.

Abstract

Cancer is among the leading causes of death worldwide, in cancer, the body's cells divide rapidly and proliferate to form malignant tumors. Tumor cells can also invade healthy tissue away from the primary tumor in a process known as metastasis. It is estimated that metastasis is the primary cause of 90% of all cancer-related deaths. Metastasis makes cancer difficult to treat, and there is an emerging need for physiologically relevant models of invasion to help study cancer progression. *In vitro* models of the tumor microenvironment are a key component of understanding cancer metastasis, the primary cause of most cancer deaths. Current models of cancer cell invasion, which precedes metastasis, lack interstitial fluid flow. The goal of this project was to design a device integrating interstitial fluid flow that could perfuse cancer cell lines through a biocompatible scaffold. Invasion could then be detected through imaging. A device was designed to hold a scaffold for cell invasion, support fluid flow through the scaffold, and be easily assembled. The device also includes a cell loading inlet with an in-line membrane to filter cell aggregates. Tests were performed to ensure that the device did not leak, and the scaffold was characterized using rheology and diffusion experiments.

Chapter 1: Introduction

Cancer is a disease in which the body's cells rapidly divide and proliferate to form malignant tumors. These abnormal cells can migrate from the primary cancer site, moving throughout the body and invading otherwise healthy tissue. Cancer cells invasion can trigger a process known as metastasis, which is when a secondary malignant tumor is formed. Metastasis is estimated to be the primary cause of nearly 90% of all cancer deaths [1].

There are current laboratory-run 3D tumor-cell invasion models that are used to study early-stage tumor cell invasion [1]. However, these models can only be so accurate, since they currently lack fluid flow, which plays a key role in regulating tumor progression. Without the inclusion of fluid flow in a model system, it is difficult to replicate the *in vivo* environment, or the environment within the body. Current models are more focused on the cell migration aspects of the design rather than mimicking the environment within the body [1].

The tumor microenvironment greatly affects the metastatic behavior of a tumor [2]. The tumor microenvironment includes the surrounding fibroblasts, blood vessels, lymphatic vessels, extracellular matrix, immune cells as well as signaling molecules, secreted factors, and proteins [2]. The interactions between these components play an important role in tumor progression and regulation. The application of our project is to create an *in vitro*, in the laboratory and outside the body, perfused tumor-tissue model for invasion analysis that will incorporate fluid flow. The inclusion of fluid flow model will greatly increase the understanding of how tumors progress and cells invade or metastasize, which in turn will benefit patient care and guide research purposes.

The goal of this project is to create a bioreactor device that will mimic certain features of the tumor microenvironment for clinical use. This device will help improve understanding of which cells are more likely to metastasize and which drugs are most effective against metastasis. In a clinical setting, laboratory technicians will be able to run individual patient's cells through this device to determine metastatic potential, then expose samples to a chosen chemotherapy drug to determine if this drug will be beneficial in treatment. This device will be able to use the patient's own cells, resulting in less trial and error from using cell lines and can potentially decrease the overall treatment timeline for a patient.

There are many current predictive approaches such as a biopsy, genomic testing, and blood sampling used to determine cancer-specific behaviors and treatments. However, these tests often cannot determine what treatment could benefit the patient most and how a patient could react to a

treatment. A bioreactor device that can perfuse a patient's cancer cells, as well as predict the effect of different therapeutic treatments could have a substantial impact to the field of oncology. The device will have multi-flow channels that allow three tests to run at once. The materials include a 3D printed device, a Gelatin-Alginate scaffold, and a Polycarbonate membrane. However, there are many key factors that must run smoothly in order for the perfusion bioreactor system to correctly model the tumor, its microenvironment, and its response to chemotherapies. First, the cell must be compatible with the scaffold material chosen. If not, the cells could either die or not invade through the scaffold. The fluid flow must also simulate the environment inside of the body. In order to test this device, the team will be using the Panc-1 cell line, which is derived from human pancreatic cells.

If successful, this design will be able to anticipate the invasiveness of a patient's cancer and provide the patient with a more accurate prognosis. In the future, this perfusion bioreactor will be able to test different therapies on cells external to the patient leading to a better, more accurate, outcome for cancer patients. Overall, this perfusion bioreactor has the potential to greatly impact oncology research with its ability to mimic the microenvironment of the tumor through the use of multi-flow channels to accurately model 3D tumor cell invasion.

Chapter 2: Literature Review

2.1 Cancerous Cells and Tumor Progression

Cancer starts when an abnormal cell begins growing and dividing out of control. This initial abnormal cell can come from an inherited genetic mutation, or a mutation developed naturally over time. These inherited genetic mutations play a major role in 5-10% of all cancers [3]. Cancer can crowd out normal cells and inhibit the tissue or organ's necessary functions [4]. All of the cells produced as a result of the division of this abnormal cell will also undergo unregulated proliferation. When these cells form a mass, it is referred to as a tumor and may begin to invade nearby tissues. An invasive tumor is considered malignant and can metastasize or establish new tumors in other locations in the body.

Tumors form from a single altered cell in a clear progression. This progression is shown in Figure 1, the first stage is known as hyperplasia when the cell begins to divide uncontrollably and form a mass in the original tissue region. At this stage, the cells still appear normal. The second stage is dysplasia, where additional genetic changes lead to continued unregulated cell growth. The cells no longer have a normal appearance and can become disorganized. The final stage before tumors begin to spread is *in situ*, at this stage, the cells and tissue look very different from normal cells but are still contained in the initial area. In some cases, cancer will stay in the *in-situ* stage and never progress any further. The final stage of tumor progression is when the tumor becomes malignant. This final stage is characterized by the tumor invading surrounding tissues and/or spreading to other areas of the body, also known as metastasis. Tumors that do not spread beyond their initial location are considered benign [5]. In the context of this project, we will be focusing

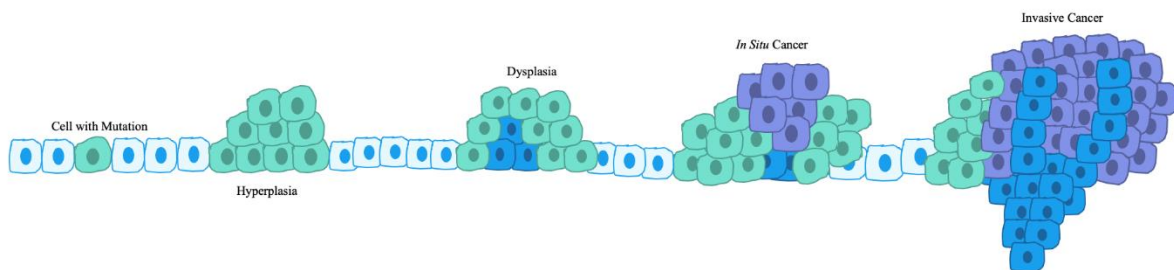


Figure 1: Stages of Tumor Progression [6]

on the final stage of tumor progression, where the cancerous cells are invading healthy tissues.

There are many characteristics used to distinguish cancer cells from normal functioning cells. Some of the main differences include a decreased requirement for growth factors, loss of

anchorage dependence, loss of cell-cycle control, resistance to apoptosis or programmed cell death, changes in cell membrane structure and function, alterations in cell surface lipids and proteins, and many more [6]. Cancer cells occasionally can also be distinguished through their physical appearance, often looking larger than normal cells and having irregularly shaped nuclei [6].

2.1.1 Tumor Microenvironment

The tumor microenvironment (TME) refers to the area surrounding the tumor. This area includes the surrounding fibroblasts, blood vessels, extracellular matrix, immune cells as well as signaling molecules, secreted factors, and proteins [2].

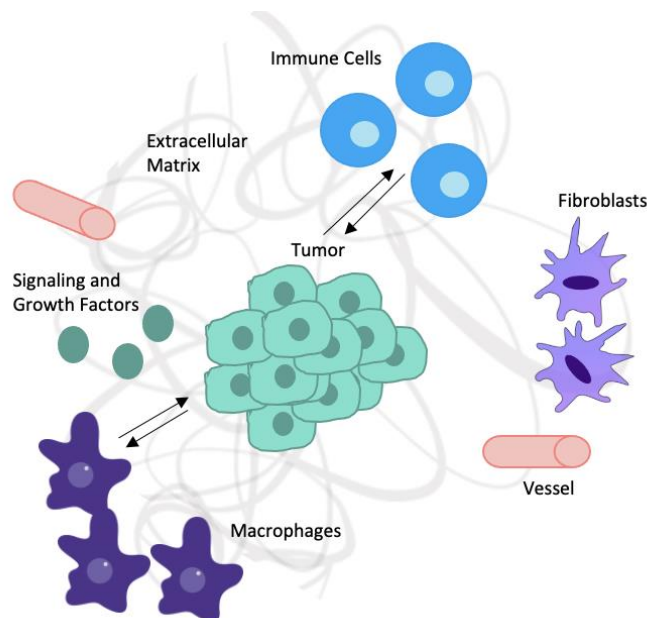


Figure 2: Interactions in the Tumor Microenvironment [7]

The interactions with these cells and molecules play an important role in tumor progression and regulation. Despite immune cells being recruited to the area, their anti-tumor properties are down regulated due to signals from the TME and sometimes end up promoting the growth of the tumor instead, as seen in Figure 2. Activation of molecular mechanisms in the TME can lead to tumor escape and eventually inhibition of normal cell function throughout the body. Specifically, the extracellular matrix (ECM) can play a key role in cancer progression. The ECM is dynamic and constantly being remodeled, restructured, and degraded. This composition and organization are regulated to control cell behaviors and differentiation. Dysregulation of these ECM dynamics

can promote tumor development [8]. Understanding the tumor microenvironment is crucial in developing ways to prevent initial tumor escape [7].

2.1.2 Clinical Practices

The current clinical practices that clinicians use to evaluate the likelihood of a primary cancer site to metastasize are performing a biopsy procedure and utilizing cancer statistics [9,10,11]. There are many different types of biopsies a clinician could perform depending on the cancer site [9]. Cancers of the blood are typically analyzed using a bone marrow biopsy. During a bone marrow biopsy, a local anesthesia is administered, and a sample of bone marrow is collected from, most commonly, the hip bone. For cancers of the bladder, lung, or colon, an endoscopic biopsy may be taken. During an endoscopic biopsy, a tube is inserted through the urinary tract, mouth, or rectum and a sample is collected from the area of concern. This procedure typically utilizes general anesthesia. A needle biopsy is a type of biopsy used on cancers which are close to the skin, such as a breast cancer, where an abnormal lump can typically be felt or seen. There are many different types of needle biopsies, such as fine-needle aspiration, core needle biopsy, vacuum-assisted biopsy, and image-guided biopsy, however all of these different methods involve using a needle and local anesthesia. For skin cancers, a skin biopsy may be taken, which involves removing skin with a razor, punch tool, or scalpel. Local anesthesia is typically used, and stitches are occasionally needed to close the open wound. Lastly, if cells cannot be harvested by any of the previously outlined biopsy methods, a surgical biopsy may be performed, where a surgeon will cut through external tissue to reach the area of concern [9].

After the biopsy, the tissue sample is then sent to a laboratory where it may be chemically treated or frozen and sliced into thin sections. The slices are then mounted to glass slides, stained, and imaged under a microscope. The results of a biopsy are typically available after a few days, though some samples may need more time if the results are inconclusive.

While biopsies are frequently used to diagnose a patient with cancer, they are also used to indicate the severity of a patient's cancer [9,10]. This is a process known as staging. Staging assigns a numeric value from one to four which essentially grades the aggressiveness of a cancer. Grade or stage one cancers are generally the least aggressive, with no current metastatic sites. Grade or stage four cancers, however, have already metastasized or formed additional tumors. The

stage of a cancer can be concluded from a biopsy by observing the cell architecture, as cancerous cells exhibit physical changes which correspond to their malignancy [10].

Statistical analysis also plays an important role in allowing a clinician to infer a patient's likelihood of metastasis, which influences the patient's prognosis [11]. This statistical analysis relies on previously documented cases of cancer to make a prediction based on how other patient's cancers have behaved. One factor taken into consideration is the type of cancer, since some cancers, such as breast or lung, have demonstrated a higher rate of metastasis. The type of cancer can also help a clinician make predictions about potential metastatic sites, as certain cancers demonstrate a higher prevalence of metastasis to certain tissues. The stage of cancer, which is concluded from a biopsy, is also factored into the statistical analysis and the age of the patient is also considered [11].

2.2 Metastatic Cancers

Cancer cells can spread through the body in a series of steps that lead to metastasis. These steps include invading nearby normal tissue, moving through blood vessels or lymph nodes, traveling through the bloodstream and lymphatic system to other organs, invading the blood vessel walls, and moving into the surrounding tissue growing in this tissue until a tumor forms. There are many different types of metastatic cancers that can spread to almost any location of the body. One of the deadliest types of metastatic cancer is pancreatic cancer, due to the cancer often not being discovered until metastasis has already occurred, mostly to the liver and lungs. Table 1 lists common cancers and the locations they most often spread to.

With respect to the current project, it was helpful to narrow down the metastatic cancer being focused on. Therefore, the team chose to focus on Pancreatic Cancer since we had access to Panc-1 cells in the laboratory. Pancreatic cancers can be classified as either exocrine or endocrine depending on which cells the tumor originated from. Each of these two categories contains several different types of pancreatic cancer. However, about 93% of pancreatic tumors are exocrine tumors and nine out of ten pancreatic cancer patients are diagnosed with pancreatic ductal adenocarcinoma (PDAC) [12]. PDAC is a very aggressive form of pancreatic cancer. PDAC is estimated to become the second leading cause of cancer-related deaths by 2030; overall 5-year survival rates have consistently remained below 10% [12,13].

Table 1: Common Metastatic Cancers and the Locations Spread to Most Often

Cancer Type	Main Sites of Metastasis
Pancreas	Liver, lung, peritoneum
Bladder	Bone, liver, lung
Breast	Bone, brain, liver, lung
Colon	Liver, lung, peritoneum
Kidney	Adrenal gland, bone, brain, liver, lung
Lung	Adrenal gland, bone, brain, liver, other lung
Melanoma	Bone, brain, liver, lung, skin, muscle
Ovary	Liver, lung, peritoneum
Prostate	Adrenal gland, bone, liver, lung
Rectal	Liver, lung, peritoneum
Stomach	Liver, lung, peritoneum
Thyroid	Bone, liver, lung
Uterus	Bone, liver, lung, peritoneum, vagina

The pancreatic TME is crucial in determining cancer treatment and prognosis, as the TME influences elements of tumor development including growth rate, invasion, and metastasis [14]. Pancreatic tumors often form dense fibrous stroma which has been shown to create resistance to chemotherapy and radiation therapy which contributes to the difficulty of treating PDAC [14,15]. The stroma also creates an environment that promotes cancer progression by enhancing tumor growth and regional and distant metastasis.

2.3 Tumor Modeling for Drug Discovery

Two types of experimental research are *in vivo* and *in vitro* studies. *In vivo* experimentation is a method of performing an established procedure within a living organism [16]. Examples of *in vivo* experimentation range from lab testing using small animals, like mice or rats, to human clinical trials [16]. *In vivo* experimentation is advantageous in cancer research because the interaction with and within a living organism can more closely mimic the environment that cancer occurs in, as well as help anticipate the way an entire system reacts to therapeutics [17]. However, performing preliminary experiments *in vivo* poses a significant risk to the animal or human model presents significant cost to researchers. Therefore, there are certain standards that must be met before an *in vivo* trial is approved, typically by an external or government agency [18]. These standards typically include substantial and significant data from *in vitro* experimentation. *In vitro* experimentation is a method of performing an established procedure outside of a living organism.

It typically takes place in a laboratory setting and involves using bacterial, animal, or human cells that are isolated then cultivated in a culture medium that supports cell growth [16]. This technique is advantageous in cancer research because experiments are relatively low cost and there is no harm done to a living organism. *In vitro* experimentation also saves time, because there are fewer prerequisites for performing an *in vitro* study.

The development and production of pharmaceutical drugs, such as chemotherapeutics, begins with significant research. An *in vitro* study is first carefully designed and conducted. If a drug performs successfully in an *in vitro* environment, it is introduced at a specific dosage *in vivo*, typically in a small animal model, to ensure it is not toxic. Around 90% of the drugs that reach this stage of testing are found to be too toxic for further development [19]. Drugs that do prove to be non-toxic then begin a human trial stage, where subjects are administered the drug at therapeutic doses. The full pharmaceutical development process is outlined in Figure 3.

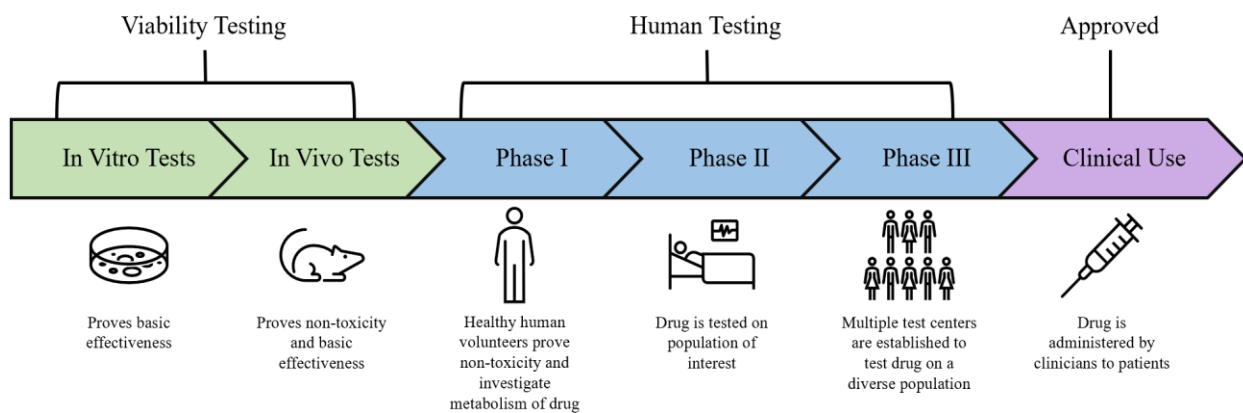


Figure 3: Pharmaceutical Development Process

While a pharmaceutical drug may pass all stages of *in vitro* and *in vivo* testing, many drugs prove to be ineffective at treating every afflicted patient [20]. The failure of a drug to improve the condition of a cancer patient can also cause unnecessary side effects for a patient, such as hair loss, nausea, and fatigue, which can worsen the patient's overall condition. In addition, the failure of a drug increases a patient's treatment timeline and the amount of time a patient must undergo different treatments before their condition improves.

This project is intended to contribute to clinical care, by utilizing *in vitro* testing of a patient's cancer cells to, first, anticipate the likelihood a patient's cancer will invade other regional

or distant tissues. A more predictive *in vitro* test will provide the patient with a more accurate prognosis and allow doctors to screen different therapeutics *in vitro* rather than subject patients to add tests and unnecessary side effects.

2.3.1 Two-Dimensional and Three-Dimensional In Vitro Cell Culture Methods

Methods of *in vitro* tumor modeling can either be two-dimensional (2D) or three-dimensional (3D). These methods are represented in Figure 4, along with some of their attributes that helped factor in making a decision of which cell culturing method would be more appropriate for the purpose of this project.

Two-dimensional modeling is an *in vitro* modeling method that has been used since the 1900s [21]. Using this method, cells are grown on a flat dish, such as a Petri dish, which is made from a material that promotes cell adhesion. 2D modeling is inexpensive, easy to image, and widely used for various applications. However, there are several drawbacks, mostly that cells grow in a monolayer, which does not represent cells in a 3D body accurately. This monolayer reduces cell-to-cell interactions in all directions, reduces cell-to-ECM interactions, and promotes changes in cell morphology, polarity, and method of cell division. Therefore, 2D modeling is less physiologically relevant [22].

For these reasons, researchers have diversified their approach in recent years, moving instead to 3D methods of *in vitro* modeling. This method improves cell-to-ECM interactions, as well as offering cell-cell interactions in every direction. 3D modeling better supports cell differentiation and better maintains different oxygen and nutrient gradients. 3D modeling more accurately represents an *in vivo* environment; however, it is used less often than 2D methods because it is more expensive and more difficult to image and analyze, largely due to the current gap in analysis tools made for 3D cell culture, because 2D cell culture is more common [23].

Three-dimensional modeling was chosen for this project because it allows for multi-directional fluid flow, which is more physiologically relevant to the interstitial fluid flow experienced by cancer cells in the body. Three-dimensional modeling also allows for migration to be effectively simulated, as using a flat plate would not allow cells to move in a way that mimics the lengths cancer cells can travel in the body. 3D modeling will be useful in a clinical application, since cells will be exposed to the drug in all three dimensions, as they would be in the body. Three-

dimensional modeling can be divided into two categories: scaffold-based methods and scaffold-free methods. These methods are discussed in the subsequent sections.

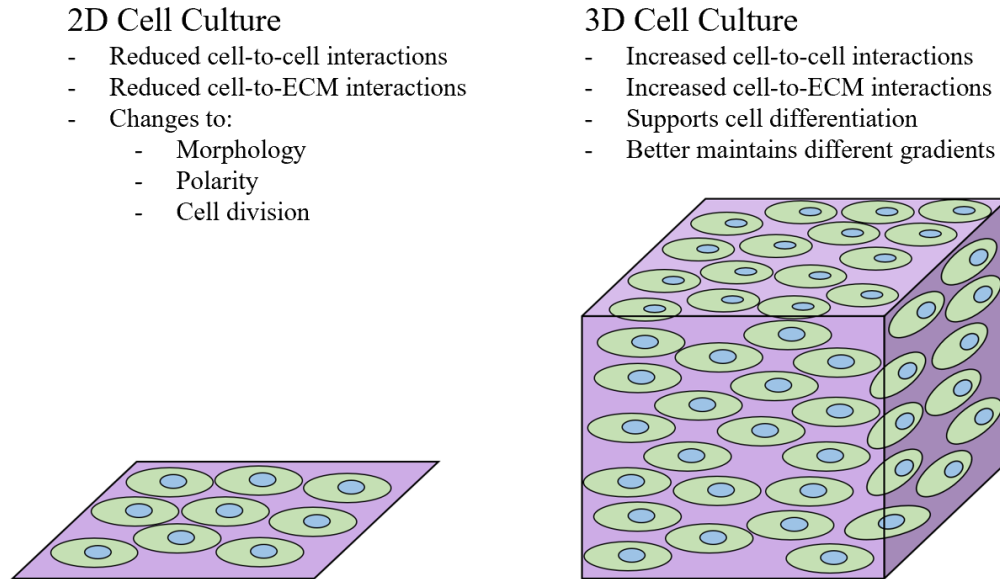


Figure 4: 2D and 3D Cell Culture Methods

2.3.2 Cancer Cell Lines

Cancer cell lines are a part of *in vitro* model systems that can be used in cancer research and drug discovery. Cancer lines have the ability to provide an indefinite source of biological material for experimental purposes and retain most of the genetic properties of the cancer of origin [24]. Cancer cell lines are used in this project in place of a patient's primary cancer cells, due to the unavailability of primary cells.

There are various cancer cell lines that originate from many different types of cancers. In order to choose a cell line for this project, the team had to evaluate cell lines based on factors important to the application of this project. The chosen cell line must be able to metastasize, be generally available, and have a relatively short doubling time (the amount of time it would take for a group of cells to double in size). A short doubling time is desirable so that the timeline of the experiment can be decreased, and the results can be obtained at a higher interval. Recommendations from the previous year's trial of a similar bioreactor system were also considered. Due to these factors, the team decided to narrow our focus to Panc-1 cells from a pancreatic cancer cell line.

This project is focused on creating a means to study tumor invasion as well as the effects of different therapeutics on tumor invasion. Therefore, cell lines that have been documented to exhibit invasive properties were prioritized when selecting a cell line, as shown in Table 2. Due to the lack of metastasis, BxPC-3 and Mia Paca2 were eliminated as a possible option. Of the remaining cell lines, Capan-1 lacks the integrin that is necessary to bind to several scaffold materials, including materials the team considered using. Panc-1 cells have demonstrated strong adhesion, migration, and integrin expression. In addition, Panc-1 cells were also readily available and recommended by the previous year's team [25,26] and this cell line was identified as the most viable option. The Panc-1 cell line is a human pancreatic cancer cell line isolated from a pancreatic carcinoma of ductal cell origin.

Table 2: Cell Line Considerations [25]

Cell Line	Metastasis	Doubling Time	Additional Comments
BxPC-3	No	48-60 hours	Not available at WPI
Mia Paca2	Not described	40 hours	Not available at WPI
Capan-1	Yes	41 hours	Lacks the integrin to bind to several scaffold materials
Panc-1	Yes	52 hours	Recommended by the previous team

2.3.3 Hydrogel Scaffolds

There are numerous methods for designing of scaffolds, and these methods can be used for a wide variety of medical applications. In tissue engineering, certain scaffolds are created as templates for new tissue formation [27]. Many types of scaffolds including polymeric scaffolds and hydrogel scaffolds are used for different biomedical applications. In general, scaffolds are usually seeded with cells, growth factors, and/or used in bioreactor systems. When creating a scaffold in tissue engineering, there are specific requirements that need to be satisfied. These requirements include the biocompatibility, biodegradability, mechanical properties, and the architecture of the scaffold [27]. Scaffolds are used in tumor models for replicating the tumor

microenvironment with a three-dimensional aspect to aid in the model. The three dimensionalities of a scaffold are also very important for modeling the tumor microenvironment. As tissue-engineered scaffolds progressively improve toward replicating the tumor microenvironment, there will be more insight into tumor behavior that will impact clinical practice, drug development, and biological or biomedical research [28].

Hydrogels are one of the most common biomaterials used for engineering scaffolds that will support cell growth due to their matrix properties. Hydrogels consist of three-dimensional hydrophilic polymeric chains that have the ability to retain water. Allowing for the hydrogel to swell or reversibly de-swell based on the amount of water it is able to hold [29]. There are different ways to prepare hydrogels depending on their intended application.

The processes of forming a hydrogel are usually prepared from polar monomers that can be created into either natural polymer hydrogels, synthetic polymer hydrogels, or can be a combination of both [29]. Natural hydrogels include polymers like collagen, hyaluronic acid, alginate, chitosan, etc. While some synthetic polymers include the use of PEG or in combination with PLA [29]. Hydrogel fabrication can be done through either physical or chemical cross-linking. More stable hydrogels can be prepared through chemical cross-linking allowing the hydrogel to have more advanced and stronger mechanical properties through their covalent bond formation. When physically cross-linking a hydrogel through hydrogen bonding or hydrophobic interactions, the mechanical properties are relatively lower than that of the chemically crosslinked hydrogels. An example of physically and chemically cross-linked hydrogels may include the use of silk fibroin (SF) via both physical and chemical crosslinking irradiated at different dosages of gamma rays (γ -rays). The physically and chemically crosslinked SF hydrogels can be compared and characterized in regard to their gel structure, swelling behavior, crystallinity, and biodegradation [30]. Even though chemically crosslinked hydrogels have better mechanical properties than physically crosslinked hydrogels, chemically cross-linking hydrogels may be less biocompatible due to their potential cytotoxicity. Therefore, combining both physical and chemical cross-linking can potentially provide the advantages of both cross-linking methods depending on their intended application [31].

Natural polymers and proteins used in the formation of hydrogel scaffolds include collagen, hyaluronic acid, fibrin, silk protein, fibronectin, alginate, agarose, and chitosan. Most often, hydrogels that are made of these natural polymers have been used in cancer cell growth and

proliferation studies [32]. After hydrogel fabrication, these hydrogels can be used in designing hydrogel scaffolds. Hydrogel scaffolds that have both biophysical and biochemical cues are often used to analyze cell behavior [31]. Depending on the use of certain hydrogel scaffolds, these scaffolds have the potential to mimic a microenvironment. As well as allow for further analysis and investigation on how different cells will behave in the scaffold microenvironment.

2.3.4 Scaffold Free Methods

Designing a multicellular tumor spheroid (MCTS) model is one of the most common scaffold-free methods to mimic the 3D aspects of a tumor [33]. There are multiple multicellular spheroid models including tumor spheres, which is a model of cancer stem cell expansion established in a serum-free medium supplemented with growth factors. Two other spheroid models include tissue-derived tumor spheres and organotypic multicellular spheroids that are obtained by tumor tissue mechanical disassociation and cutting [33]. These three spheroid models can be used in designing the MCTS models. MCTS models are 3D *in vitro* models that are used for many different applications. Some 3D cell cultures can be grown without a present supporting scaffold, these scaffold free methods rely on the cells to form into their own spheroids or clusters. These three common scaffold free methods to form spheroid models are through low adhesion plates, micropatterned surfaces, and hanging drop. Low adhesion plates are plates that are coated with a hydrophilic polymer to prevent cells from sticking to the surface, so they would clump together to form their own spheroid. Micropatterned surfaces are modified plastic surfaces to provide microwells much allows cells to form in clusters. The hanging drop scaffold free method has cells placed in a suspended drop of medium, allowing cells to cluster and form a spheroid structure [34]. MCTS models can also be used to analyze cell proliferation, tumor growth, immune interactions, and drug screenings [35]. The formation of MCTS models is often completed using non-adhesive culture procedures like liquid overlay or rotational culturing. These procedures heavily rely on the cell's ability to form cell to cell interactions [33]. The ability to form MCTS models is important in replicating a solid human tumor by relying only on the cell-to-cell interactions, no other alterations are required. Even though the design process of MCTS models is relatively simple, the process may take up to weeks to be completed.

2.4 In Vitro Techniques for Studying Cell Migration and Invasion

Cancer metastasis, or the spread of tumor cells, is correlated to the more invasive cancer types. Metastasis incorporates, both, invasion, and migration. For example, Pancreatic Ductal Adenocarcinoma is just one of many invasive cancers where the cells migrate from the tumor site to other parts of the body, and invade other bodily tissue, such as the lungs or lymph nodes.

2.4.1 Scratch Assay and Cell Exclusion Zone Assay

A scratch assay is an easy method for studying cell migration *in vitro* in terms of mimicking wound healing *in vivo*. An artificial scratch is made in a cell monolayer and the sample is imaged at different time points. The cells then migrate towards the scratch, filling the gap (Figure 5). This technique is useful when quantifying migration rates of different cell lines or to study cell-matrix or cell-cell interactions [36].

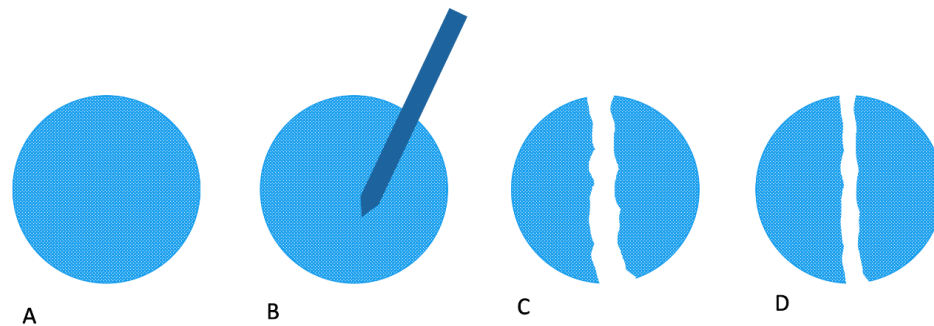


Figure 5: Experimental process of a scratch assay [37]

The cell exclusion zone assay is a widely used technique to study cancer cell migration and quick resurfacing. Cells are plated around the perimeter of a container with a silicone stopper in the center. The stopper is removed once the cells have adhered to the bottom of the container, leaving an empty circular area for which the cells will migrate (Figure 6). In order to create this experiment in 3D, add the coated matrix on top of the cell layer while the stopper is in the middle. Once the matrix has set and the cells have adhered, remove the stopper [38]. The cell exclusion zone assay can reveal information about cell morphology, distance, velocity, and direction of migration [38]. In previous studies, researchers have used the cell exclusion zone assay to determine a faster evaluation of how cells migrate. This method is highly reproducible and allows for the continuous imaging of living cells.

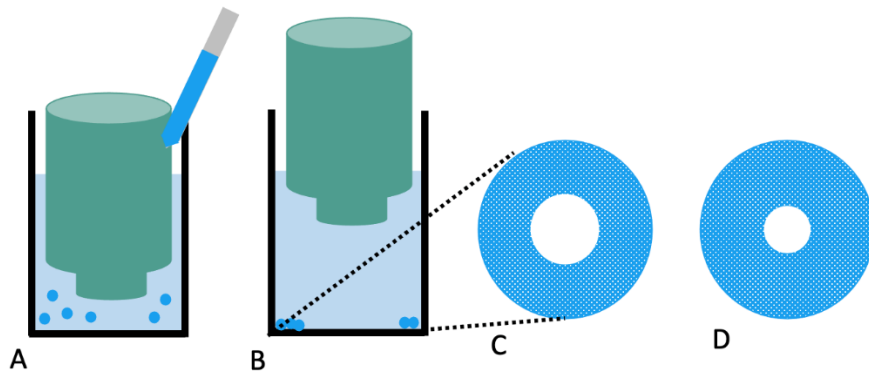


Figure 6: Experimental Process of the Cell Exclusion Zone Assay [38]

2.4.2 Boyden Chamber Assay and Transwell Migration Assay

The Boyden Chamber assay is the most commonly accepted cell migration technique for research purposes. Detailed in Figure 7, this system is made of a hollow chamber that is sealed at one end with a porous membrane. The chamber is placed above a container filled with chemo attractants or medium. Cells are seeded inside the open end of the chamber and are left to migrate through the membrane and into the container [39].

The size of the porous membrane depends on which cells are being studied. Cells can range in size from 30 μm to 50 μm . However, they can migrate through pore sizes that are much smaller. For example, fibroblasts cells and macrophages can migrate through a 5 μm pore size. Most cell types, such as epithelial cells, can migrate through a pore size of 8 μm [39].

The Transwell Migration assay is a modified version of the Boyden Chamber assay. The difference being that the porous membrane is covered with an extracellular matrix component, such as collagen or Matrigel, to facilitate migration. The incubation period can range from 3 to 18 hours and the cells that have migrated after this incubation are stained and counted [40].

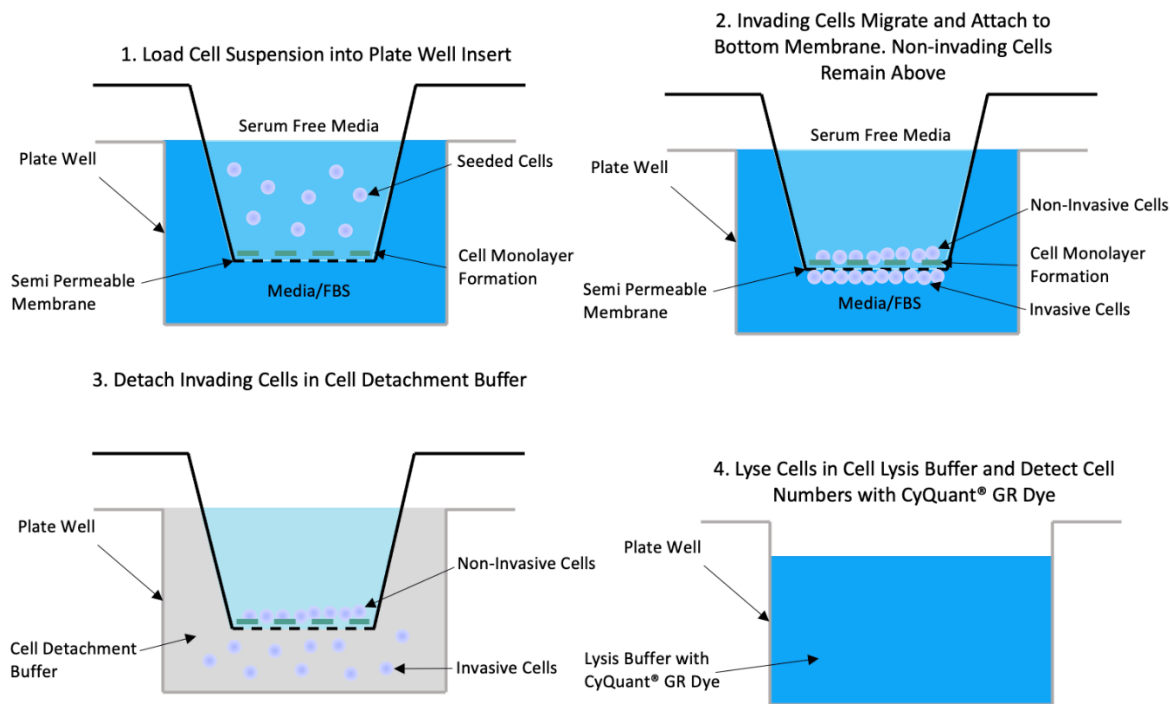


Figure 7: Experimental Process of the Boyden Chamber Assay

2.4.3 3D Tumor Tissue Invasion for High-throughput High Content Phenotypic Drug Screening

Puls et. al developed a novel 3D tumor tissue invasion model for phenotypic drug screening in 2018. Some of the main benefits of the model they developed include a rapid and reproducible setup, as well as user-definition of the tumor and surrounding tissue. They created custom high-density tumor compartments and used type I collagen to mimic *in vivo* extracellular matrix properties. Another benefit to the model that was created for this study was its compatibility with automated imaging and analysis to enable high throughput and high content drug screening, potentially helpful in the identification of new cancer therapies. One limitation of this study is that the model does not incorporate physiologically relevant fluid flow [41].

2.4.4 Image Analysis

A key component of studying cell migration and invasion is the imaging of results to obtain measurable outcomes. There are many different imaging techniques to measure invasion of cells

into a scaffold or hydrogel. Commonly, light microscopy is used for imaging of fixed specimens, and for measurement of invasion can be used at different time periods to track the movement of cells through the model material. For increased specificity and cell visibility, a fluorescence microscope can be used, which incorporates a fluorescent dye and is beneficial to visualize more specific cell structures [42]. When imaging with the goal of observing invasion, often these microscope techniques are used in tandem with a software like ImageJ, CellProfiler™, or MATLAB® to make the quantification aspect of measurement easier and slightly automated [43].

2.5 Fluid Flow in Cancer

2.5.1 Perfusion and Blood Flow

Perfusion is defined as “the volume of blood flowing through capillary networks and extracellular matrices of tissue per unit time” [44]. Blood perfusion is responsible for regulating the nutrients, oxygen, and waste products throughout the body which ultimately benefits the physiology of normal tissue [45]. The tumor microenvironment has a heterogeneous distribution of blood flow due to structurally abnormal blood vessels, resulting in hypoxia. Hypoxia is caused by the deprivation of oxygen to an area of the body. These regions tend to be resistant to chemotherapeutics resulting in a favorable environment for metastatic cells.

Further, angiogenesis, or the development of blood vessels, contribute to the progression of cancer. These blood vessels form from already existing perfused vessels [46]. Tumor cells secrete a vascular endothelial growth factor, along with other secretions, to induce angiogenesis. The newly formed blood vessels are typically irregular in shape, which causes gaps in the endothelial cell layer and a lack of smooth muscle coverage [47]. These inconsistencies allow for the increased influx of fluid into the tumor and further demonstrate the connection between angiogenesis and fluid flow [47]. Exploring the impact of perfusion in relation to metastasis can greatly improve the understanding of how tumors develop and grow.

2.5.2 Interstitial Fluid Flow

Interstitial fluid is defined as the movement of fluid through the extracellular matrix in tissues and blood vessels that plays an important role in morphogenesis [48].

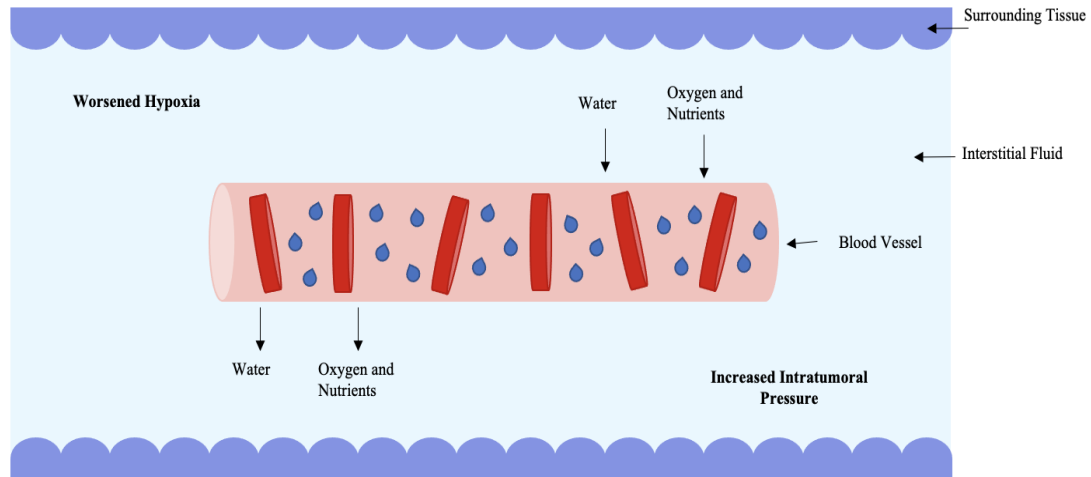


Figure 8: Interstitial Flow Between Tissue Cells and Blood Vessels

Tumor blood vessels are unstable compared to healthy blood vessels. This is due to a weakened ability for the fluid to drain from the stroma in cancerous tissue. This instability causes an increase in the interstitial fluid flow and pressure within the tumor, which ultimately leads to changes in perfusion rates. This increase in interstitial fluid within the tumor ultimately leads to an increase in cell migration from the tumor site. Further, side effects of this increased interstitial fluid worsens hypoxia as a result of decreased oxygen delivery to the tumor (Figure 8).

2.6 Types of Bioreactor Systems

Bioreactors allow biological processes to take place within closed systems under tightly controlled conditions. Bioreactors are an attractive component for *in vitro* tumor modeling due to their abilities for cell growth and modeling of biochemical and mechanical factors on the cells. There are many different types of bioreactors that are used in bioprocesses with each type having different benefits over standard static culture mechanisms. To mimic the tumor microenvironment most accurately, hybrid bioreactors can be used which incorporate specific characteristics from multiple standard bioreactors [49].

The first type of bioreactor is a perfusion bioreactor also sometimes referred to as flow bioreactors. Perfusion bioreactors have a pump and an incubation chamber with tubes to form an open or closed loop. An overpressure is created by the pump providing consistent medium flow through the scaffold. A benefit of perfusion bioreactors is that they are considered the most accurate way to mimic the *in vivo* mass transfer process. In perfusion bioreactors, cells are

suspended on 3D scaffolds which allow for uniform cell distribution and proliferation. 3D scaffolds can be beneficial for showing the invasion abilities of cancer lines, but the size and material inconsistencies can occasionally lead to unequal nutrient distribution [49].

Stirring bioreactors consist of a tank vessel with a built-in spinning element to form a vortex of fluid flows. These bioreactors improve the mass transfer between cells and culture medium. Typically, a culture is placed into the vessel and fed with medium and then either placed on a shaking/vibrating element or the built-in instrument is started and runs for a set period of time. Stirring bioreactors are advantageous because sampling is easily accessible, computational models are available and cell mass can be easily increased. Potential drawbacks include high shear stress and the balance with mass transfer, as well as unequal cell distribution due to medium not penetrating the entire scaffold [49].

A third type of bioreactor to consider is a rotary bioreactor. Rotary bioreactors can be vertical or horizontal and involve a cylindrical container and spinning walls filled with the culture medium. Cells are seeded on a scaffold which freely floats among the culture medium. Rotary bioreactors are advantageous when it comes to determining gene and growth factor expression, but they are limited due to the influence of shear stress and in terms of tumor modeling, do not provide a means to quantify invasion [49].

Hollow fiber bioreactors consist of a closed vessel with cells suspended on a scaffold permeable to the culture medium. The scaffold contains hollow fibers to mimic blood vessels and tumor metabolism. The main benefit of this design is that the hollow fibers allow for a unique ability to deliver nutrients and remove waste to and from the depths of the growing tissue. Drawbacks include that this type of bioreactor is not accommodating of 3D scaffolds, and the scaffolds must be removed from the main vessel to be examined, potentially damaging the tissues [49].

Finally, there are microfluidic bioreactors, essentially a specialized perfusion bioreactor these systems are used to study cells in small quantities. The functions are the same as that of the perfusion bioreactor but at a much smaller scale. Microfluidic bioreactors use a glass substrate covered with biocompatible silicone material that is arranged as a microchannel or container. Mass transfer occurs by perfusion of the culture medium through the channels. These systems are beneficial for studying the progression of tumors, angiogenesis, invasion as well as other stages of metastasis. The disadvantages of microfluidic bioreactors include the small cell count as well as

the price and complexity associated with the manufacturing of the device [49]. The bioreactor systems mentioned above are summarized in Table 3.

Table 3: Summary of Types of Bioreactors

Bioreactor Type	Benefits	Drawbacks
<i>Perfusion Bioreactor</i>	<ul style="list-style-type: none"> • Incorporates flow • Mimics <i>in vivo</i> mass transfer • Quantifying invasion 	<ul style="list-style-type: none"> • Size and material inconsistencies • Unequal nutrient distribution
<i>Stirring Bioreactor</i>	<ul style="list-style-type: none"> • Pre-existing computational models • Easily accessible for sampling 	<ul style="list-style-type: none"> • High shear stress • Unequal cell distribution due to poor medium/scaffold penetration
<i>Rotary Bioreactor</i>	<ul style="list-style-type: none"> • Determining gene and growth factor expression 	<ul style="list-style-type: none"> • Influence of shear stress • Unable to quantify invasion
<i>Hollow Fiber Bioreactor</i>	<ul style="list-style-type: none"> • Deliver nutrients and remove waste mimicking tissue 	<ul style="list-style-type: none"> • Unable to accommodate 3D scaffolds • Scaffolds must be completely removed for sampling/imaging
<i>Microfluidic Bioreactor</i>	<ul style="list-style-type: none"> • Useful for studying tumor progression, invasion, and metastasis 	<ul style="list-style-type: none"> • Small amount of cells • Expensive and complex to manufacture

2.7 Modeling Cancerous Interstitial Fluid Flow In Vitro

Current research has been done related to the effect of interstitial fluid flow on cancer cell invasion in many different cancer types. The process of cancer cell invasion is what allows cancers to resist therapeutics. Interstitial fluid flow is inconsistent, and changes in interstitial fluid pressure have been found in the tumor microenvironment due to changes in angiogenesis that is correlated

with the progression of cancer [50]. Modeling the cancerous interstitial fluid flow in bioreactors will aid in identifying and understanding the effects of fluid flow to the tumor microenvironment.

Darcy's Law is an equation that derives the flow of fluid through a porous medium [51]. It is the relationship between instantaneous discharge rate through a porous medium, the viscosity of fluid, and the pressure change. The equation is only valid for slow, viscous fluid, as shown in Equation 1. The permeability k , of a porous scaffold can be determined by following Equation 2.

$$Q = \frac{-kA(pb - pa)}{\mu L}$$

Equation 1: Darcy's Law for Fluid Flow through Porous Medium [51]

$$k = \frac{Q * \mu * h}{A * \Delta P}$$

Equation 2: Permeability Coefficient Calculation

Where, Q is the volumetric flow rate, μ is the dynamic viscosity of water at 37°C, h is the height, A is the area of the scaffold biomaterial, and $\Delta P(p_b - p_a)$ is the pressure change.

It is important to understand other models of cancerous interstitial fluid flow in bioreactors. There have been *in vitro* studies experimenting and examining the effects of shear flow and continuous fluid flow on cancerous cells. These studies have been done using different types of cancer models, experimental setups, and flow types.

2.7.1 Microfluidics

Microfluidics refers to the science of directing picolitres of fluids in microchannels ranging from 1 μ m to 1000 μ m in size. It can be used in a variety of applications such as manipulating RNA, proteins, cells using biosensors, and cell assays for disease diagnosis [52]. There are many benefits to using microfluidics in cancer research, including reduced sample size, reduced reagent consumption, and short processing times [52]. It can provide a non-invasive way to diagnose cancer in patients, as it can analyze bodily fluids, such as saliva or blood.

The earliest microfluidic devices that have been established in the biomedical realm involve the Polymerase chain reaction, electrophoresis on chip, and DNA microarrays [52]. There are a variety of materials that have been used when preparing a microfluidic device, including:

silicon, glass, and elastomers. The ability to use elastomers in microfluidics research enhanced the biocompatibility and non-invasiveness of these devices as well as lowered their cost.

2.7.2 Shear Flow Study: Human Epithelial Ovarian Cancer

Shear flow and stresses are often experienced in cancer cells. It is important to understand the forces of shear stresses that different cancer cell lines experience during flow. In 2013, a study experimented using an OVCAR-3 cancer cell model. The experiment included a microfluidic chamber with seeded cells in two dimensions. The cells were then exposed to a pump-driven shear flow (0.5-1.5 dyne/cm²). After completion of this experiment, the gathered results explained that the cells in this model elongated and developed long thin stress fibers due to the flow [53]. Shear flow is an important topic to discuss in regard to replicating the tumor microenvironment and the forces that cells experience. The models and experiments provide important data to advance the understanding and effects of shear flow to cells within the body.

2.7.3 Continuous Interstitial Flow Study: Human Breast Carcinoma

Continuous interstitial fluid flow is another important concept to understand with how the continuous flow effects cancer cells in the body. Creating a modeling system to replicate continuous interstitial fluid flow and its effects on cancer cells. There are current modeling systems that incorporate this concept. In 2014, a study experimented using an MDAMB231 cancer cell model. This experiment included cells in three-dimensional collagen matrices. These cells were then exposed to driven pressure flow across the matrix (4.6 μm/second). After completion of this experiment, the gathered results explained that the interstitial fluid flow reorganized the focal adhesions of the cells. The cells were reorganized at the surface of the matrices [54]. Continuous interstitial fluid flow is another important topic to discuss when evaluating the effects of flow on cancer cells within the body. These models are designed and used to closely replicate the effects of interstitial fluid flow in the body. Gathering data from these studies and models allow for further research to be done and may also provide a better understanding on the underlying effects of interstitial fluid flow. Evaluating both the benefits and drawbacks of many different studies modeling cancerous interstitial fluid flow will be considered when designing our bioreactor system.

2.8 State of the Art Devices and Methods of Invasion Analysis

2.8.1 Perfused Tumor Tissue Model for Invasion Analysis

In 2019-2020 Callahan, Ferguson, Steigerwald, and Waskowicz designed a perfused tumor tissue model for invasion analysis for their senior capstone project at Worcester Polytechnic Institute, detailed in Figure 9. The bioreactor model was intended to “perfuse 3D tumor tissue constructs at physiologically relevant flow rates using a multi-channel syringe pump and allows for image analysis of cellular invasion”. The design was a clear acrylic CCH unit with parallel wells and a multi-channel syringe pump. A 10% gelatin hydrogel was crosslinked with 0.2% glutaraldehyde to form the scaffold. Image analysis was performed using light microscopy and a MATLAB® quantification program. Drawbacks of the model include poor quantification of cell invasion, as well as inconclusive evidence for the scaffold supporting cell invasion [26].

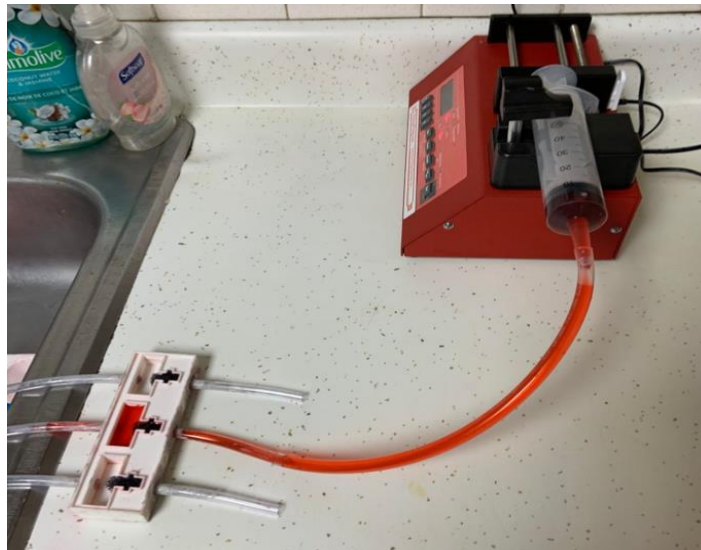


Figure 9: Set-Up of Perfusion Bioreactor from 2019-2020 MQP Group

2.8.2 Microfluidic Cell Migration Assay for Glioblastoma Patients

Wong et. al developed a microfluidic assay to quantify cell migration and proliferation and “categorize patients with glioblastoma according to progression-free survival.” The assay was developed to measure both the migratory and proliferative potentials for breast cancer cells to assess the metastatic capabilities and screen for possible therapeutics. The assay consisted of parallel seeding and medium channels connected by microchannels to mimic the complex topography of the *in vivo* environment. By quantifying the number of cells that traverse the

microchannels they demonstrated that the assay could predict individual patient survival and time to recurrence. This study demonstrates the importance of studying invasion as it relates to patient prognosis and outcomes, and these specific methods and techniques provide valuable insight for quantifying migratory behaviors within physiologically relevant conditions. One drawback of this technique is that it was designed specifically for Glioblastoma and not invasive cancers as a whole [55].

2.8.3 Perfusion Bioreactor System for Engineered Breast Cancer Surrogates for Preclinical Testing

Marshall et. al developed a new perfusion flow bioreactor in 2017 to improve and fill gaps in preclinical testing. They hoped to predict the efficacy, safety, and pharmacokinetics of different cancer therapies better than existing models. The benefit of using a bioreactor system was the ability to model cancers in large volumes and over a long period of time. Carbon foams and extracellular matrix hydrogels were used to seed breast cancer cells. Microchannels were included and it was found that cell viability was increased with the presence of the microchannels compared to models that do not include them. Another benefit of this model relevant to the current project is that it was easily imageable through the PDMS flow chamber. The use of carbon foam was critical to maintaining the integrity of the microchannels over time. This study demonstrates the ability to image from a perfusion bioreactor system, as well as methods to improve cell viability and applications for clinical testing through the incorporation of flow. Drawbacks of this model include material limitations with carbon foam and uncertainty surrounding incorporation of an ECM hydrogel using collagen [56].

Chapter 3: Project Strategy

3.1: Client Statement

The initial client statement presented to the team was to:

“Design a device that is able to perfuse multiple in vitro tumor constructs simultaneously in a tissue culture incubator and be transferred to a microscope for daily monitoring of cell activity with minimal handling over multiple days.”

This client statement emphasized sterility and the ability for cells to be imaged throughout the process of migration and invasion. This client statement was conducive to use in an academic research environment, however, the team decided early on to shift focus to a clinical setting.

Due to this change in focus, the team contacted Dr. David Ebb, a Pediatric Oncologist at Massachusetts General Hospital, to discuss the implications of the project goal and gain insight on the needs of a clinician. From this discussion, a revised client statement was formed that states:

“Design a device that is able to model interstitial fluid flow to perfuse multiple different types of cancer cells into a biocompatible scaffold that can be imaged in order to quantify a cell line’s tendency to migrate to and invade secondary tissues.”

This statement emphasizes that the device be able to be used on different types of cancer cells so that it can have applications using an individual patient’s cancer cells as taken from a biopsy. This client statement, like the initial client statement, requires the use of imaging. However, the cells only need imaging at the conclusion of an experiment and not multiple times throughout the process.

3.2 Technical Design Requirements

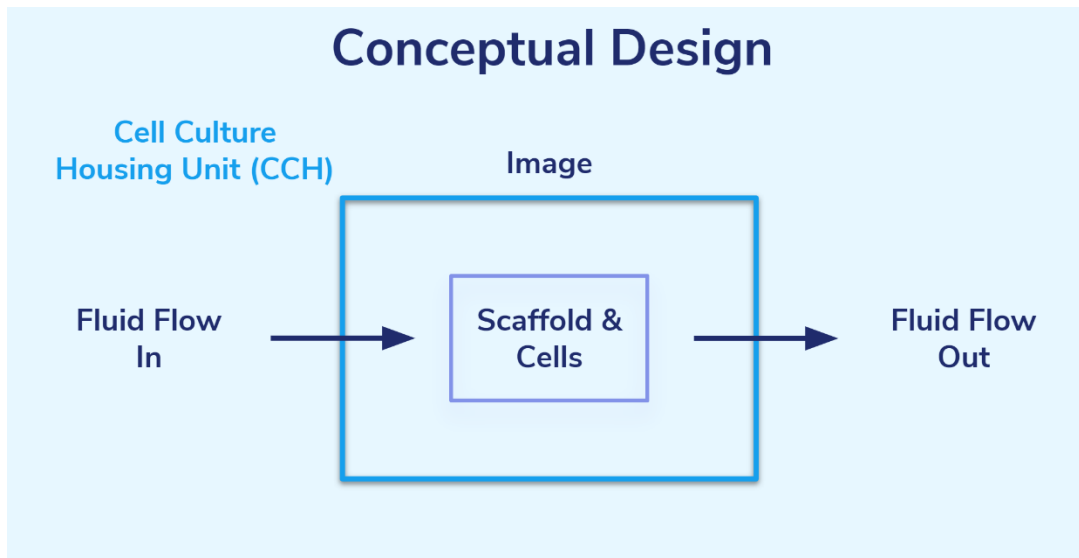


Figure 10: Conceptual Schematic of Device Design

Following our revised client statement, our team created a schematic that identifies the important components of our proposed conceptual design (Figure 10). The most important components include fluid flow and scaffold imaging. At the start of our design flow chart, we will generate an inlet fluid flow with a specific cell line that will lead to a scaffold that mimics the tumor microenvironment. That scaffold will be held in a cell culture housing unit and later imaged and analyzed for cell invasion. Finally, fluid will exit the system.

The team developed the following list of technical design objectives:

1. The model should support cancer cell invasion into a scaffold.
2. Scaffolds and cells should be contained within the Cell Culture Housing (CCH) unit and be able to be imaged.
3. Fluid should perfuse through the CCH with variable flow speeds.
4. The device should be easily manufactured, assembled, and maintain sterility.
5. The device can be used in a clinical setting.

The team has identified five main objectives for this project. Our **first objective** is that the design should support invasion of metastatic cell lines through a porous scaffold. To do this we

need to make sure that the metastatic cancer cells can be seeded on and invade a scaffold which is able to achieve high disease state properties and not impede cell invasion. Our **second objective** is that the scaffold and cells should be contained within the cell culture housing unit and be able to be imaged. To accomplish this objective, it is important for the cell culture housing unit to not impede cell viability, allow for imaging of the scaffold using a standard microscope, and be analyzed using semi-automated image analysis. Our **third objective** is that fluid should perfuse through the cell culture housing unit with variable flow speeds. The flow speeds should be comparable to the in vivo tumor microenvironment and not hinder cell proliferation and viability. Our **fourth objective** is that the device should be easily manufactured, assembled, and maintain sterility so that it can work properly while still being user friendly. The device will be printed as one complete fabricated design. The design will also include a pump that will be connected via tubing to the device. Our **fifth objective** is for the device to be applicable in a clinical setting. For this objective, the system should be reusable and easily sterilized. The design will have multiple flow channels to run test.

These design splits the project into four primary areas of focus: 1) flow through the system, 2) quantifiable cell invasion, 3) scaffold fabrication with cells, and 4) bringing this device into the industry and clinic. The objectives were paired with the appropriate functional requirements to describe what that objective should accomplish. The functional requirements were then paired with means to illustrate how the functional requirements would be achieved.

3.3 Objectives for Invasion

Table 4: Invasion Functional Requirements and Means

Objective	Functions	Means
The model should support cancer cell invasion into the scaffold	The metastatic cancer cells will invade the scaffold	<ul style="list-style-type: none"> • Pore size and stiffness will be chosen to mimic the properties of tumor tissue • Scaffold will contain a chemoattractant that will promote invasion
	The cell invasion is detectable through microscopy	<ul style="list-style-type: none"> • Cells will be stained (e.g., nucleus) for visualization on a standard light microscope • Scaffold thickness will be made to match the working distance of the microscope

Objective 1 is to develop a model that is supportive of Panc-1 cell invasion into the scaffold for a proof of concept of our final design (Table 4). The functions of this objective are that Panc-1 cells will invade the scaffold and the invasion is detectable through microscopy. To achieve these functions, it is important that the pore size and stiffness of the chosen scaffold material mimics the properties of an *in vivo* tumor microenvironment. The scaffold will need to have a chemoattractant that will promote cellular invasion into the scaffold. Further, the nucleus of the cells will be stained to achieve a visualization under a standard light microscope and the scaffold thickness will be made to match the working distance of the microscope. If this objective is achieved, it will pave the way for future studies in exploring cellular response under different conditions.

Table 5: Invasion Design Criteria

Functional Requirements	Design Criteria
The metastatic cancer cells will invade the scaffold	Designing different flow channels that will connect to their assigned scaffold chamber will allow for metastatic cells to travel and invade the scaffold.
The cell invasion is detectable through microscopy	Scaffolds will be designed to fit into the three scaffold chambers. These chambers will hold any invaded cells from the inlet flow channels into the scaffold. Utilizing microscopy techniques, each chamber will be analyzed individually to detect any invaded cells.

The design criteria for the functional requirements of invasion are explained in Table 5 and are important requirements for the functionality of our device. To make sure that metastatic cancer cells will invade the scaffold there will be separate flow channels for each of the three scaffolds. This allows for multiple tests to be run simultaneously at variable flow speeds. Second, to ensure the invasion is detectable through microscopy the scaffold will be sized to fit within the 3D printed chambers, which can be imaged individually using either fluorescence or light microscopy.

3.4 Objectives for Scaffold and Membrane

Table 6: Scaffold Functional Requirements and Means

Objective	Functions	Means
Scaffold and cells should be contained within the CCH unit and be able to be imaged	Scaffold does not impede cell viability	<ul style="list-style-type: none"> • The chosen scaffold material will be biocompatible and sterile so that cancer cells can be seeded on it • The system will be closed off for sterility to not effect cell viability
	CCH unit allows for imaging of scaffold using a standard microscope	<ul style="list-style-type: none"> • The chosen CCH unit material will be clear so that scaffolds can be imaged without needing to be removed from the device • CCH unit has to fit the boundaries of a standard light microscope

Our second objective is that the scaffold and cells should be contained within the CCH unit and be able to be imaged (Table 6). Functions of this objective include CCH unit not impeding cell viability, and CCH unit capability of being imaged by a standard light microscope. To meet these functions the CCH unit material will be biocompatible with metastatic cell lines and the system will be closed off to the outside for sterility. This is important because the cells need to be able to survive under the conditions in the CCH unit. The conditions should mimic the *in vivo*

tumor microenvironment. The CCH unit material will be clear so the invasion is detectable, and the size of the device will fit the boundaries of a standard light microscope. This allows for scaffold to be easily imageable while maintaining ease of assembly.

Table 7: Scaffold Design Criteria

Functional Requirements	Design Criteria
CCH does not impede cell viability	CCH unit will be sterilized, and tests will be run within an incubator so that conditions mimic the <i>in vivo</i> tumor microenvironment
CCH allows for imaging of scaffold using a standard microscope	Dimensions of each scaffold chamber are 1-inch in diameter and 0.65 inches deep, this size allows for the chamber of the CCH design to be placed on and imaged using a standard microscope.

The design criteria for the functional requirements of the scaffold are explained in Table 7 and are important requirements for the functionality of our device. The functional requirements for our scaffold design include sterility between CCH unit and the scaffold, CCH unit not impeding cell viability, and CCH unit allows for imaging of the scaffold. The user needs to ensure that every component of the system including the CCH unit are sterilized properly to not impede cell viability. For imaging of the scaffolds using a standard microscope, dimensions of each scaffold chamber will be sized properly to fit onto a standard microscope.

3.5 Objectives for System Flow

Table 8: System Flow Functional Requirements and Means

Objective	Functions	Means
Fluid should perfuse through the CCH unit with variable flow speeds	Flow is comparable to <i>in vivo</i> TME	<ul style="list-style-type: none"> • Flow will be controlled by using a programmable automatic syringe pump • Chosen scaffold mimics tumor tissue with variability in porosity and stiffness properties
	The flow will not hinder cell proliferation and viability	<ul style="list-style-type: none"> • The flow will be in a closed loop to maintain sterility • Fluid to induce flow will consist of proper cell culture medium

The third objective for this device is that the bioreactor can perfuse through the CCH unit with varying flow speeds (Table 8). The CCH unit design includes three inlet and outlet flow channels that are connected to 0.25-inch tubing to model continuous flow at variable flow speeds. The two important functions for this device are that flow is comparable to *in vivo* tumor microenvironment and that flow does not hinder cell viability. The means to meet these functions are that the flow will be controllable and the chosen scaffold material mimics *in vivo* tumor tissues. Additionally, the flow will be in a closed-loop to maintain sterility and the fluid used to induce flow will be the proper cell medium for Panc-1 cells. The fluid flow through the system can be summed up into Equation 3.

$$Q = Av$$

$Q = \text{volumetric flow rate}, A = \text{area of tubing}, v = \text{velocity}$

Equation 3: Speed to Volumetric Flow Rate

Table 9: System Flow Design Criteria

Functional Requirements	Design Criteria
Flow is comparable to <i>in vivo</i> TME	Fluid flow will be administered using a syringe pump connected to tubing with a 0.25-inch outer diameter. This tubing will then connect to inlet flow channels of the CCH allowing for fluid to travel through the individual channels leading to the scaffold.
The flow will not hinder cell proliferation and viability	The rate of flow being driven through the 3 flow channels will be consistent while using a syringe pump and not promote cell proliferation and viability.

The design criteria for the functional requirements of system fluid flow are explained in Table 9 and are important requirements for the functionality of our device. The fluid flow will be administered by the specifications of the user. Each channel can be programmed to administer different fluid flow rates; however, the flow will be uniform for means of testing. This is important because the rate of flow through the device and scaffold could affect the timing at which cellular invasion into the scaffold occurs. However, as stated by the second functional requirement of the team, the flow should not hinder cell proliferation or viability. So, while there is a chance that an increased flow could increase cellular invasion, an increased flow should not cause cellular death or impede multiplication.

3.6 Objectives for Device Fabrication

The device will be printed as one complete CCH unit out of one material to allow for ease of assembly between the tubing, syringes, and syringe pump. The functions and means are shown in Table 10. The design will include a pump that will be connected via tubing to the device.

Table 10: Objectives for Device Fabrication

Objective	Functions	Means
The device should be easily manufactured, assembled, and maintain sterility	Multiple channels will be in one CCH unit	<ul style="list-style-type: none"> The device will have a custom design that can be printed
	Scaffolds remain sterile with the CCH unit	<ul style="list-style-type: none"> The material chosen for the scaffolds will be easily sterilized using an autoclave or vacuum filter The scaffold will be loaded into the CCH unit in the biosafety cabinet

The device will be printed to a size that is able to include multiple flow channels and scaffold chambers in one CCH unit for multiple scaffolds to be tested simultaneously (Table 11). The dimensions provided in the design criteria allow for these channels and chambers to be evenly spaced between each other. Sterility will be achieved through autoclaving the high-temperature resin design. Further, the scaffolds can be sterilized by either autoclaving or vacuum filtering the individual materials before mixing the solution in a biosafety cabinet. To further add to sterility, the device would need to have a lid that will close the system to keep it sterile if the experiments were done outside of a biosafety cabinet.

Table 11: Functional Requirements and Design Objectives for Device Fabrication

Functional Requirements	Design Criteria
Multiple channels will be in one CCH unit	Device will be 3D printed and fabricated as one design that is 5.25in x 4.50in x 0.75in to align with the microscope stage size and fit within a standard incubator
Scaffolds remains sterile with the CCH	Device will be 3D printed of high temperature resin, which is able to be autoclaved to maintain sterility

3.7 Objectives for Industry Use

Table 12: Industry Use Functional Requirements and Means

Objective	Functions	Means
The device can be used in a clinical setting	Reusable and easily sanitized and cleaned	<ul style="list-style-type: none"> • CCH material and internal materials (scaffolds) will be easily autoclaved, vacuum filtered, or wiped down with ethanol
	The device takes three days to obtain accurate clinical data	<ul style="list-style-type: none"> • The CCH device will be continuously run in parallel with the syringe pump • Cells will begin to invade the scaffold material, be imaged, and quantified using an open-source program, within three days

The fifth and final objective is for the device to be applicable for use in a clinical setting as shown in Table 12. To achieve this objective the device should be capable of testing chemotherapies on the patient’s cells as well as reduce the patient’s treatment timeline. To achieve these functions chemotherapies should be able to be perfused through the system, the model can externally test patient’s cells as well as reduce the trial and error associated with typical testing. This objective is the end timeline point of this device. However, for means of this current project, the clinical setting objective is set as a future direction. All previous objectives: however, lead this device to be used in a clinical setting.

Table 13: Industry Use Design Criteria

Functional Requirements	Design Criteria
Reusable and easily sanitized and cleaned	The CCH housing unit material will be high temperature Resin which can be autoclaved for sterilization
The device takes three days to obtain accurate clinical data	Design will have multiple flow channels to run tests continuously, effectively, and efficiently to then deliver faster results to patients.

The design criteria for the functional requirements of industry use are explained in Table 13 and are important requirements for the functionality of our device. As stated previously, the device would need to be made of a material that is easily sterilized so that laboratory technicians can reuse the device between tests. As proved in research, it takes about three days for a cell to break off one tumor and form another [56]. Therefore, the team chose the timeline of three days to allow for cells to invade the scaffold.

3.8 Standards for Design Requirements

The design and verification process for the device followed standards that are developed by several regulatory bodies. The standards listed ensured that the experiments and procedures used for this project are comparable to other projects in the field and allows for repeatability of the completed protocols. The relevant standards from these bodies are listed below:

FDA: The FDA outlines good laboratory practices for non-clinical laboratory studies in 21CFR58

ISO: This project included the use of several ISO standards throughout the development of the bioreactor system.

- ISO 24998:2008: All cell culture dishes, and conical tubes used in cell culture procedures were properly sterilized and maintained.
- ISO 14937:2009: General sterilization methods for a bioreactor
- ISO 17665-1:2006: This standard was followed for autoclaving the gelatin powder for cell viability testing.
- ISO 128:2003: All SolidWorks drawings follow the drafting standard outlined.

ASTM: The guide ASTM F2150-19 was followed for the characterization and testing of the biomaterial scaffold.

Chapter 4: Design Process

4.1 Needs Analysis by Pairwise Comparison

After revising the client statement and defining clear objectives, the team defined several considerations that would influence the preliminary device designs. Firstly, the device must be able to support cell invasion of a scaffold. The device must also be easy to assemble, both in the team's building process and for any future users. The device should also meet our project goal of introducing fluid flow and designing a device that would be a closed-loop system could maintain this flow. Additionally, the device must be imageable in order for cell counting to be performed for quantifiable results. Finally, the device should be applicable for use in a clinical setting.

The team conducted a Needs Analysis using a Pairwise Comparison to evaluate the considerations that should be of highest priority when designing preliminary devices. This Pairwise Comparison is shown in Table 14. Each feature on the top row was evaluated to determine whether it was more important (1) or less important (0) than the feature in the leftmost column. The values in each column were added together to produce a final ranking.

Table 14: Needs Analysis by Pairwise Comparison

	Cell Invasion	Imageable	Clinical Setting	Fluid Flow	Ease of Assembly
Cell Invasion		0	0	0	0
Imageable	1		0	1	1
Clinical Setting	1	1		1	1
Fluid Flow	1	0	0		0
Ease of Assembly	1	0	0	1	
Total	4	1	0	3	2

Based on the pairwise comparison, the three most important features of the final design are:

1. Cell Invasion
2. Fluid flow
3. Ease of assembly

4.2 Overall System Design

4.2.1 Preliminary Designs

Following the design process, the team considered some preliminary designs:

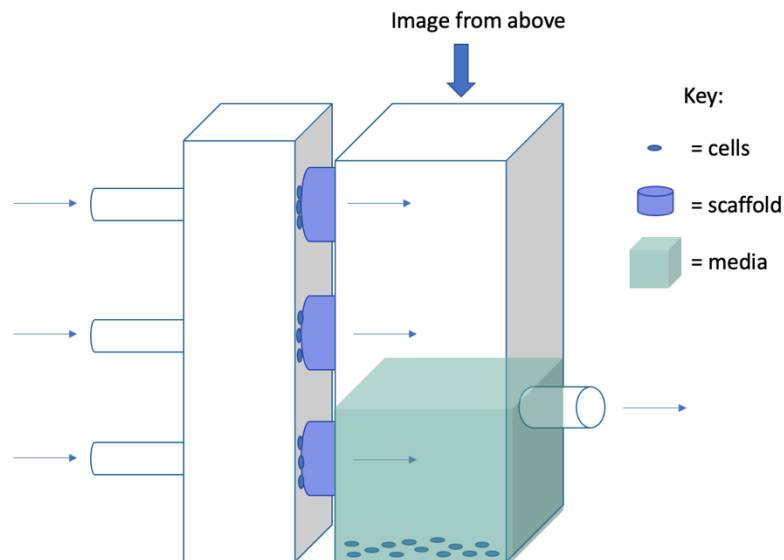


Figure 11: Preliminary Design 1 (Two-Chamber)

The first preliminary design is an idea the team had created that included two different chambers as shown in Figure 11. The two chambers are connected with tubing and the scaffolds are placed between the two parts and inside the tubing. Fluid flow is added to the inlet channels and flows into the next chamber. The second part is hollowed out and is where the invaded cells are collected from the scaffolds. Using a standard microscope, image the number of cells that were collected into the following chamber. A limitation to this design is that the ability for the cells to readily detach from the scaffold and entering the second chamber is very unlikely, giving a pooled population from all three scaffold and not each one individually.

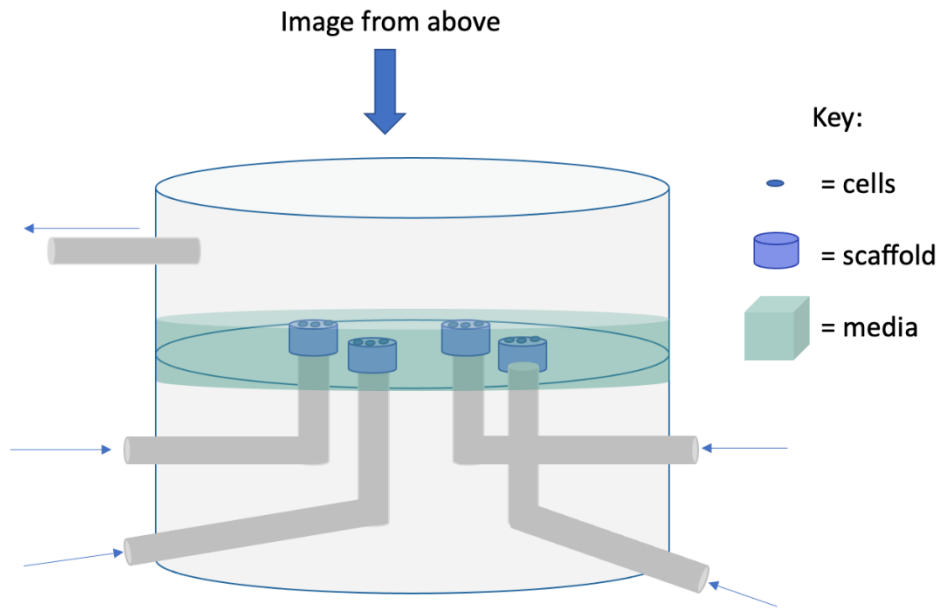


Figure 12: Preliminary Design 2 (4 Channel Flow Bioreactor)

Our second preliminary design was based off of a similar research project that designed a multi-flow channel bioreactor that is able to monitor real time cellular dynamics in 3D engineered tissue [57]. As shown in Figure 12, this preliminary design includes four different inlet flow channels, leading up to a scaffold. Cells will then invade the scaffold and the scaffold will then be imaged from above. A single outlet flow channel will collect any of the excess medium or cells that do not invade the scaffold. A limitation to this design is the idea of only one outlet flow channel, not allowing for continuous fluid flow in and out of each individual scaffold.

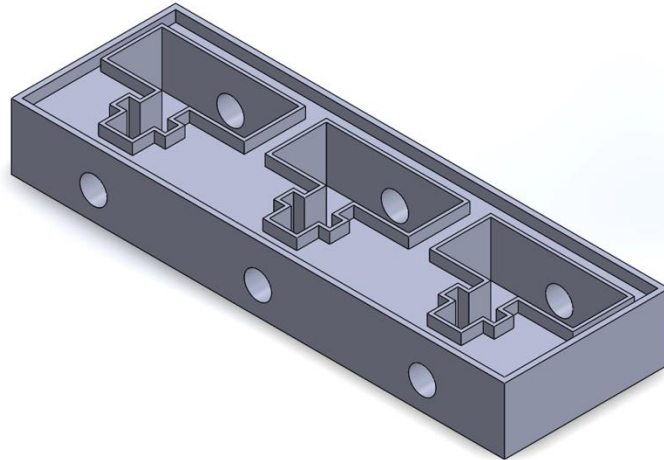


Figure 13: Preliminary Design 3 (Previous MQP Team Design)

Our third preliminary design consideration was simply utilizing last year's MQP team's design [26]. As shown in Figure 13, their design includes three flow channels that will lead to a scaffold, so cells will invade the scaffold and empty into a chamber. Using a microscope, images of the leftover cells were taken in the three individual chambers. Three outlet flow channels were also included to expel any excess medium that was accumulated in the cell imaging chambers. A limitation to this design is the extra step of having to seed cells to their scaffold prior to placing it into their housing unit.

Our final preliminary design (Figure 14) depicts the concepts and components of the overall system design that we proposed. The components of the system design include flow channels, structural supports (chambers), scaffolds, membranes, and cells. The final design has three parallel extended individual flow channels with an inlet for the flow of cell culture medium and a separate inlet for adding cells. There are three individual chambers after the cell inlet to hold a membrane to filter any larger aggregates. A channel leads from the membrane to the chamber that holds a scaffold. This design allows for three scaffolds to be used simultaneously.

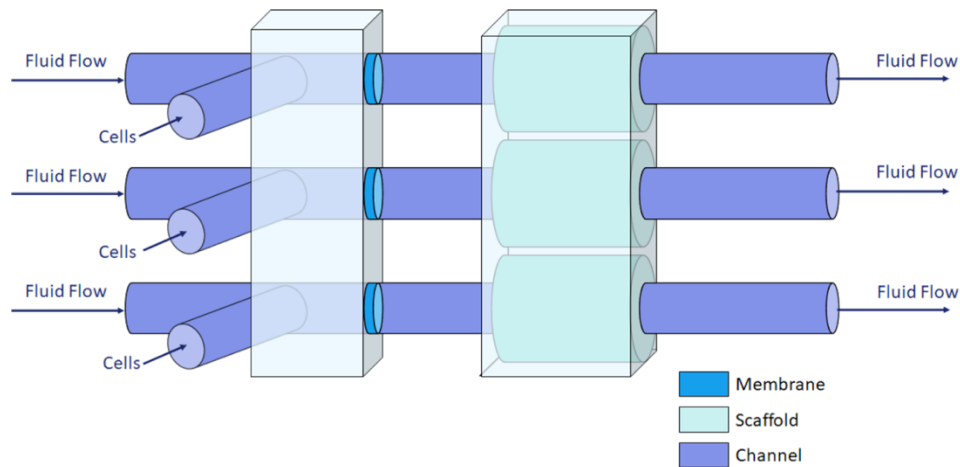


Figure 14: Conceptual Design of Bioreactor System

With understanding the different components and limitations to the preliminary designs, the team was able to create a decision matrix as show in Table 15 above comparing the three preliminary design considerations and our team design concept to a baseline. The baseline that the designs are being compared to is a Transwell migration assay with a patient's primary cells. This was chosen as a comparison because it is a standard practice for measuring invasion *in vitro* but considering it using a patient's primary cells making it more of a clinical application. After completing the decision matrix, our conceptual design is the most suitable design that will meet the requirements and objectives.

Table 15: Decision Matrix with Preliminary Designs

Requirement	Weight	Baseline	Two-Chamber	Previous MQP Team Design	4 Channel Flow Bioreactor	Our Team Design Concept
Ability to measure cell invasion	4	0	0	1	1	1
Imageability of scaffold and cells	1	0	0	-1	1	1
Use in a clinical setting	0	0	0	0	0	0
Incorporates fluid flow	3	0	1	1	1	1
Ease of assembly	2	0	-1	1	-1	1
RANK SCORE			1	8	6	10

4.3 Developing Image Analysis Methodology

It was important for the team to develop a way to easily measure cell counts and distance within the scaffold without having to take the device apart after each trial. There were three main image processing goals for developing an image analysis program:

- 1) Be able to measure distance, in μm , between cells on a scaffold in two dimensions.
- 2) Be able to quantify the number of cells present within the scaffold images captured in two dimensions.
- 3) Be able to create a z-stack of images so that cells can be analyzed, in accordance with goals one and two, in three dimensions.

The team designed a combination of image analysis models based on a MATLAB® (MathWorks) program that was developed by the previous MQP team (Appendix F) and the open-source program, CellProfiler™, developed out of the Broad Institute of MIT and Harvard (Appendix G). MATLAB® was developed for the analysis of design systems with the capabilities of data analysis, graphics, algorithm development, app building, and more [58]. CellProfiler™ is an open-source image analysis software allowing for the identification, measurements, and analysis of cell-based images [59,60] This specific combination was chosen because each program has different strengths that help the team accomplish the three goals listed above.

4.3.1 Image Analysis Method: MATLAB®

A custom graphical user interface (GUI) was developed by the previous MQP team that incorporates cell counting, invasion distance, and three dimensionality into one program. However, its strength was in calibrating distance, and three dimensionality. It displays a control panel that shows two main functions: Image processing options and distance measurement options, as shown in Figure 15.

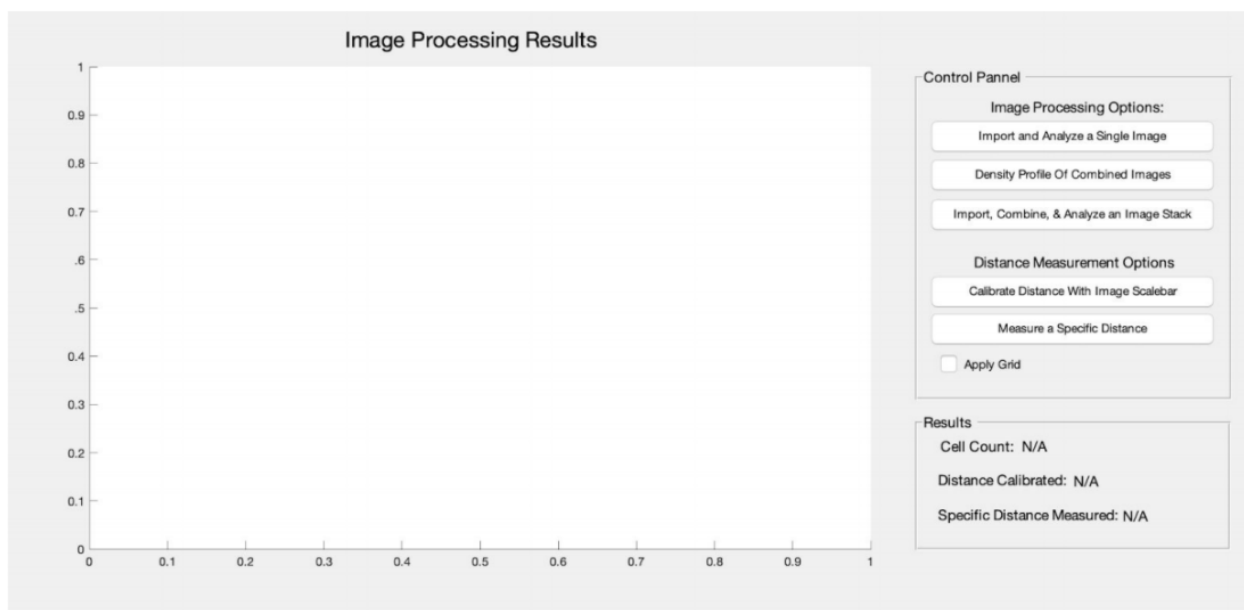


Figure 15: The User Interface of the MATLAB® Program (Developed by Previous MQP Team for Cell Counting and Invasion Distances)

The first function, “Image Processing,” allows for the analysis of a singular image as well as an image stack from scaffold slices in the z-plane. An image can be selected from any file on a

computer and imported into the program. From there, an automatic cell count will take place and the final number will appear under the “results” tab below.

If the image has a scale bar, the user can manually enter the length, in μm , by clicking on one end of the scale bar, dragging the mouse to the other end of the scale bar, and double clicking. Then, the user can type in the value, as shown in Figure 16. The “Distance Measurement” also allows the user to measure the distance between two cells. The distance will appear under the “results” tab as a value in pixels per scale bar distance.

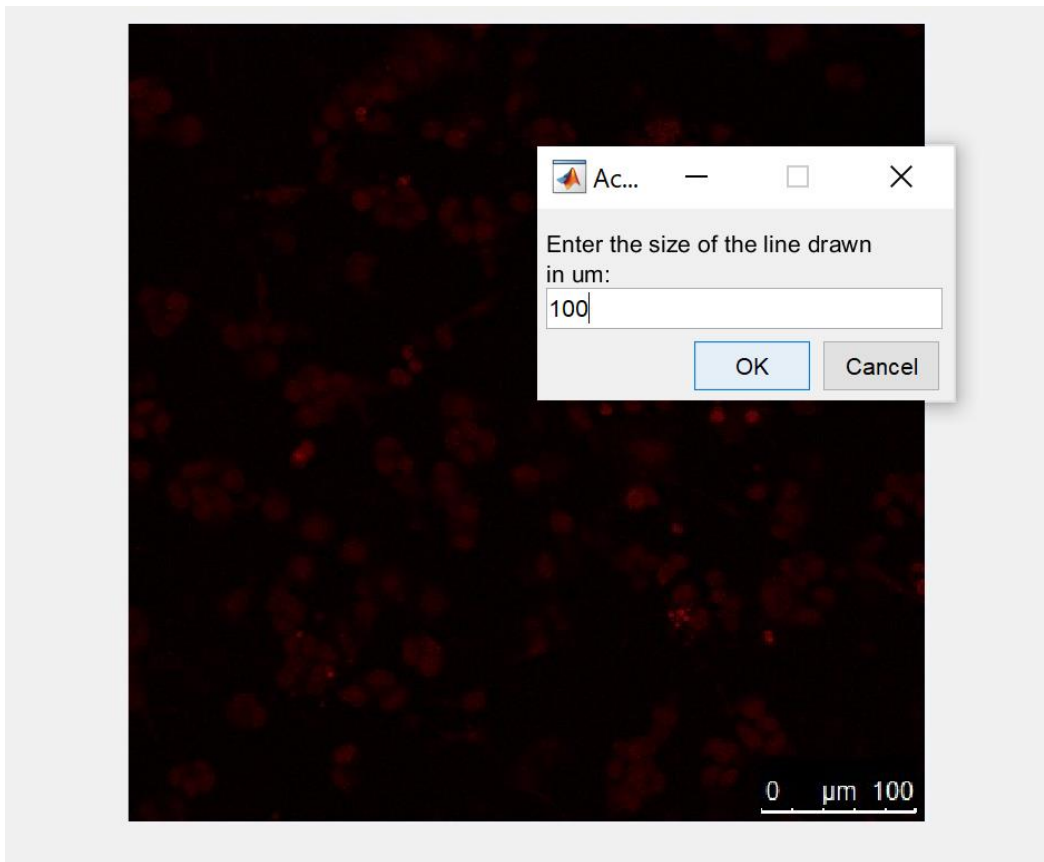


Figure 16: Popup Window that Allows User to Enter Specified Distance of Scale Bar (in μm)

After the distance is calibrated as 100 pixels per 100 μm , the user is then able to measure any distance desirable. In the control panel, the user clicks on the “measure a specific distance” button, single clicks on the starting point, and double clicks on the ending point. For example, Figure 17 shows a reference line across the image measuring from one cell to another. The distance is specified as 287 μm .

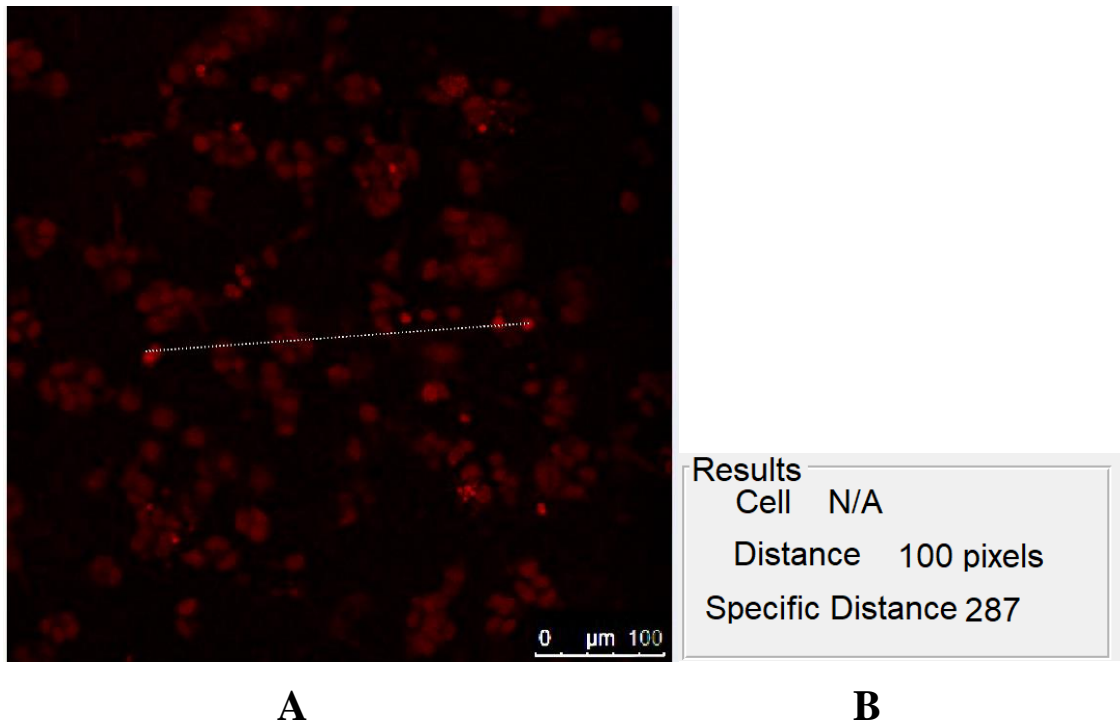


Figure 17: (A) The reference line that shows the visual distance between point one and two on a Sample Image of Panc-1 cells. (B) The results panel displaying the specific distance of the line, in μm

The second strength of the program was accounting for three dimensionality when analyzing multiple images from 3D image stacks (z-plane). This method was accomplished through the “Density Profile of Combined Images” function within the control panel. The density profile allows the user to import a folder of images, manually selected, and the program combines them together in an overlap display, as shown in Figure 18.

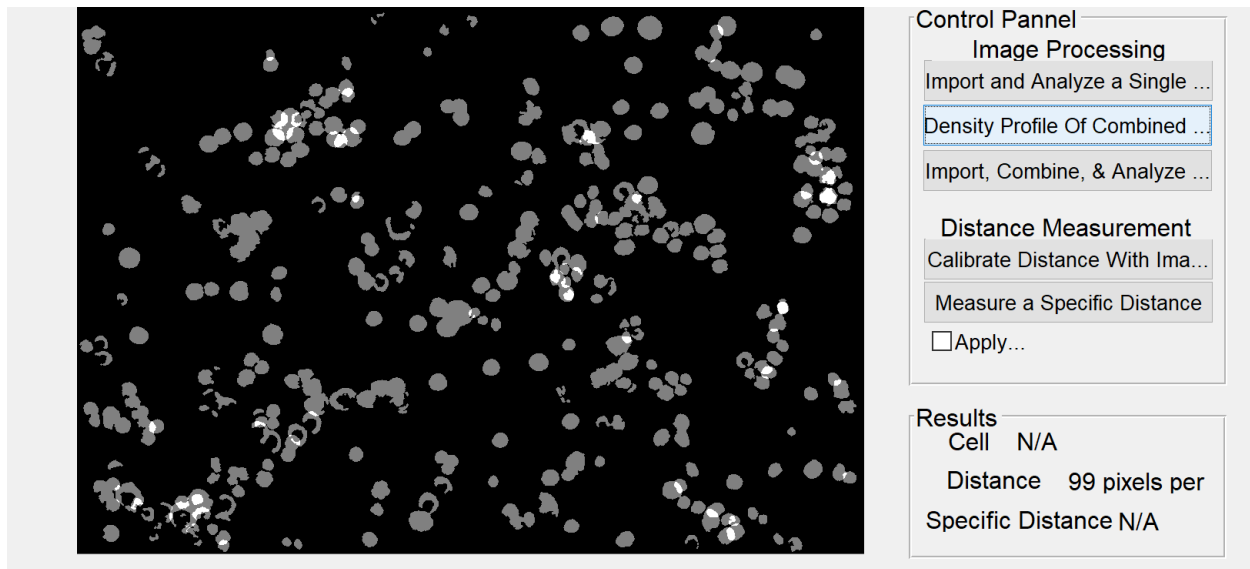


Figure 18: Sample Panc-1 cell Image output and results from using the density profile of combined images function [26]

The overlapped cells are the ones shown in grey. This is representative of how many cells are present throughout the thickness of the scaffold slices and helps to differentiate new cells, the ones in white, from the ones that have already been counted. It is also helpful in determining the thickness of each slice (i.e., distance between slices) during image acquisition. Once this information is processed, the user could use this in determining cellular invasion into the scaffold. The main limitation of the MATLAB® program is cell counting, as shown in Figure 19 which is why the team looked to another program in order to achieve a better assessment of cell count per image or stack.

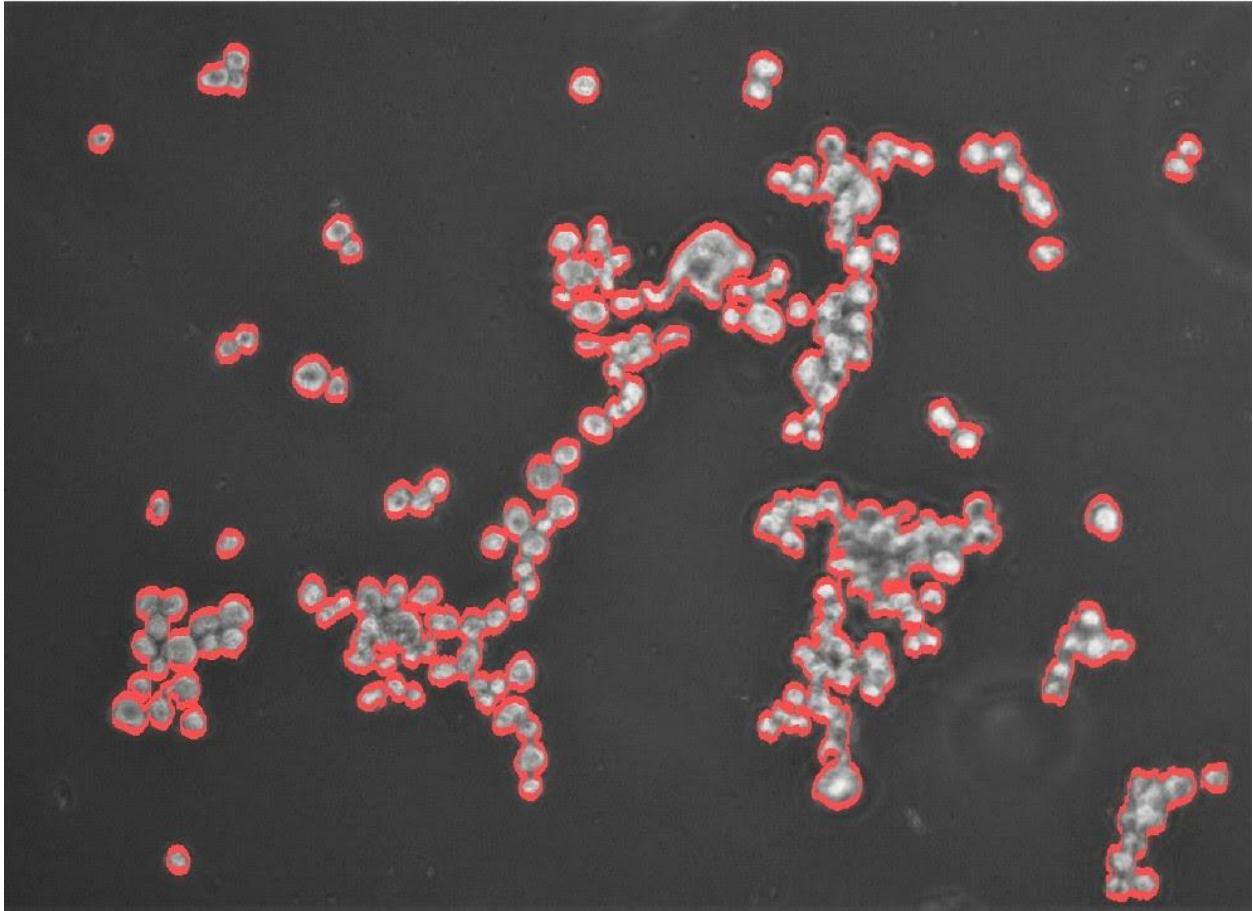


Figure 19: MATLAB® Portrayal of Clustered Cell Count on Sample Image of Panc-1 cells

4.3.2 Image Analysis Method: CellProfiler™

A pipeline was developed by the team to solve the cell count discrepancy presented by the previous MATLAB® program. Since cell count was the team's main focus, the pipeline was kept simple. The program was created by employing a series of image processing and analysis functions built into CellProfiler™. After the pipeline is finalized, an image or multiple images can be added, as shown in Figure 20.

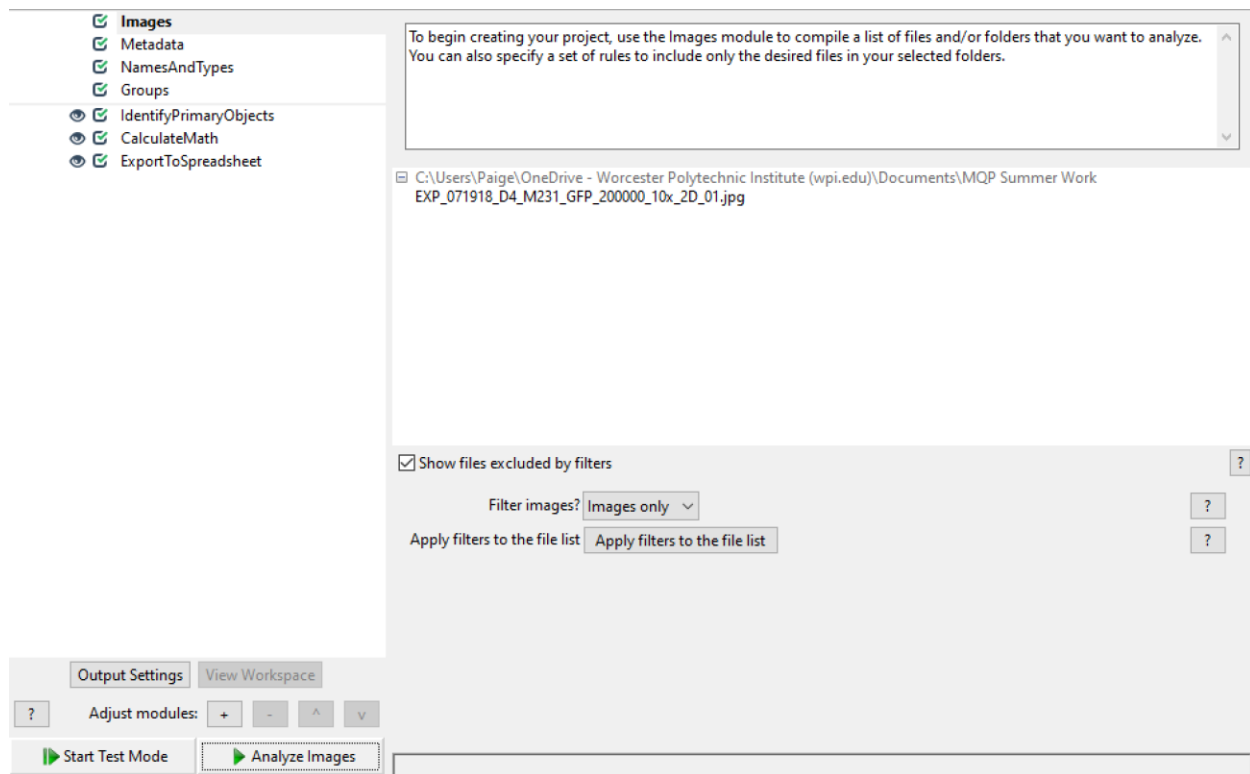


Figure 20: Cell Profiler Main Screen Displaying Pipeline (left) and Sample Imported Image (right)

The user then clicks the “Analyze Images” button, and the program goes through the pipeline, following these steps:

1. **Images:** The user imports the specified images to be analyzed individually by dragging the file or folder into the display window.
2. **Metadata:** The user can attach further data about the images into this module. The program will extract the data, such as the image type, height, width, or timepoints to name a few, from a specified location.
3. **NamesAndTypes:** The user is able to rename their images or define a relationship between multiple images. This module is where the user decides to test the data as a two dimensional or three-dimensional image set.
4. **Groups:** The user is able to further sub-divide the images into similar groups. The program will go on to analyze these images in their specific groupings.
5. **IdentifyPrimaryObjects:** This module allows the user to identify the object of interest. This could include organisms, nuclei, and cells. The image is converted to a grayscale image. The output displays a figure with three images attached. As shown in

Figure 21, the top left image shows the input. The top right image shows a colored version of the identified objects. Each individual object is labeled as an arbitrarily distinct color, to differentiate boundaries. Finally, the lower left image displays the original image with an overlay of dotted outlines of different colors. The three colors designate the likelihood of the object being counted. The green dots represent the objects that have passed all criteria added to the pipeline, the purple dots represent the objects that are not counted because they are outside the size range selected within the pipeline, and the yellow dots represent the objects that are not counted due to their positioning against the border of the image. These specifications can be manually altered to fit the criteria of the specific user [61].

6. **CalculateMath:** The user is able to perform simple arithmetic operations that allows for image-based or object-based calculations. This module can display the percentage of area occupied by the objects versus the background that further helps the user distinguish certain boundaries.
7. **ExportToSpreadsheet:** The user is able to export the data into a separate file, such as an excel spreadsheet or other programs [61].

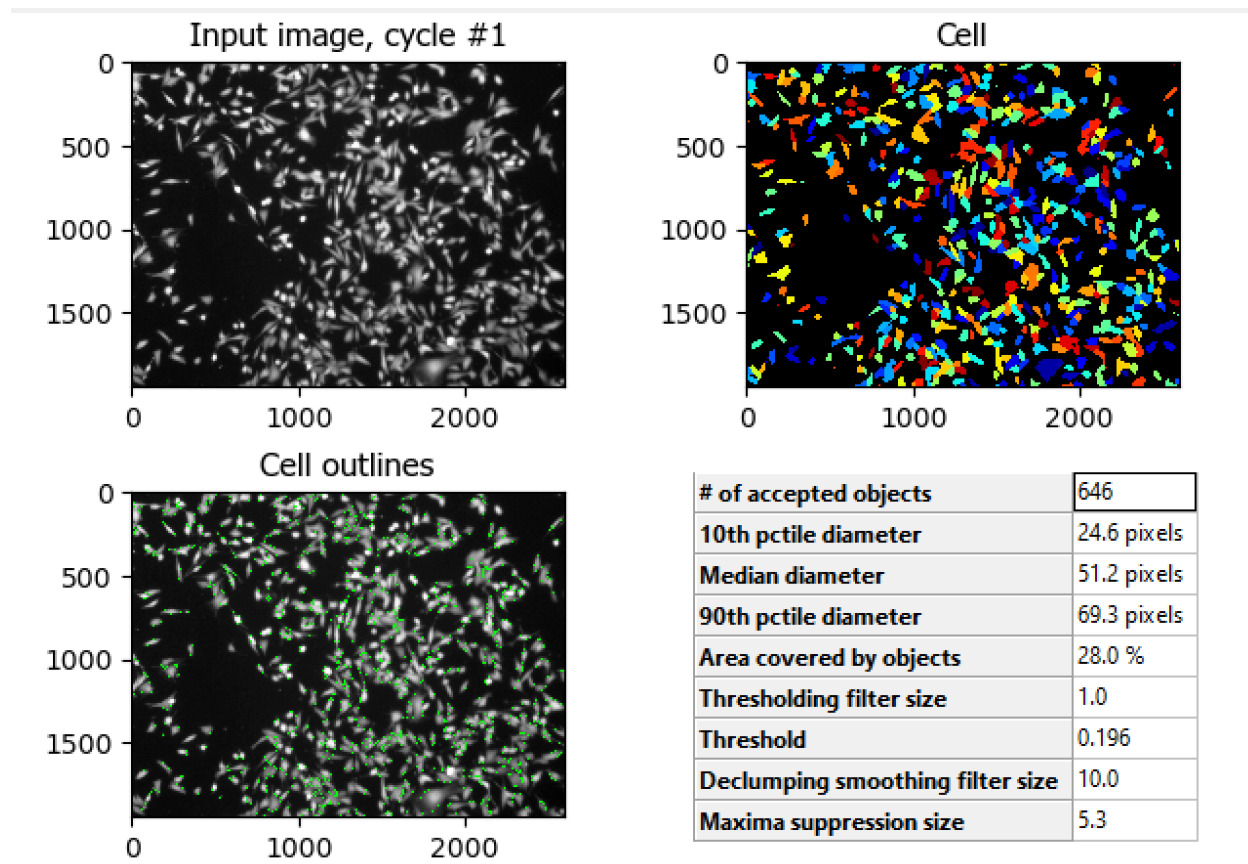


Figure 21: Raw Sample Image of MDA-MB-231 cell line Displayed (Top Left), Separation Boundaries of Identified Objects (Top Right), Object Outlines Based on Pipeline Criteria (Bottom Left)

The bottom right corner of the sample image, Figure 21, displays the “# of accepted objects,” in this case the cell count, 646. The user can manually choose to discard the objects outside of the given diameter range as well as discard objects that are in contact with the border. This feature is useful if there is an image with background noise or inconsistent staining. The window also displays various other criteria that was set up in the pipeline, such as the “Area covered by objects” equaling 28%.

4.4 Scaffold Testing

Once our scaffold and cross-linking agent were chosen the team developed a process for formulation and testing of the hydrogel based on the criteria outlined in Section 3.4. Our main concerns were surrounding sterility, cell viability and imaging. We needed to determine the best

ways to form the scaffolds, ensure they could withstand flow, have the desired porosity as well as the ability for metastatic cancer cells to be seeded on and invade the scaffold. The remainder of this section details the protocols the team developed for each of these areas.

4.4.1 Requirements for Scaffolding

The requirements for designing a scaffold include 1) biocompatibility, 2) biodegradability, 3) mechanical integrity, and 4) scaffold architecture, as shown in Table 16, the Needs Analysis chart for Scaffold Criteria. First, a scaffold for tissue engineering must be biocompatible. Cells must be able to adhere to the surface, successfully migrate through the scaffold, and eventually begin to proliferate. Second, the scaffold for this project must be relatively acceptable and low cost to fit within our time and budget constraints. Third, the scaffold must have the necessary mechanical properties for its intended application. This includes materials that need to be highly flexible or stable. Finally, the most important characteristic is that the scaffold must have the necessary architecture. Scaffolds must have an interconnected pore structure and high porosity. This will ensure successful cell penetration into the scaffold while allowing for a sufficient amount of nutrients to flow into the extracellular matrix formed from these cells [27].

Table 16: Needs Analysis for Scaffold Criteria

	Accessibility	Cost	Biocompatibility	Moldability
Accessibility		0	1	0
Cost	1		1	0
Biocompatibility	0	0		0
Moldability	1	1	1	
Total	2	1	3	0

4.4.2 Scaffold Base Material Considerations

Scaffold Material 1: Gelatin

Gelatin is a biocompatible and non-immunogenic natural polymer that has been used in a variety of both culinary and scientific measures. It is a protein created by the denaturalization of collagen, usually bovine skin or porcine skin and found in either a random coil or helical states [62]. When the temperature goes beyond 35°C, Gelatin is found in liquid form. If the temperature decreases below 35°C, then Gelatin will start to form interchained hydrogen bonds. Chemical crosslinkers can change the viscosity and gelling properties of Gelatin. It displays a clear color, is hydrophilic, and is a very flexible material, which makes for a good scaffold. The material is further subcategorized into Gelatin Type A and Gelatin Type B. Type A is the result of an acid hydrolysis method of culturing Gelatin. Type B is obtained from a basic hydrolysis method that yields Gelatin [62]. Gelatin can be mixed with a variety of crosslinkers, such as Glutaraldehyde, Carbodiimide, and Genipin. The stiffness is easily altered by changing the concentrations of Gelatin and its crosslinker. This technique allows the user to specify the material to its own specifications. However, Gelatin can easily be transformed into a hydrogel by crosslinking the material with water at a concentration around 2% weight per volume [63]. Gelatin powder can be purchased at a price range of \$20.00-\$40.00 per 100 grams [64]. The team has the ability to access Gelatin, type A and type B as they are both relatively cost-effective materials.

Scaffold Material 2: Alginate

Alginate is a nontoxic biomaterial that is derived from brown algae and used in a variety of biomedical applications, such as wound healing, drug delivery, and hydrogel formation [65]. There are over 200 different types of alginates that vary in molecular weight, ranging between 32,000 and 400,000 g/mol. Alginate is a viscous material that increases viscosity as the pH of a solution decreases. In recent studies, Alginate is being used as a model system for cell culture studies. This material is easily modified and mixes well with calcium-based solutions. Calcium is needed due to its ability to either be bonded ionically, covalently, or thermally [65]. The price ranges from \$49.70-\$129.00 per 100 grams [66].

Scaffold Material 3: Native Type I Collagen

Collagen is a fibrillar protein that can be found in skin, blood vessels, and other connective tissues [67]. Type I Collagen controls the structural composition of many of these tissues. Native Type I Collagen is used in many engineered scaffold models because of its ability to mimic the *in vivo* tumor microenvironment. This ability is partly due to Collagen comprising 25% of the total protein in the extracellular matrix [68]. There are four main types of Collagen: Type I, Type II, Type III, and Type IV. Type I, as stated above, is a protein found in many connective tissues. Type II Collagen is a protein found in cartilage and bone. Type III Collagen is a fibrillar collagen that is secreted by fibroblasts and mesenchymal cells [69]. Finally, Type IV Collagen is found in the basement membrane that lines epithelial and endothelial cells, separating various tissues [70]. Type I collagen is used often in academia, laboratory, and industry practices for 3D cell culture models. However, it is very costly, ranging from \$220.00-\$243.00 for 10 mL [71].

4.4.3 Crosslinkers

Crosslinker 1: Glutaraldehyde

Based on the suggestion of the previous MQP team, our team decided to look into Glutaraldehyde as a crosslinking agent. Glutaraldehyde is a clear liquid used in a variety of different applications, some including disinfectant for surgical equipment, crosslinking agent, antimicrobial for water-treatment systems, preservative in cosmetics, and more [72]. Glutaraldehyde is also widely known in the context of crosslinking Gelatin. The gelatin times vary based on the concentration of the polymer and crosslinker. A concentration of 5% Gelatin and 1% Glutaraldehyde will usually gel within the first ten minutes [73]. Glutaraldehyde is successful as a crosslinking agent due to its quick gelation rates. However, the material can be toxic at higher concentrations and therefore could cause problems when working with cells. A 25 mL bottle of Glutaraldehyde at 50 wt. % in H₂O is roughly \$45.00 [74].

Crosslinker 2: Calcium Chloride

Calcium Chloride (CaCl₂) is a very successful crosslinker of Alginate. It works to ionically crosslink the Alginate at increased temperatures. Along with increased temperatures, higher concentrations of CaCl₂, lead to rapid gelation rates [75]. This mixture of Alginate and the crosslinker creates a clear colored gel, allowing for better image capture and cell work. The team

had access to this crosslinking agent through the MQP workspace at WPI. Lab grade CaCl₂ powder is very cheap to purchase. A bottle containing 500 grams of CaCl₂ powder is roughly \$11.00 [76].

4.5 Membrane Considerations

A membrane is utilized within our design in order to accommodate future application of this device in a clinical setting. One of the team’s major goals was that a technician should be able to utilize a raw sample from a patient’s biopsy and place the tissue into the bioreactor in order for a clinician to interpret the results and make inferences pertaining to the likelihood of a patient’s cancer to migrate, invade, and metastasize. However, a raw sample may contain undesirable tissues in addition to the cancer cells. A membrane can be used to filter out these undesirable materials.

4.5.1 Objectives for Membrane within the CCH Unit

The membrane should ensure the perfusion of only cancer cells, but not obstruct the fluid flow or cell migration. These functions and means are outlined in Table 17.

Table 17: Membrane Functional Requirements and Means

Objective	Functions	Means
Undesirable raw materials from a patient biopsy should be filtered out	Membrane will allow for only cancer cells to perfuse into the scaffold	Membrane will have a pore size comparable to that of the cancer cells
	Membrane will not hinder fluid flow or cell diffusion	Membrane will have a high pore density
		Membrane will be thin to not significantly disrupt the path of cell migration

In order to achieve the functional requirements, design criteria had to be determined. The first functional requirement concerned allowing for the flow of cancer cells through the membrane. This is affected by the pore size, which should accommodate the cell diameter. The second functional requirement concerned fluid flow, which is also affected by pore size, as well as pore

density and membrane thickness. This functional requirement also considered properties of cell diffusion, which is affected by the material properties of the membrane and whether or not these properties encourage cell adhesion to the membrane. The design criteria helped inform the decisions made concerning the material properties of the final membrane. The corresponding functional requirement and criteria are outlined in Table 18.

Table 18: Membrane Design Criteria

Functional Requirements	Design Criteria
Membrane will allow for only cancer cells to perfuse into the scaffold	The membrane should have a pore size similar to the cancer cell size, with a pore size no more than 10 μ m smaller than the average cancer cell size, which differs based on the cancer type.
Membrane will not hinder fluid flow or cell diffusion	The membrane should have a high pore density of 50,000 pore per square centimeter. The membrane should also have a thickness of 6 μ m so as not to significantly alter the cell migration. The membrane should be made of a material that does not encourage cell adhesion.

4.5.2 Material Considerations for Membrane Within the CCH Unit

The functional requirements of the membrane included allowing for only cancer cells to cross the membrane and not obstructing fluid flow or cell diffusion. Several different types of membranes that could meet the corresponding design requirements were researched. These included using polydimethylsiloxane (PDMS), polyester, and polycarbonate. In order to make a more informed decision on which material to use, the requirements for the membrane were ranked using a pairwise comparison, which is shown in Table 19.

Table 19: Pairwise Comparison for Membrane Requirements

	Accessibility	Cost	Fluid Flow	No Cell Adhesion
Accessibility		0	0	0
Cost	1		1	1
Fluid Flow	1	0		0.5
No Cell Adhesion	1	0	0.5	
Total	3	0	1.5	1.5

Beyond the functional requirements of allowing for fluid flow and cell adhesion, cost and accessibility were also taken into consideration. Accessibility in this case refers to the team’s ability to obtain or create the material with available tools. Accessibility ranked as the most important component, while fluid flow and cell adhesion followed, and then cost. Cost was considered least important due to all considered membranes not exceeding the team’s budget. The three materials considered for the membrane were compared in Table 20.

Table 20: Comparison of Membrane Materials

Consideration	PDMS	Polyester	Polycarbonate
Is the process accessible?	No	Yes	Yes
Is it cost-effective?	Yes	Yes	Yes
Does it allow for fluid flow?	Yes	Yes	Yes
Does it not encourage cell adhesion?	Yes	No	Yes

PDMS was eliminated as a consideration, due to the creation of a PDMS membrane requiring lithography to manufacture a custom aluminum mask that would require the use of tools not available to the team [77]. Polyester and polycarbonate were then compared and based on polyester’s tendency to encourage cell adhesion; polyester was eliminated. The team decided to use polycarbonate as the membrane material.

Research into commercially available polycarbonate membranes showed that membranes of this material are more widely available in pore sizes ranging from 0.01 μm to 10.0 μm . The median cell size of Panc-1 cells is approximately 24 μm [78]. This was a cause of concern, as the majority of the cells the team intended on using for testing were larger than the pore that they would have to fit through. Based on accessibility, the team then decided to purchase a pack of 100 polycarbonate membranes with a pore size of 14 μm , pore density of 50,000 pores per square centimeter, and thickness of 6 μm from Sterlitech for \$91.94. The membrane is shown in Figure 22 below.

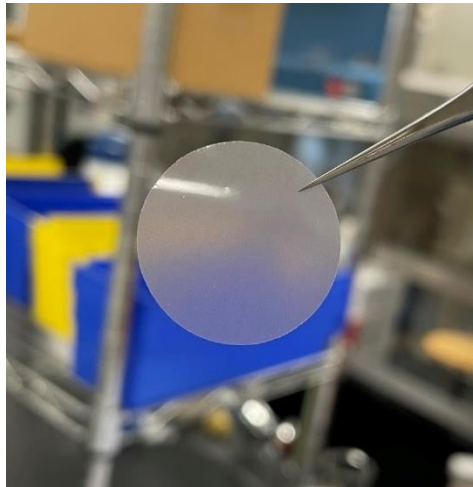


Figure 22: Polycarbonate Membrane Face On, Handled with Forceps

Chapter 5: Design Verification and Validation Testing

5.1 Design Viability Testing and Verification

The components of full system design, including the CCH unit and tubing connections needed to be both leakproof and have the ability to hold a scaffold under flow conditions. To ensure that the design met these requirements, testing was done with individual components and then as a full system setup.

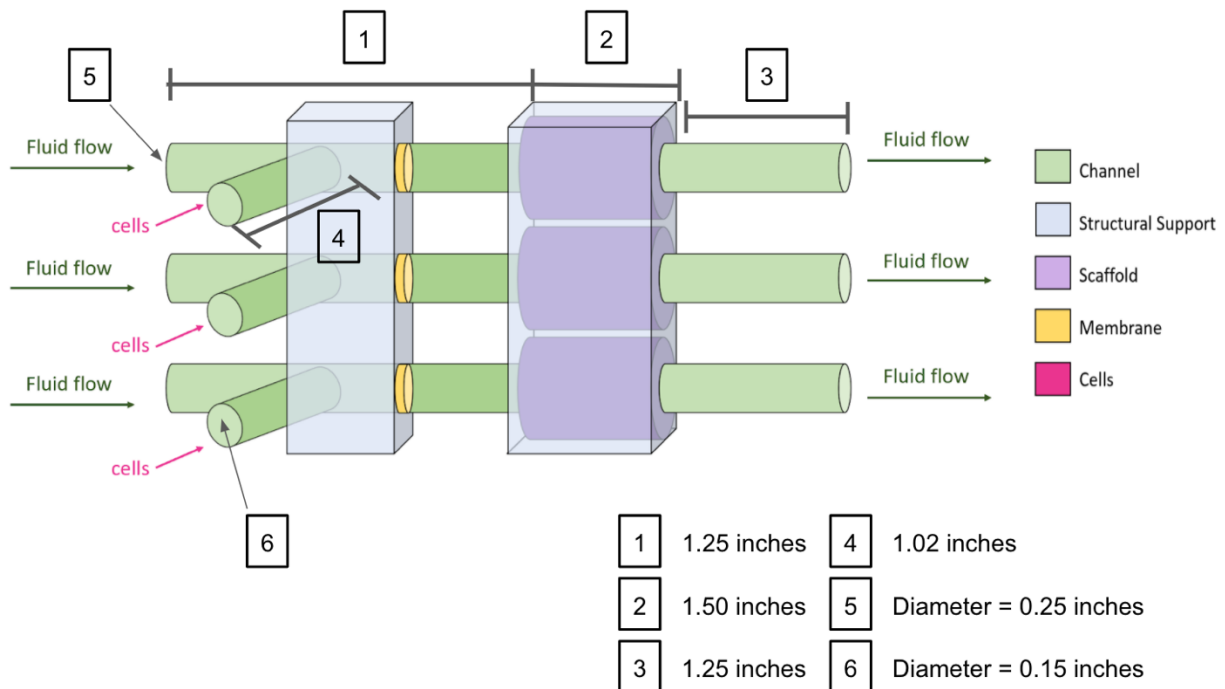


Figure 23: Conceptual Device Design with Dimensions (not to scale)

Following Figure 23 above, there are three different inlet medium flow channels (point 5) directing fluid flow through the system using three different syringes attached to a syringe pump. Cells will be injected through another inlet channel (point 6) that will connect with the initial inlet medium flow channel. Cells will then travel through the membrane (yellow), and eventually migrate and invade the scaffold (purple). Three outlet flow channels (point 3) will be used to collect on excess medium or cells that travel through the entire scaffold. The overall system includes concepts of both cell migration from membrane to the scaffold and cell invasion into the scaffold. The CCH unit was 3D printed and the iterations of earlier designs are shown in Appendices D and E.

5.1.1 CCH Unit and Tubing Leakage Testing

The CCH unit was filled with room temperature water to test for any leaks in the unit that could have formed as a result of any manufacturing defects. The room temperature water was dyed blue to aid in visualizing any potential leaks in the unit. The CCH unit filled with the blue dyed water was then placed onto a white paper towel for 24 hours. If any signs of leakage were identified on the paper towel, then the test would fail. The same testing procedure was carried out with the connections between the tubing connected to the CCH unit. These connections were also filled with room temperature water that was dyed blue to aid in visualizing any potential leaks in the connectors. This setup was also placed on a white paper towel for 24 hours. If any signs of leakage were visible on the paper towel, then this test would fail.

If the any of the leakage tests do fail, visual observations were made to identify any visible cracks in the unit or tubing that may lead to leakages and were appropriately fixed. If there are no signs of leaking within the 24 hours, then the device would formally pass the leakage test.

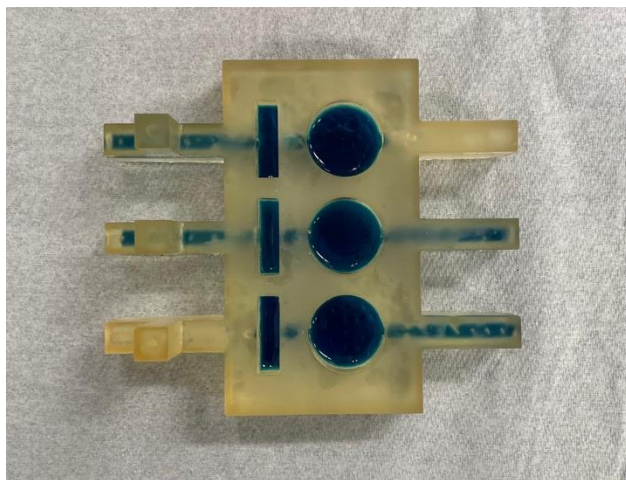


Figure 24: Setup of Individual CCH Unit Leakage Test

5.1.2 CCH Unit Material Cytotoxicity Testing

The CCH unit is fabricated and printed out of a high-temperature (HT) resin material that will be autoclaved for sterility. The purpose of this testing method is to determine if the device material HT resin is cytotoxic. One hundred thousand cells are seeded to a number of well plates in a multi well plate. Within the multi-well plate, a third of the wells are seeded with the cells and contain a small piece of the autoclaved HT resin material. Then, a third of the wells will be seeded

with just the cells, acting as the control. Finally, dimethyl sulfoxide (DMSO) is known to be toxic to cells when the concentration is greater than 1% [79]. So, the last third of the wells will be seeded with the cells and contain a small piece of autoclaved HT resin soaked in 1% DMSO, acting as the negative control. The multi-well plate with the cells were left in the incubator at 37°C, and imaged at 24 hours, then again at 48 hours. The cells with the autoclaved HT resin material were compared to both the control (cells with no material) and the negative control (cells with DMSO soaked material). If the cells in the well plate with the autoclaved HT resin material behaved similarly to the cells in the control well plates, then the material would be considered non-toxic. The cells in the well plate with the autoclaved HT resin material would also be compared to the negative control well plates. If the cells in the well plates had the opposite effects of those in the negative control well plates, then the material would also be confirmed as non-toxic to the cells.

5.1.3 Full System Flow Verification Testing

In addition to checking for leakage, the system was tested at a set flow rate to verify that it is able to deliver consistent amounts of volume between each chamber. The syringe pump was a KD Scientific 220 Multi-Syringe Infusion Pump, capable of holding three syringes simultaneously and programmable to specific rates. The pump was set up to deliver 10 mL of blue-dyed room temperature water at 5 mL/minute. First, we attached 0.25-inch tubing securely to both the inlet and outlet channels, along with a syringe to the tubing at the inlet channel to deliver the dyed water through the device. A paper towel was placed under the full system again to identify any potential leakages in the CCH, tubing, or syringe. Conical tubes were also placed at the end of the outlet flow channels to collect and catch the water that outflowed. The flow was tested with both empty scaffold chambers and blocked scaffold chambers, a sample setup is shown in Figure 25 below. The blocked scaffold chambers were filled with taped together tissues to perfectly fit the chamber. The 3 syringe-syringe pump system was run for two minutes at the set flow rate of 5 mL/minute with both situations for each scaffold chamber. After tests were run, the results from each chamber were compared with the amount of outflow collected in each of the conical tubes. If the conical tubes accumulate the same amount of water without any leakage in the system after each trial, then the device system flow set up was verified. If there are any signs of leakage or inconsistent amounts

of fluid accumulated in the conical tubes between each chamber, then the device fluid flow system would then be considered inconsistent.

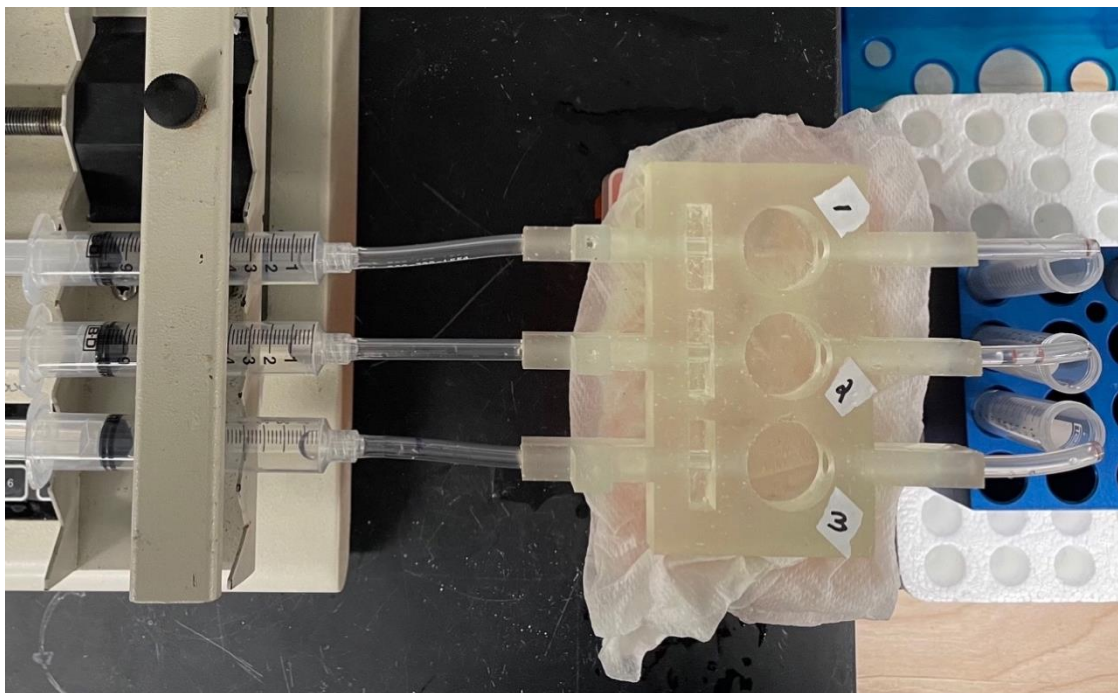


Figure 25: Empty Scaffold Chamber Flow Testing Setup Including Syringe Pump, Three Syringes, Tubing, CCH Unit, and 15mL Conical Tubes

5.2 Verifying Cell Quantification Method

After reading the future work report section of the previous MQP team, our team realized that MATLAB® would not be sufficient in accurately extracting cell counts from images. The CellProfiler™ pipeline was established and seemed promising in its capabilities of designating and counting objects. Images were processed through the program and compared to the average hand count of the team to determine the accuracy of CellProfiler™ performance.

Four sample images were given to the team in order to verify our cell quantification programs. The images were taken with a 10x objective. A larger sample set of images were unable to be obtained due to unforeseen limitations in the sterile scaffold procedure that limited our access to cell images. The images were sent out to the team members and counted individually. The values were then averaged together to be used as the “accepted value” in Equation 4. The images were then run through the CellProfiler™ pipeline and the cell counts were obtained. For further

comparison, the images were also run through the MATLAB® program and cell counts were recorded.

The percent error for the CellProfiler™ program and the MATLAB® program were calculated using Equation 4 and compared against the accepted percent error threshold range of ten percent [80]. The “experimental value” is the cell count recorded by the program, and the “accepted value” is the average hand count of the team.

$$\text{Percent Error} = \frac{|\text{Accepted Value} - \text{Experimental Value}|}{\text{Accepted Value}} * 100$$

Accepted Value = Average of the Team’s Hand Count of Cells

Experimental Value = Program Cell Count

Equation 4: Percent Error Equation

5.3 Hydrogel Characterization Methods

After initial formulations of the various scaffold materials, the team decided on a base material to generate the scaffolds for our project. The team then had to formulate an efficient process to create these hydrogels and analyze their properties based on the specifications we set in Section 4.4. These steps included the most efficient process for hydrogel formation, and the ability of the scaffold to obtain a stiffness comparable to an *in vivo* tumor microenvironment.

5.3.1 Hydrogel Formation

Scaffold Material 1: Gelatin

Based upon a literature review and last year’s project group’s procedure, a protocol was formed for gelatin hydrogels (Appendix M). The gelatin was dissolved in Dulbecco’s phosphate-buffered saline (DPBS (-)) and stirred for one hour. The solution was then pipetted into a 12-well plate and specific percentages of Glutaraldehyde were mixed in to each well. The team explored various concentrations of Glutaraldehyde within the gelatin solutions, as shown in Table 21.

Table 21: Differing Glutaraldehyde Concentrations for Hydrogel Formation

Final Concentration Gelatin (Stock: 9% Gelatin)	Volume of 25 wt. % Glutaraldehyde Solution	Final Glutaraldehyde Concentration in Gelatin Solution
9.0%	0.01 mL	0.1%
9.0%	0.02 mL	0.2%
9.0%	0.04 mL	0.5%
9.0%	0.08 mL	1%
9.0%	0.12 mL	1.2%
9.0%	0.16 mL	1.8%

Scaffold Material 2: Alginate

Once the team discovered some challenges, further described in Section 6.3, a new approach was taken, based upon a literature review and consultation with the project advisor that would incorporate the second material, Alginate. To make these gelatin-alginate scaffolds, gelatin was dissolved in DPBS (-), alginate solution was added to the mixture, stirred, and heated at 60°C for one hour. The heat was then turned off and left to stir for another hour. The team explored different concentrations of CaCl₂ solution within the gelatin-alginate solutions, shown in Table 22.

Table 22: Differing CaCl₂ Concentrations for Hydrogel Formation

Final Concentration Gelatin (Stock: 9% Gelatin)	Final Concentration Alginate (Stock: 4% Alginate)	Final CaCl ₂ Concentration (Stock: 100 mM CaCl ₂)
8.6%	0.19%	42.86 mM
8.6%	0.19%	33 mM
8.6%	0.19%	31.03 mM
9.0%	0.0%	4.76 mM
9.0%	0.0%	0.0 mM

5.3.2 Rheological Testing

Rheological testing was used to characterize the stiffness of the scaffold. Determining the stiffness of the hydrogel scaffold was critical so that the team could develop a formulation that closely represents a stiffness value of the tumor microenvironment found in a high disease state. In pancreatic cancers, high disease states are characterized as those with a stiffness value greater

than 1,000Pa [81]. The rheometer used in this study was the MCR 302 WESP Rheometer from Anton Paar, as seen in Figure 26.



Figure 26: MCR 302 WESP Rheometer Used for Testing Hydrogel Stiffness Properties

A 25 mm flat geometry tool for parallel plate configuration was attached to the machine following the protocol in Appendix I. The gelatin-alginate gels were formed in a 12-well plate due to the similarity in diameter of the geometry tool. When it came time to test, the gels were removed from the well plate using tweezers and a small scoop to ensure that the hydrogels stayed intact. The hydrogel was then placed in the center of the peltier stage of the rheometer, and the gap distance was set to 5 mm, based on the height of the 2 mL hydrogel.

A frequency sweep from 0.1-1000 rad/s in oscillatory shear mode was performed a constant amplitude and at a 1% strain. This test allowed the team to determine the viscoelastic properties of different materials and samples; for example, the shear storage modulus (G') of each varying scaffold concentrations. The amplitude was kept constant, and the testing was performed at room temperature. Each test was approximately 7 minutes in length, and the machine was cleaned and

reset between each trial. Three independent frequency sweep tests were conducted on hydrogel samples of the same concentrations.

5.3.3 Cell Viability Testing

Cell seeding is the first step of cell attachment and the distribution of cells across a scaffold can be an indicator of biocompatibility [82]. The team created a cell seeding experiment, detailed in Appendix Q that would provide information on the biocompatibility of the scaffold which can be tested by seeing if the cells survive after being pipetted onto the scaffold material.

The first aspect of the cell viability testing for the scaffold, was to make scaffolds in a sterile environment for the cells to be seeded on. All work needed to take place in a biosafety cabinet with the user wearing proper personal protective equipment. Both the calcium chloride and alginate solutions needed to be sterilized using a vacuum filter with a pore size of 22 μm . Due to the viscosity of the gelatin solution, the vacuum filter was not an option. Based on discussion with Prof. Destin Heilman it was decided that autoclaving the gelatin powder was a viable option. The gelatin was placed in an autoclave safe container and autoclaved using the regular pressure settings and a temperature of 121°C. Once each material was sterilized the scaffolds were formed in the biosafety cabinet and plated for cell seeding. The scaffold formulations chosen for this test would those which best approximated the desired stiffness based off of the rheological data.

Once the scaffolds were plated and refrigerated for 24 hours, cells could be seeded on top of each scaffold. Panc-1 cells were used as a representative of a metastatic cell line that was easily accessible to the team. One hundred thousand cells were seeded onto each of the 6 scaffolds and the plate was kept in the incubator. To assess cell viability, 50 μL of Trypan Blue was added to each well. Trypan Blue enters cells with compromised membranes that are not viable, and stains them blue. When imaging, the stained (non-viable) cells appear distinctly darker than the viable cells and percent viability was calculated.

5.3.4 Diffusivity Testing

A glucose diffusion experiment was conducted to determine the feasibility and rate of diffusion through the scaffold. Aside-by-side Franz cell setup was used for this test, as shown in Figure 27. The setup included two 50 mL plastic containers with rubber stoppers, a glass capillary, rubber membrane, and clamp.

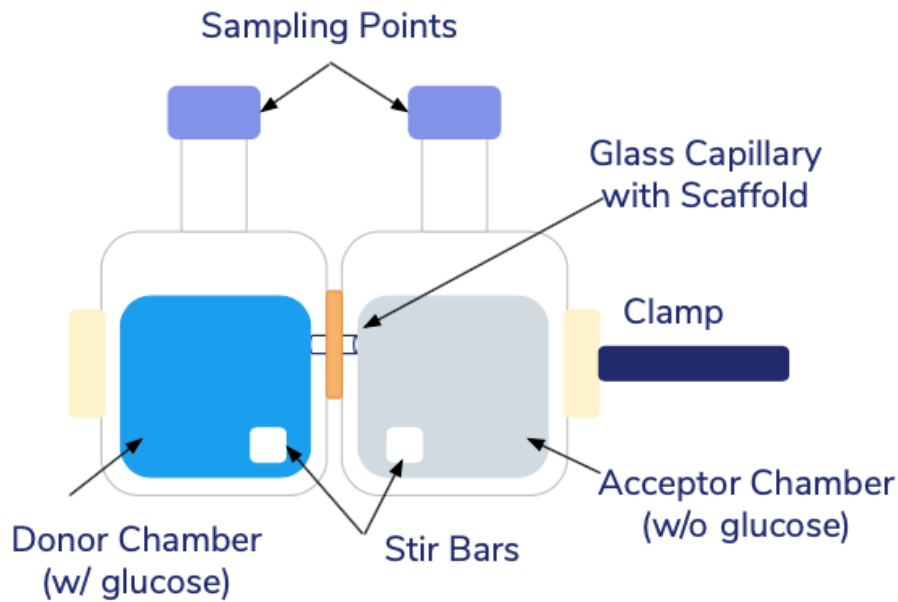


Figure 27: Glucose Diffusion through Scaffold Setup Schematic

The scaffold was loaded into the glass capillary which was then fitted through the rubber membrane and tightly secured between the two containers with a clamp. A glucose solution was made by combining 9 grams of Dextrose with 20 mL of DPBS+ (Dulbecco's Phosphate Buffered Saline) with heating and stirring. Later, blue dye was added to the glucose solution to act as a visual for diffusion between the chambers. A stir bar was placed in each container and 40 mL of DI water was loaded into each of the plastic chambers simultaneously so as not to create convective transport which could dislodge the scaffold from the glass capillary. For the donor chamber 400 μL of the glucose solution was added, and 400 μL of DI water added to the receptor chamber to equalize the chamber volumes. The setup was placed on a stir plate, set to a medium speed (Figure 28). Glucose readings were taken from each chamber over a span of 24 hours. For each sampling period, a 1 mL sample was extracted from each chamber using a syringe and mixed in a centrifuge tube with an equal amount of DPBS. Using glucose strips, the sample was read by a glucose meter (ContourNextEZ) and reported in mg/dL. This protocol was completed for three trials and is described in Appendix N.



Figure 28: Experimental Setup of Glucose Scaffold Diffusion Test on Stir Plate

5.4 Membrane Characterization Methods

The team devised three experimental protocols to assess the ability of the polycarbonate membrane to meet the predetermined functional requirements. These three experiments included (1) assessing the flow of water through the membrane, (2) assessing the flow of cell culture medium through the membrane, and (3) assessing the tendency of cells to adhere to the membrane.

5.4.1 Membrane Fluid Flow Testing

Both fluid flow experiments utilized the same apparatus of a funnel, two 0.5-inch tubes with length of 30cm, a tubing connector with internal diameter of 9.9mm, and 50mL graduated cylinder. A schematic of the apparatus is shown in Figure 29.

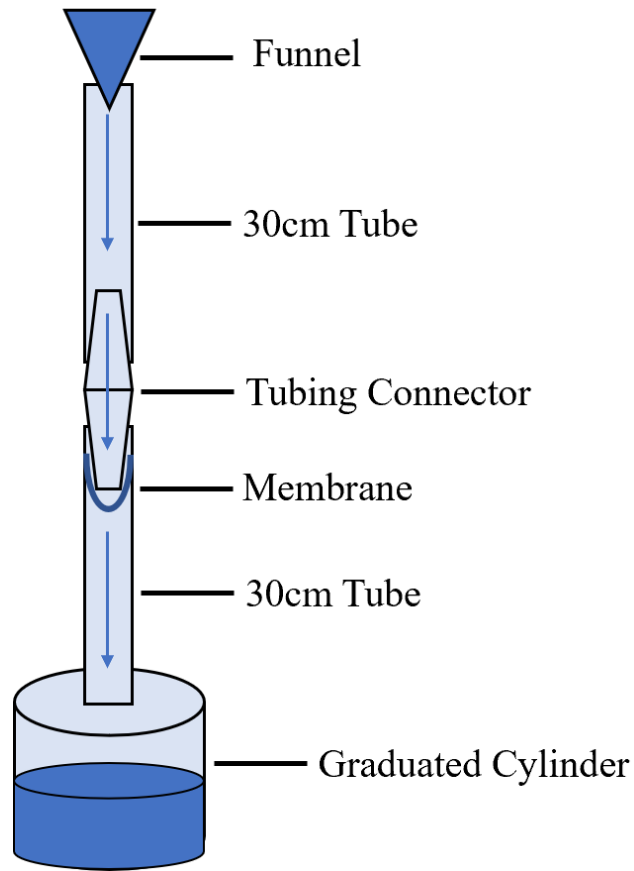


Figure 29: Experimental Setup for Fluid Flow Experiments

As shown in Figure 30, the membrane was clamped between the tubing connector and the internal wall of the bottom tube. This allowed for the fluid to flow through the membrane without dislodging the membrane or diverting the flow around the membrane.

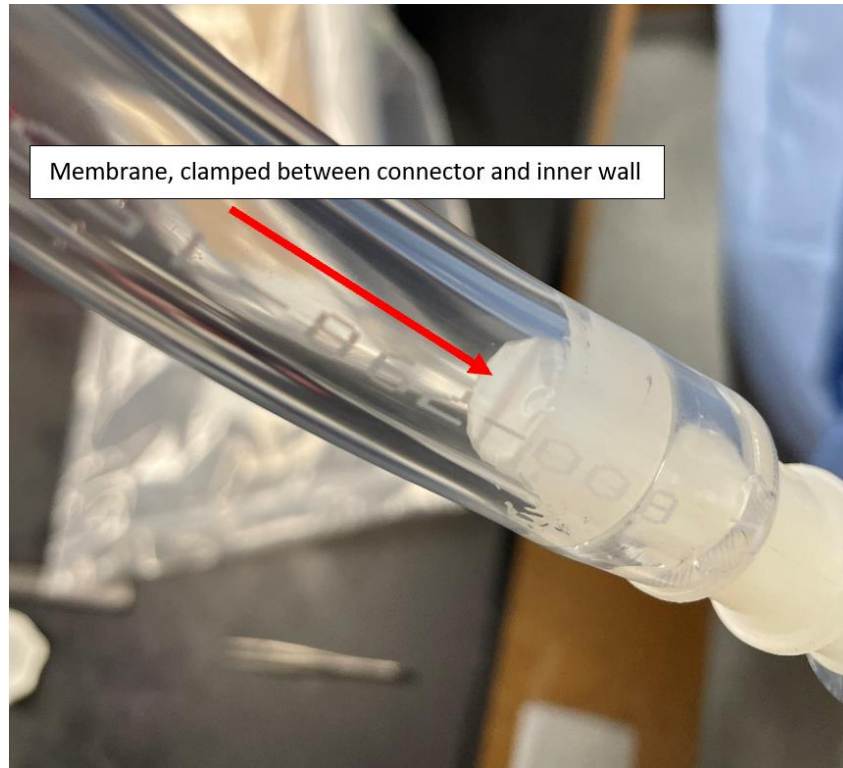


Figure 30: The Membrane Clamped by Tubing Connector

In the water flow experiment, a stopwatch was started as 50 mL of water was poured into the top of the setup and into the first tube. The water then flowed down the tube and into the tubing connector, where the membrane was clamped at the bottom. The water then flowed through the membrane and through the second tube, where it flowed into a collection reservoir. When all of the water had drained through the tubing, the stopwatch was stopped. The experiment was conducted with three different membranes and three different trials each. The experiment was also conducted without a membrane in three trials, which served as the control for the experiment.

In cell culture medium experiment, the same protocol as the water flow experiment was used, but with cell culture medium instead of water. This experiment was also conducted with three different membranes and three different trials each, as well as conducted without a membrane in three trials, which served as the control for the experiment.

5.4.2 Membrane Cell Adhesion Testing

In the cellular adhesion experiment, a separate apparatus was built. This apparatus is composed of 0.5-inch tubing, a tubing connector of an inner diameter of 9.9mm, and rubber stoppers. A photograph of the apparatus is shown in Figure 31.

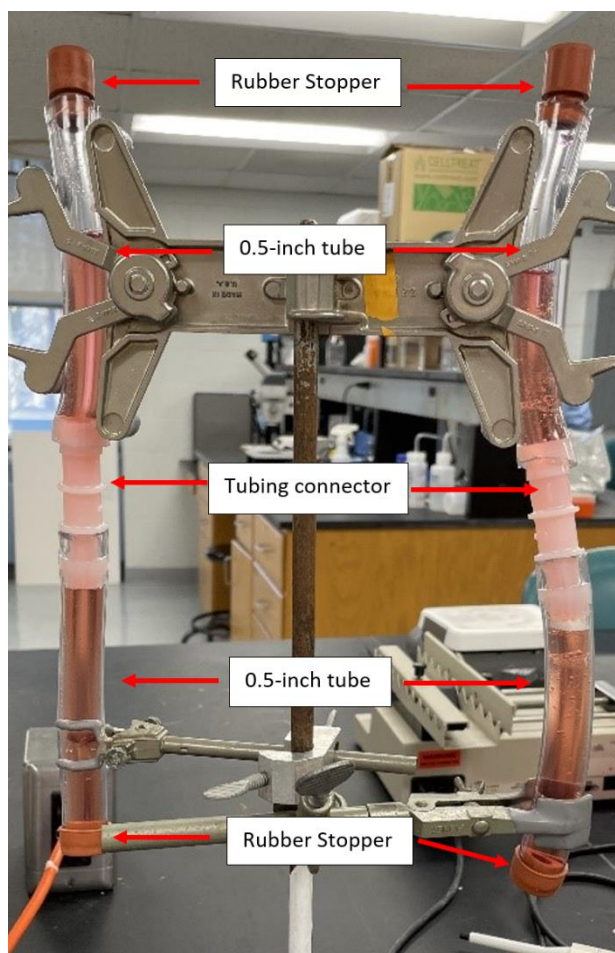


Figure 31: Apparatus Used in the Cellular Adhesion Experiment to Evaluate the Flow of Cells through the Membrane

In the cellular adhesion experiment, two trials were conducted using the two apparatuses shown. Each apparatus was loaded with cell culture medium. 3T3 cells from mouse embryonic fibroblasts were used in this experiment due to their accessibility and their diameter of $19\ \mu\text{m}$, which is similar to the $24\ \mu\text{m}$ diameter of Panc-1 cells [78]. Five hundred thousand 3T3 cells were injected into the top tubes of each of the apparatuses after they were loaded with the cell culture medium. The cells were then allowed 48 hours to flow down the top tube, through the membrane, and into the bottom tube. After 48 hours, the contents of the bottom tubes were emptied into a petri dish and analyzed under a Ziess Primovert inverted microscope with a 100X objective. The membrane was also removed from each apparatus and analyzed as well.

Chapter 6: Results and Discussion

6.1 Basic Design Viability Testing Results

6.1.1 CCH Unit and Tubing Leakage Testing

After performing the leakage test for the CCH unit individually, the test confirmed that there were no signs of leakage in or around the housing unit after 24 hours (Figure 32). The unit was then visually analyzed and there were also no signs of cracks in the flow channels or the individual chambers. After performing the leakage testing for the connections between the tubing and the CCH unit as described in Section 5.1.1, the results confirmed that there were also no signs of leakage with the connections after 24 hours. When visually analyzing the CCH unit individually and with the connections, no further changes needed to be made to prevent leakage.

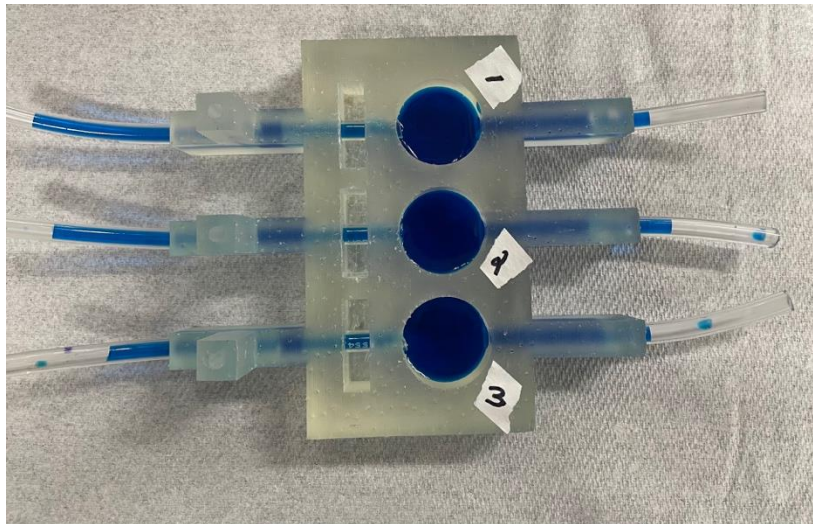


Figure 32: No Leakage Between Tubing Connections and CCH Unit

6.1.2 Full System Flow Verification Testing

The results from the flow verification tests did verify that no water (0 mL) was able to flow through the system with blocked scaffold chambers, and the output volumes between each of the scaffold chambers delivered inconsistent volumes in each of the conical tubes. After 10 mL of water was run through the system at 5 mL/minute, the left, middle, and right chambers all delivered different output volumes according to Table 23.

Table 23: Results of output flow volume between each empty scaffold chamber in the CCH unit (last row represents mean \pm standard deviation)

Scaffold Chamber	Left	Middle	Right
Test 1 (mL)	6.5	5.0	5.5
Test 2 (mL)	7.5	6.0	7.0
Test 3 (mL)	7.0	5.0	6.0
Mean (mL)	7.0 \pm 0.5 mL	5.3 \pm 0.58 mL	6.17 \pm 0.76 mL

Overall, these results do verify that fluid can flow directly through the CCH unit, but each scaffold chamber is unable to produce consistent results. For the full system to be used effectively in a clinical setting, the system setup must be able to deliver consistent results. Therefore, either design and/or system changes need to be made to confirm a viable system setup and CCH unit design.

6.2 Verifying Cell Quantification Methods

The results of the image analysis programs showed that CellProfiler™ was significantly more accurate in cell counts than MATLAB®. CellProfiler™ overestimated the quantity in each image compared to the average hand count of the team. The percent error was calculated for each image analyzed and displayed in Figure 33.

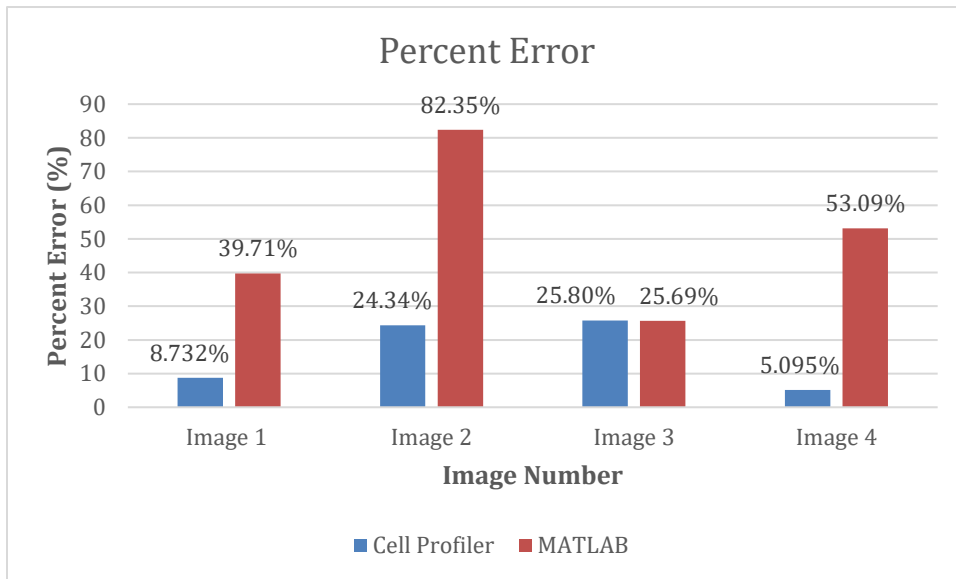
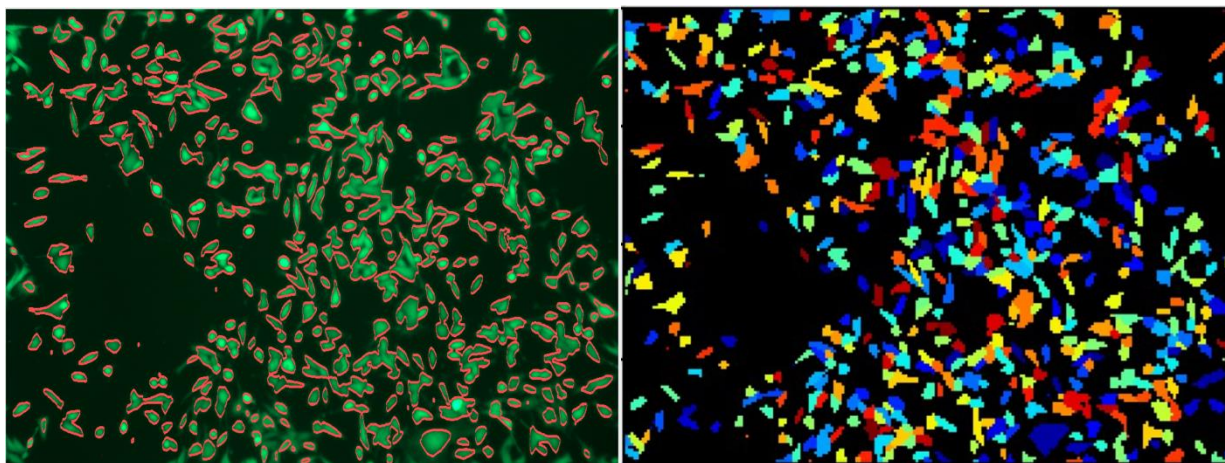


Figure 33: Percent Error Results for CellProfiler™ versus MATLAB® Cell Counts

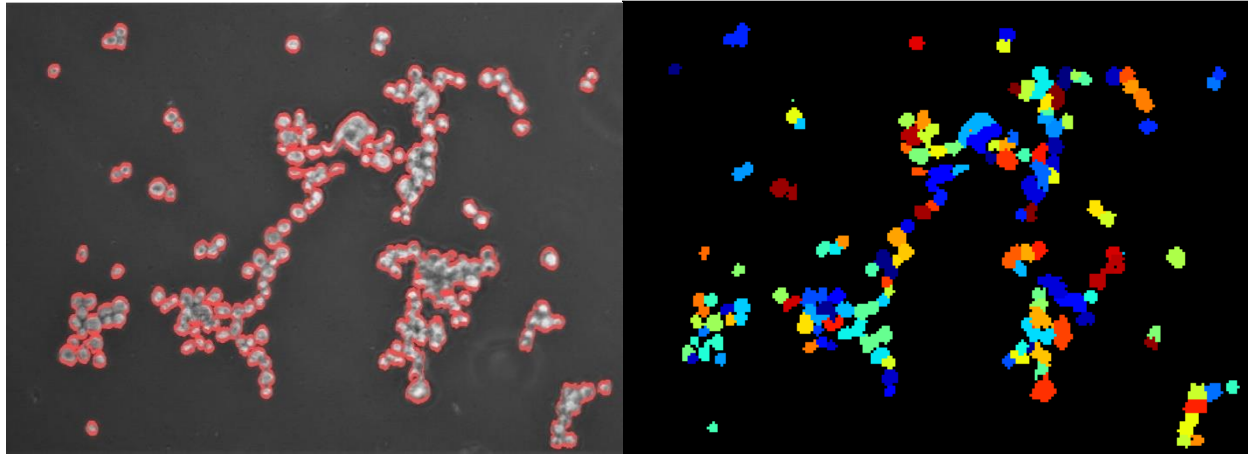
Based on the images tested, CellProfiler™ cell counts were close to, or below, the allowable ten percent error range. MATLAB® cell counts were well above this range, clearly showing that CellProfiler™ was a more reliable source. The MATLAB® program had a difficult time differentiating individual cells from a cluster. When comparing cell count to the average hand count of the team, or CellProfiler™, it was clear that the MATLAB® program lacked the ability to properly display the accurate cell count needed to prove its reliability. As shown in Figure 34, the MATLAB® program clustered most cells, unable to differentiate cell boundaries and counted a total of 290 cells. This was compared to the 523 cells that the CellProfiler™ pipeline counted and the hand count average of the team at 481 cells.



MATLAB® Cell Count: 290 cells
CellProfiler™ Cell Count: 523 cells
Hand Count Average: 481 cells

Figure 34: MATLAB® cell count of Image 1 (left) and CellProfiler™ cell count of Image 1 (right)

The CellProfiler™ program overestimates the number of cells in an image. This could be due to the user's ability to decide whether or not to count objects touching the border, or objects outside the specified size range. For the purpose of these experiments, all objects were counted which could potentially lead to a higher cell count than what was hand counted by the team. The CellProfiler™ analyzed image had a percent error of only 8.732%, lower than the accepted threshold range, whereas the MATLAB® analyzed image had a percent error of 39.71%.



MATLAB® Cell Count: 35 cells
CellProfiler™ Cell Count: 150 cells
Hand Count Average: 198 cells

Figure 35: MATLAB® cell count of Image 2 (left) and CellProfiler™ cell count of Image 2 (right)

A similar analysis can be done for Figure 35, where the cell count based on the MATLAB® program was 35 cells. This count compares to the CellProfiler™ count of 150 cells and an average hand count of 198 cells. The percent errors for these images are both above the given threshold range of ten percent. However, the CellProfiler™ analysis outweighs the MATLAB® program with a value of 24.24% compared to 82.35%. The CellProfiler™ program is more sufficient for counting cells in images with a high degree of cell-cell contact and overlap.

6.3 Hydrogel Characterization

6.3.1 Hydrogel Formation

Scaffold Material 1: Gelatin

The team conducted initial scaffold experiments with different concentrations of glutaraldehyde. After 9 grams of gelatin was heated in 100 mL DPBS for one hour, 2 mL was placed in each well of two 12-well plates. Then, different concentrations of glutaraldehyde were placed in each row of the well-plate and fully mixed with the solution using a pipette. The team decided to use the combination of 0.1%, 0.2%, 0.5%, 1.0%, 1.2%, and 1.8% of 25 wt% volume glutaraldehyde solution in the 9.0% gelatin formula. The images below depict the results of the

procedure above, further listed in Appendix M. As the concentration of glutaraldehyde increased, the color changed from a yellow to a brown and the stiffness increased. It was notably more difficult to stir the glutaraldehyde into the gelatin without the consistency changing with each stir. There were inconsistencies in the pipetting for the 0.5% and 1.0% of glutaraldehyde, which describes why the images show a variety in color within each row. Further iterations of this experiment need to be done in order to verify the team's findings.

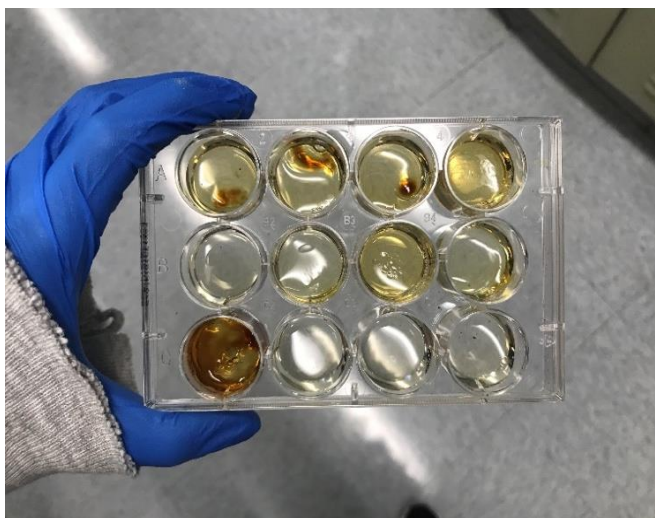


Figure 36: Scaffold Formation using Gelatin and Glutaraldehyde.

Scaffold Material 2: Alginate

The team researched other combinations in which the scaffolds could be formed, as the consistency and reproducibility was not suitable for imaging. The next combination tried was a mixture of Alginate, DPBS (-), and Gelatin. First, Alginic acid was mixed with DPBS (-) and left on the stir plate for three hours to create a 4% Alginate solution. Next, 100mL of DPBS (-) was poured into a beaker and mixed with 5 mL of the Alginate solution and 9 grams of Gelatin to create an 8.6% Gelatin, 0.19% Alginate gel solution. This mixture was left on a stir plate for two hours to combine and heat was added during the first hour of stirring. Further, a 100 mM solution of CaCl_2 was prepared, to be added into the gel solution when pipetting into the well plate. The procedure is listed in Appendix M. As the concentration of CaCl_2 solution increased, the gels turned a cloudy color as seen in Figure 37. These gels were polymerizing at much slower rates than the previous gels made of gelatin and glutaraldehyde, giving the team more time to pipette and form various gel formulations.

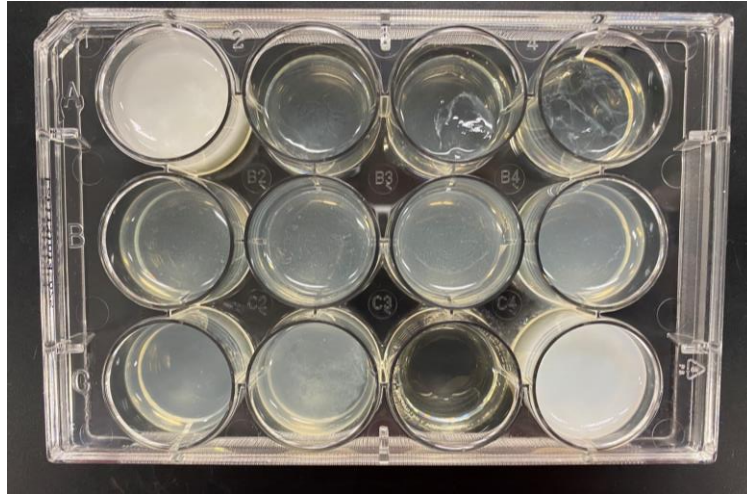


Figure 37: Variations of Gelatin and Alginate Gels After Polymerization

The team worked with three different variations of Gelatin-Alginate and CaCl_2 concentrations, as well as two variations of a pure Gelatin hydrogel for comparison, as was shown in Table 23, in Section 5.3.1.

6.3.2 Rheological Testing

A frequency sweep in oscillatory shear was run from 0.1 to 1000 radians per second at 1% strain and the output was shear storage modulus as shown on the representative graph in Figure 38. All graphs have this general curve shape showing that stiffness was not dependent on frequency between 1-10 radians per second but decreased drastically above 100 radians per second, which is expected of a fully gelled material. No gelatin-alginate formulation reached above 1000 Pa, but the hydrogel with 8.6% Gelatin, 0.19% Alginate, and 33 mM Calcium Chloride had the closest stiffness value and was chosen for subsequent studies.

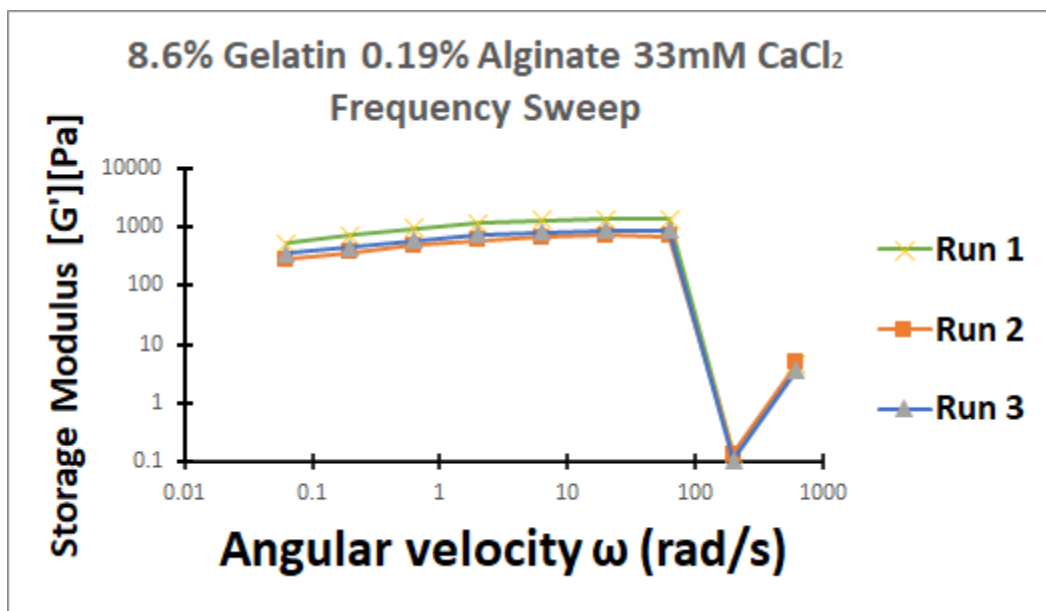


Figure 38: Oscillatory shear testing performed on three independent samples of 8.6% gelatin, 0.19% alginate and 33 mM calcium chloride (graph is in logarithmic scale)

The mean and standard deviation of each test was calculated and displayed in Table 24. Overall, there was no observable trend with decreasing calcium chloride concentration, and there were high standard deviations which shows a high degree of variability within each test and possible inconsistency in the rheological testing result.

Table 24: Scaffold Formulations Tested in Triplicate/Duplicate and the Average \pm Standard Deviation

Sample	Storage Modulus [G'] [Pa]
8.6% Gelatin/ 0.19% Alginate/ 42.86 mM CaCl ₂	431.25 \pm 24.765
8.6% Gelatin/ 0.19% Alginate/ 33 mM CaCl ₂	719.74 \pm 80.918
8.6% Gelatin/ 0.19% Alginate/ 31.03 mM CaCl ₂	303.04 \pm 12.867
9.0% Gelatin/ 4.76 mM CaCl ₂	871.13 \pm 8.657
9.0% Gelatin/ 0.0 mM CaCl ₂	846.25 \pm 27.817

The large standard deviations can be due to a variety of reasons: variability in gap distance and sample height as well as uneven surfaces or damage caused by the removal of the hydrogel from the 12-well plate. Further rheology testing and troubleshooting was limited due to laboratory access and external factors.

6.3.3 Cell Viability Testing: Scaffold

The cell viability protocol was followed per Section 5.3.3 however, there were some unforeseen challenges with forming the gelatin-alginate scaffolds at concentrations identified from rheometer stiffness, with sterilized materials. When forming the scaffolds with unsterilized materials, the viscosity of the hydrogel solutions was low, fairly easy to pipette, and consistent between trials. When using the autoclaved gelatin powder, the solution thickened very quickly and could not be precisely pipetted into the wells of the plate. The solution was still added to the wells, and the varying amounts of 100 mM calcium chloride mixed in. Once the calcium chloride was added, instead of gelling like had been observed with the non-sterile scaffolds, the consistency became less viscous and remained liquid throughout stirring.

After remaining in the refrigerator overnight, the scaffolds were transferred to a biosafety cabinet, where 100,000 Panc-1 cells were seeded on top of each scaffold and the plate was transferred to the incubator. After 24 hours the scaffolds were still entirely liquid, so the medium could not be aspirated off of the scaffold without also removing the scaffold. Although it would be a deviation from the standard protocol of a Trypan Blue exclusion assay, 50 μ L of trypan blue was added to each well to determine whether any of the cells remained viable. Images were taken of each scaffold after the trypan blue was added to the wells using a standard light microscope, using a 10x objective. The viable cells were still distinguishable from those that had taken in the trypan blue; however, the results were inconsistent from one scaffold to another, with some scaffolds having visible stained and non-stained cells, and other scaffolds having lots of noise making it difficult to visualize the staining. An example image is shown in Figure 39.

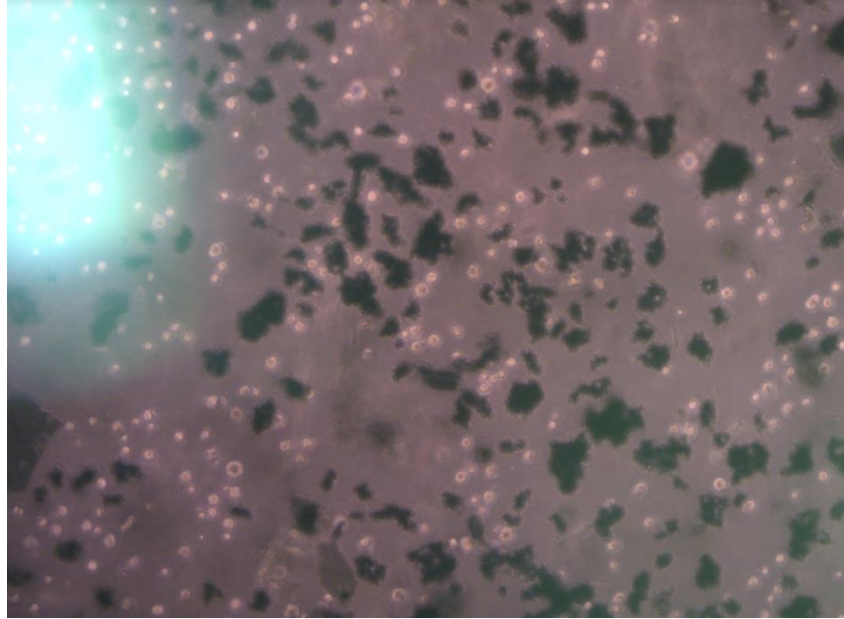


Figure 39: Non-Viable Cells Stained with Trypan Blue on Scaffold (8.6% Gelatin, 0.19% Alginate, 33mM Calcium Chloride)

6.3.4 Diffusivity Testing: Scaffold

The diffusion testing was completed per the protocol described in Section 5.3.4. As the system was running with water in each chamber, and glucose added to the donor chamber, samples were taken sporadically over a period of 24 hours. A sample was taken from each chamber (donor and receptor) at each sampling period. To get an accurate glucose reading an equal amount of DPBS was added to each sample and the output reading (mg/dL) was multiplied by two. Through the three trials the receptor chamber only yielded a reading of “lo” indicating that there was little to no diffusion from the donor chamber with the glucose through the scaffold to the receptor chamber. During one of the trials there was noted leakage, but the results were otherwise consistent with the other two trials. Also of note, over time the glucose reading of the donor chamber would decrease, but this was not reflected by an increase in the receptor chamber so does not indicate that diffusion was occurring through the scaffold. A representative graph, shown in Figure 40, from Trial 2 shows the readings of glucose in the donor chamber over the 24-hour period.

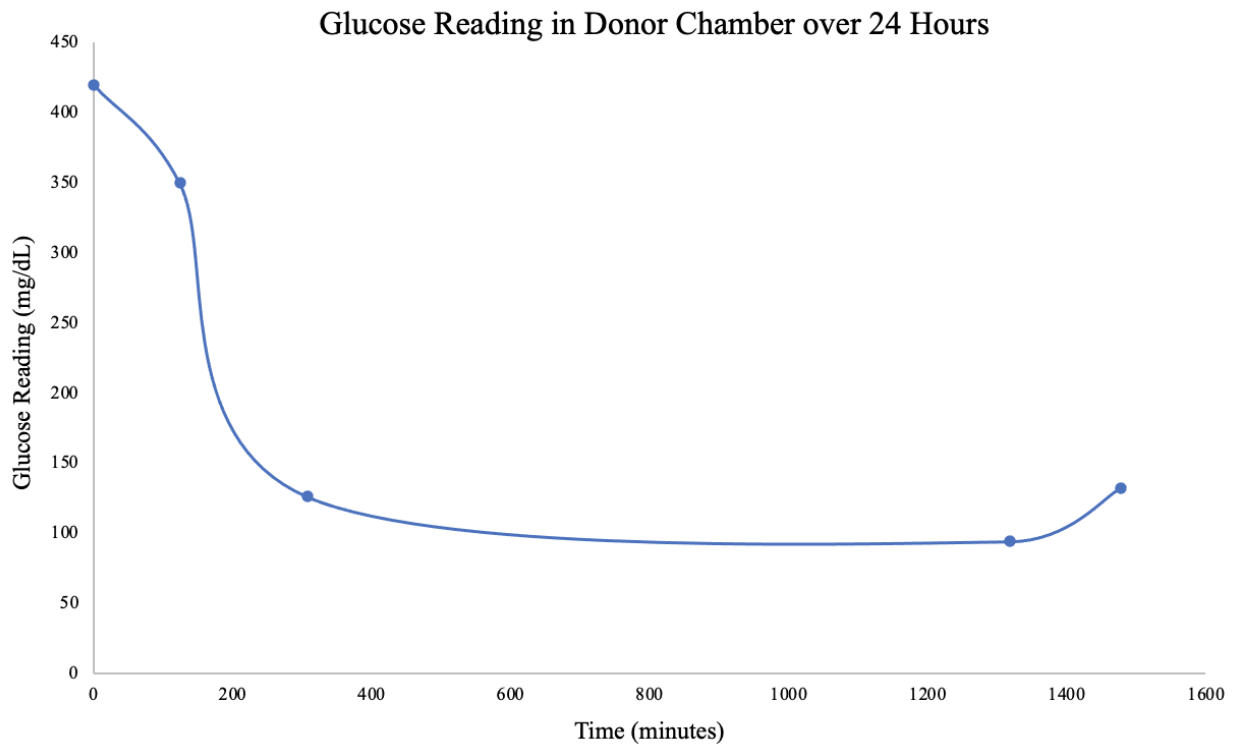


Figure 40: Glucose Reading in Donor Chamber (mg/dL) Over 24 Hours

6.4 Membrane Characterization

6.4.1 Membrane Fluid Flow Testing

The membrane fluid flow testing was performed on the polycarbonate membrane with pore size of 14 μ m in accordance with the protocol described in Appendix O. The time durations for each experimental iteration are shown in Table 25, as well as the averages for each membrane, grouping of membranes, and the controls.

Table 25: Time Durations of Membrane Fluid Flow Experiment Trials

Condition		Trial 1 (s)	Trial 2 (s)	Trial 3 (s)	Average (s)	Average (s)
Water	Membrane 1	21.56	22.85	23.61	22.67	24.07±1.64
	Membrane 2	26.28	24.52	25.83	25.54	
	Membrane 3	24.32	21.86	25.85	24.01	
	No Membrane (Control)	3.23	3.40	3.79	3.47	3.47±0.23
Cell Media	Membrane 1	54.06	58.76	53.39	55.40	52.91±4.78
	Membrane 2	51.26	54.86	58.38	54.83	
	Membrane 3	41.98	49.42	54.07	48.49	
	No Membrane (Control)	5.23	5.33	5.49	5.35	5.35±0.11

From these results, the flow rate was calculated using Equation 5:

$$Q = \frac{V}{t}$$

Equation 5: Flow Rate

where Q is the flow rate, V is the fluid volume, and t is time. The volume for each trial was kept consistent at 50 mL. The flow rates for each condition and membrane were calculated and the results are summarized in Table 26.

Table 26: Flow Rates of Membrane Fluid Flow Experiment Trials

Condition		Trial 1 (mL/s)	Trial 2 (mL/s)	Trial 3 (mL/s)	Average (mL/s)	Average (mL/s)
Water	Membrane 1	2.32	2.19	2.12	2.21	2.09±0.14
	Membrane 2	1.90	2.04	1.94	1.96	
	Membrane 3	2.06	2.29	1.93	2.09	
	No Membrane (Control)	15.48	14.71	13.19	14.46	14.46±0.95
Cell Media	Membrane 1	0.92	0.85	0.94	0.90	0.95±0.10
	Membrane 2	0.98	0.91	0.86	0.92	
	Membrane 3	1.19	1.01	0.92	1.04	
	No Membrane (Control)	9.56	9.38	9.11	9.35	9.35±0.18

From the results of both experiments, the presence of the membrane does significantly slow the flow rates. In the first experiment, the flow rate of water was slowed to a seventh of the flow rate through the tubing without a membrane present. In the second experiment, the flow rate of cell culture medium was slowed to approximately a tenth of the flow rate through the same tubing without a membrane present. While the fluid flow is hindered by the presence of the membrane, the flow was not fully obstructed, which could allow for the functional requirement of maintaining fluid flow to be achieved. This assists the achievement of our fifth objective, which involves the devices utilization in a clinical setting.

While the functional requirement was met, the results could also be improved. One of the main requirements of the membrane was to not significantly hinder fluid flow. This could be achieved by using a membrane with a great pore size, a higher pore density, or a combination of the two.

6.4.2 Cellular Adhesion Testing

The membrane cellular adhesion testing was performed in accordance with the protocol described in Appendix P. After 48 hours where the 3T3 cells were allowed to flow through the apparatus, the bottom tube was removed, and the contents were emptied into a petri dish. The membrane was also removed and placed in a petri dish. Both the contents of the bottom tube and

the membrane were imaged under a microscope. The cellular adhesion testing was conducted in two simultaneous trials using two separate apparatuses. Trial 1 yielded no cell movement, but it was determined that a likely cause was the formation of a vacuum within the apparatus, as the cells and culture medium were not being pumped through the apparatus and the tubing was closed at both ends. Trial 2 did not seem to form a vacuum, which could have been due to the rubber stopper at the top of the apparatus being placed more loosely. Trial 2 did result in some net movement of the cells and an image capture of the partial contents of the bottom tube is shown in Figure 41.



Figure 41: Image of the Contents of the Bottom Tube in Trial 2

While there was some cell movement through the membrane, there were originally 500,000 cells injected into the top tube of the apparatus. The number of cells that were observed in the bottom tube after 48 hours was not high enough to conclude that this polycarbonate membrane

was well-suited for this application. The membrane was then analyzed under the microscope to determine if cells had adhered to the membrane. An image capture of the partial membrane from Trial 2 is shown in Figure 42.

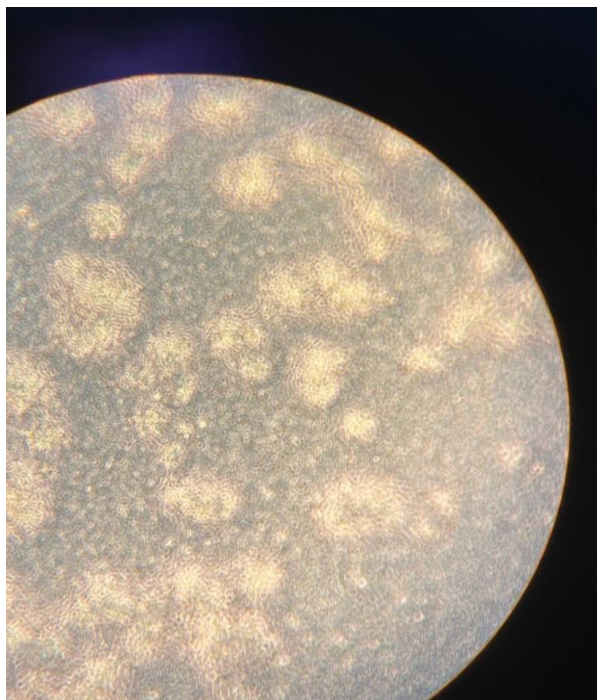


Figure 42: Membrane with 3T3 Cells Adhered

The high density of cell adhesion to the membrane allowed the team to conclude that this membrane with a pore size of 14 μm should not be utilized in the final device, as it did not allow for the functional requirement of allowing unhindered flow of cells through the membrane to be achieved. While the results of this experiment were not desirable for the application of the membrane, they are consistent with documented literature. A polycarbonate membrane with a pore size of 14 μm is typically not utilized for this application. The adhesion to the membrane was almost certainly due to the pore size of the membrane being smaller than the diameter of most 3T3 cells. This would only be worsened for PANC-1 cells, as their diameter is even larger than that of the 3T3 cells. Suggestions for future improvements to the membrane are outlined in Section 8.5.

6.5 Project Impact

The project impact had to be considered in a variety of areas throughout the development stages. These areas included the economic, environmental, societal and sustainability impacts. As well as ethical, health and safety, and manufacturing concerns.

6.5.1 Economic Impact

An important overall design consideration for the project was cost. The overall budget for the project was \$1000 and therefore it was important to consider materials that were efficient and low cost. An inexpensive *in vitro* model for invasion potential would be useful in both academia and a clinical setting. The model being low cost means that it would be more accessible for researchers and clinicians. Additionally, after further development of this model to resemble the physiological conditions of the tumor microenvironment more accurately, costs could be reduced in other areas. For example, this model could reduce the need for expensive clinical procedures for patients and laboratory animals for testing.

6.5.2 Environmental Impact

This bioreactor system has minimal environmental impacts. All device components are made from non-toxic materials. Additionally, the associated tubing and membrane clamps can be easily sterilized using ethanol, ethylene oxide sterilization or autoclaving. The device is small enough in size to fit in a standard laboratory incubator when cells are housed in the unit, reducing the need for a specialized environment with custom equipment. Throughout the duration of the development process, the team prioritized not wasting materials, by avoiding making excess solution and using only the amounts needed of the reagents. We ensured that all created waste was disposed of in accordance with the environmental health and safety standards.

6.5.3 Societal Impact

With additional iterations, the bioreactor system has the potential to make a large positive societal impact. Creating a more physiologically relevant *in vitro* model for tumor cell invasion can benefit researchers and clinicians. Researchers will have a better model for testing different cancer therapeutics for drug discover and delivery. Clinicians will be able to understand the

invasion potential of a patient's cancer and provide a more accurate prognosis and better treatment plan.

6.5.4 Ethical Concerns

The bioreactor system poses few ethical concerns itself but could potentially alleviate some ethical considerations surrounding the use of animals in a laboratory setting. The gelatin used in the formation of the scaffold is bovine derived and therefore an animal product, however alternative natural and synthetic materials could be considered as a scaffold material to reduce the reliance on animal products. Currently, *in vitro* models of invasion do not incorporate interstitial fluid flow and many fail to integrate three-dimensional cell culture, so *in vivo* models are considered more physiologically relevant. A bioreactor device combining three-dimensional cell culture with interstitial fluid flow to measure invasion would make for a physiologically relevant *in vitro* model, which can reduce the need for animal models.

6.5.5 Health and Safety

The bioreactor system is a minimal risk to health and safety for the user. The small size of the housing unit allows for easy handling of the device by the user. The largest risk to health and safety is the use of the calcium chloride solution in the scaffold formation protocol. Calcium chloride can cause skin irritation if contact is made, and ingested calcium chloride can cause burns, vomiting, and other potentially severe health impacts. It is important that the potential hazards are understood when using these materials and that they are handled in the proper workspace and the user is wearing adequate personal protective equipment.

6.5.6 Manufacturing Concerns

The manufacturing concerns for this device fall into three main categories, the cell culture housing unit, the scaffold, and the associated external parts and software.

Three-dimensional printing was used for formation of the CCH to allow for quick and repeat iterations at a low cost. Polylactic acid (PLA) was used for the first iterations of the CCH and later a switch was made to high temperature resin. Both materials are low cost and would be accessible at most machine shops. The manufacturing process was relatively simple and can be

performed by anyone following basic machine shop training. If training or equipment were unavailable, the manufacturing of the CCH could be outsourced.

Manufacturing of the scaffold does not pose any major concerns. The materials needed for the formation include, Gelatin, Alginate, DPBS, and Calcium Chloride. All of these materials are accessible through most laboratory supply distributors. All of the laboratory work for the scaffold formation can be completed in a Class II Biosafety Cabinet.

The associated external parts include 0.25-inch tubing and a syringe pump. These materials can often be found in research laboratories or otherwise purchased from a laboratory supply distributor. The associated software includes the programs MATLAB®, and CellProfiler™, which can be used on any computer on which these programs are downloaded.

6.5.7 Sustainability Impact

The CCH unit and associated tubing were developed with the idea of easy sterilization in mind. Since both components can be readily cleaned with ethanol, ethylene oxide sterilization, or autoclaving, they can be reused over and over again for many trials. This minimizes unnecessary waste that accompanies single use systems. Additionally, the size of the device means that it could fit in a standard incubator and there is not a need for a specialized temperature-controlled environment. Throughout the device fabrication process, the team was careful to only use the exact amount of reagents needed to not create any unnecessary waste, all waste that was created was disposed of according to the laboratory guidelines. The development of this device had a minimal impact on water and energy consumption.

Chapter 7: Final Design and Project Impact

7.1 Final System Design

The final system design of our perfusion bioreactor would utilize a three syringe-syringe pump to flow cell culture medium and cells through the CCH unit that housed a hydrogel scaffold to support cell invasion. The cell invasion into the scaffold would be imaged using a microscope and quantified using the CellProfiler™ program. The components listed below would be used in the final system design:

- 3D printed CCH unit made using high temperature resin
- 0.25-inch tubing
- Syringe pump
- Cell culture medium
- Hydrogel Scaffold: 8.6% gelatin, 0.19% alginate, and 33mM CaCl₂
- Three 30 mL syringes
- Three 15 mL conical tubes

The syringe pump would be set-up according to the manufacturer's procedure. The three 30 mL syringes would be filled with 20 mL of cell culture medium and then placed directly into the syringe pump. The CCH unit would be sterilized using an autoclave, and the tubing will be sterilized with ethylene oxide. To set up the bioreactor system, tubing would be connected to the inlet and outlet flow channels of the CCH unit including the syringes. Next, the CCH unit would be placed inside of an incubator, with the syringe pump and tubing running outside of it. The sterile hydrogel scaffold would then be inserted into the scaffold chambers, and a lid would be placed on top of the CCH unit to maintain sterility. When the user is ready to begin testing, they would inject the cells into the designated cell inlet. The syringe pump will be programmed to run at a rate of 0.06 mL/hour, and the bioreactor system would run for three days. After three days, the CCH unit would be placed under a microscope and the scaffolds in each of the scaffold chambers would be imaged. The images would then be analyzed using the CellProfiler™ program to measure cell invasion into the z-plane of the hydrogel scaffold through cell counts and distance measurements.

7.2 Industry Standards

The following standards were incorporated into the project. If further validation testing were to support large scale commercial production of this device, additional cleanroom and production protocols would need to be followed.

FDA: The FDA outlines good laboratory practices for non-clinical laboratory studies in 21CFR58

ISO: This project included the use of several ISO standards throughout the development of the bioreactor system.

- ISO 24998:2008: All cell culture dishes, and conical tubes used in cell culture procedures were properly sterilized and maintained.
- ISO 14937:2009: General sterilization methods for a bioreactor
- ISO 17665-1:2006: This standard was followed for autoclaving the gelatin powder for cell viability testing.
- ISO 128:2003: All SolidWorks drawings follow the drafting standard outlined.

ASTM: The guide ASTM F2150-19 was followed for the characterization and testing of the biomaterial scaffold.

Chapter 8: Future Work and Conclusions

8.1 Full System Implementation

Although the initial testing of flow through the system was successful, the system did not meet the requirements of scaffold imaging and sterility. Additional testing with the scaffold in the chambers and the ability to image and measure invasion through the scaffold must be done in future work. Sterility of the scaffolds inside of a sterilized CCH unit must also be carried out to meet the full system flow requirements.

8.1.1 Syringe Pump

The syringe pump in the laboratory was able to hold multiple syringes for flow testing between each channel and scaffold chamber. This allowed for the possibility of running fluid through each channel in the CCH unit simultaneously in parallel. The timeline of this project did not leave room for the team to test the different functions of the syringe pump. The team was able to test leakage of the device by using the syringe pump to flow fluid through the system, at a constant rate. Multiple syringes were used in this testing for proof of concept. Future work includes adjusting and testing different flow speeds, that mimic different flows within the tumor tissue, using the syringe pump. This will allow for more conclusive data on optimal flow rates for the device and full system setup. Further, the length of these tests are dependent on the rate at which fluid is flowing. This information will be helpful in getting this device into clinical practice.

8.1.2 CCH Unit Design

The final design of the CCH unit experienced no signs of leaking, but more testing and verification needs to be done with the CCH unit. The device was printed from high temperature resin, a clear material that is helpful for imageability purposes. This material is also able to be autoclaved, for easier application in a clinical setting. The limitation of this design is that it was built to implement a membrane and membrane clamps. Therefore, a membrane must be used in this design. The user is not able to stray and implement a cell strainer or any other porous material. Further, this device is not a closed-loop system currently. A lid would need to be printed in order to close off the top of the device. This ensures the sterility of the device as a whole and promotes

cell viability. This also will allow for testing of a fully closed system with the sterile scaffold and cells in the full system design.

The initial testing of the final design of the CCH unit did verify that fluid has the ability to flow through each of the channels and scaffold chambers. However, fluid flow between each scaffold chamber delivered different output volumes. This could have been due to pressure gradients within the tubing, air bubbles in the syringes, size or shape of the scaffold chamber and channels. The output of each chamber should have been equal since the input flowrate was identical among all channels. Alterations to the size and shape of the chambers should be considered in the future.

8.1.3 Full System Testing

The team was unable to perform a full system test. This was due to limitations in the diffusivity testing of the scaffold. The scaffolds that were formulated did not have the proper porosity needed to allow fluid to flow through the material. For future work, flow testing would have to be done with the scaffold in the scaffold chamber. The fluid flow at both a constant rate and varying rates would need to be tested with the scaffold and membrane loaded into the device. This will allow the team to gain information on the output rates when the device is fully equipped.

The CCH unit was unable to be imaged with the scaffold and membrane inside. Further, cells were unable to be processed through the device and imaged within the unit. More testing needs to be completed to verify that medium and cells are able to freely move through the chambers and invade into the hydrogel scaffold. As described in Section 8.4, the team had some challenges in creating the sterile scaffolds. Therefore, there was a lack of cell work able to be done and the inability of placing a sterile scaffold into the device and testing it. Future work can also be done in exploring how to set up the full system design experiment in an incubator, while the syringe pump, tubing and syringes remain outside of the incubator. This testing will allow the team to come up with more conclusive evidence on full system flow testing for cell invasion.

8.2 Simulation Future Work

To gain an even better understanding of how fluid flow would work with this device it would be beneficial to develop a mathematical/visual simulation representing fluid flow in different tumor conditions. There are two main software options that are commonly used for this

application, COMSOL and ANSYS. COMSOL was used in part by the previous MQP team as a model of fluid flow and is known to be user friendly. One drawback of this program is that it does not support 3D modeling. ANSYS was recommended by the previous MQP group due to its compatibility with SOLIDWORKS drawing files which can be imported into the program easily. ANSYS is more of an industry standard and better supports 3D modeling.

8.3 Image Processing Future Work

The image analysis work aimed to achieve Objective 2 “Scaffold and cells should be contained within the CCH unit and be able to be imaged.” The objective was partially met in that the two programs were evaluated and accomplished the goal of imaging cellular invasion in two dimension and three dimensions and obtain an accurate cell count per image. However, the team was unable to obtain the images from scaffolds in the current device. From the sample images used in verification, the percent errors for CellProfiler™ were much lower than that of the custom MATLAB® program. In future studies, cell images from the scaffolds made from the team would be useful in analysis. This would round out the image analysis aspect of the project and relate it back to the system as a whole.

It would be helpful if one program could accomplish all three goals. As of now, the team has a combination of CellProfiler™ and MATLAB®. Where, CellProfiler™ is used to count the cells in either a 2D image or in an image z-stack. The MATLAB® program is used to overlap the images in the z-stack and measure distances between the independent cells. One way to accomplish the one program goal would be to create a time-lapse video of the cells invading the scaffold. This way, the video could be uploaded into CellProfiler™ and analyzed per frame. This would give an accurate depiction of cells per frame as well as invasion distance each cell traveled. In order to accomplish this, the team would need to set up a microscope with a video camera within an incubator or take one image every few hours in order to track the individual cell movement. Further, since CellProfiler™ is an open-source program, it is always being updated and retransformed. There potentially could be new iterations of the program in the next few months that would allow for better analysis of a three-dimensional setting.

8.4 Scaffold Future Work

Objective 4 “Support cancer cell invasion into scaffold” was only partially met, as there was no conclusive evidence that supported cell viability or three-dimensional cellular invasion into the scaffold. There is significant room for improvement in the cellular aspect of the scaffold work, as well as changes to the hydrogel formulation and overall scaffold validation.

The current formulation of the gelatin-alginate scaffold does not allow for any diffusive properties. This could be due to the stiffness of the high disease state trying to be achieved. Further, the team kept a constant concentration of both Gelatin and Alginate throughout each formulation while just changing the concentration of CaCl_2 . Different concentrations of Gelatin and Alginate could be attempted in order to obtain a more porous material. Once a more porous material is achieved the diffusion testing could be conducted again to calculate and verify the diffusivity of the scaffold. Additional diffusivity testing can be performed with cells, and future diffusion tests should take place within the CCH unit.

Scanning electron microscopy could be implemented into the scaffold process to help verify porosity and microstructure of the hydrogel. Further, contact angles were not able to be performed in order to test the hydrophobicity of each scaffold formation. Doing these tests earlier into the scaffold formation process might save the team some time in determining which scaffolds will be used for subsequent studies. More research will need to be done to determine if stiffness correlates to porosity at all in terms of the specific materials chosen.

A time sweep on the Rheometer could be a beneficial way of determining the gelation time of a material. This could inform future studies on how long the hydrogels would need to sit before work is done. The use of a 3D printed PDMS mold would also be beneficial in any transfer processes that the scaffold might endure during testing (e.g., rheological testing, microstructural analysis). This would allow for the minimization of cracks, breaks, and uneven surfaces during polymerization and transfer.

Another limitation of the group was the idea that Alginate loses viscosity if autoclaved. This prevented the group from autoclaving the hydrogel as a whole. It forced the group to sterilize individual materials before being formulated. Another sterilization limitation the team encountered was with Gelatin. The Gelatin powder was autoclaved, which made the powder very hard and ultimately resulted in a much higher viscosity for the Gelatin-Alginate solution. Alternative sterilization methods should be considered for the formation of the sterile scaffolds so that they

maintain the viscosity, stiffness and other characteristics that were observed in the non-sterile scaffolds. Once it is determined that scaffolds are consistent when formed in a sterile or non-sterile environment, the cell seeding experiment can be performed again to get a more accurate understanding of the scaffold's impact on cell viability. The team was unable to gain accurate information from the cell viability testing done, since the sterilized materials changed the texture and gelation properties of the hydrogel. The hydrogels lost all gelling abilities due to the sterilization technique that was implemented on the Gelatin material. Therefore, if the team can tackle the sterilization limitation, it will pave the way for future studies.

8.5 Membrane Future Work

8.5.1 Material Alterations and Replacements

The cellular adhesion testing performed on the polycarbonate membrane concluded that the cells had a high affinity for adhering to the membrane. This is most likely due to the pore size of the membrane being a smaller diameter than the 3T3 cells used, which is also smaller than the PANC-1 cells that are desired for future testing and modeling. An alteration that should be made is switching to the use of a cell strainer to filter potentially larger aggregates that come from patient biopsies. Cell strainers are sterile sieving devices that fit onto the rim of most conical tubes and allow for cell suspensions. Cell strainers are desirable for this application because they come in a range of pore sizes from 1 micrometer to 1000 μm . The most appropriate pore size would be 40 μm to 60 μm , but fluid flow and cellular adhesion testing should be performed on cell strainers of several different sizes to determine which is most suited for meeting the functional requirements. The CCH unit would potentially be altered to accommodate for the change from a flat membrane to an indented cell strainer.

8.5.2 Validation Methods

Cell adhesion testing should be conducted with an invasive cell line in order to better mimic the desired clinical application. Additional cell flow testing should also be completed on a membrane or sieving device, where cells in cell culture medium are pumped into an apparatus that holds the membrane or sieving device. This will better assess the membrane's ability to

accommodate flow without hindering cellular migration and better represent the membrane's application within the device.

8.6 Conclusions

The goal of this project was to design a device integrating interstitial fluid flow that could perfuse cancer cell lines through a biocompatible scaffold. Invasion could then be detected through imaging. A device was designed to hold a scaffold for cell invasion, support fluid flow through the scaffold, and be easily assembled. In conclusion, the results from current tests demonstrate partial fulfillment of objectives. Objective 1 concerned cell invasion of the scaffold, while cell invasion was not measured, the stiffness of the scaffold was characterized and compared to the *in vivo* disease state. Objective 2 surrounded the scaffold in the housing unit and imageability. Cell imaging was not conducted within the CCH unit, but the scaffolds were able to be housed in the unit and removed easily. Objective 3 was met, as fluid was able to flow through the housing unit, although the three chambers had varying flow outputs. Objective 4 concerned device assembly and sterility, this objective was partially met through the material choice of high-temperature resin for the CCH unit for sterilization, and the use of SOLIDWORKS and 3D printing for easy manufacturing of the device. Objective 5 was not met but could be a direction for future work to translate the device that was developed to work practically in a clinical setting.

Chapter 9: Appendices

Appendix A: Solidworks Drawing Iteration 1

2 **1**

B **B**

A **A**

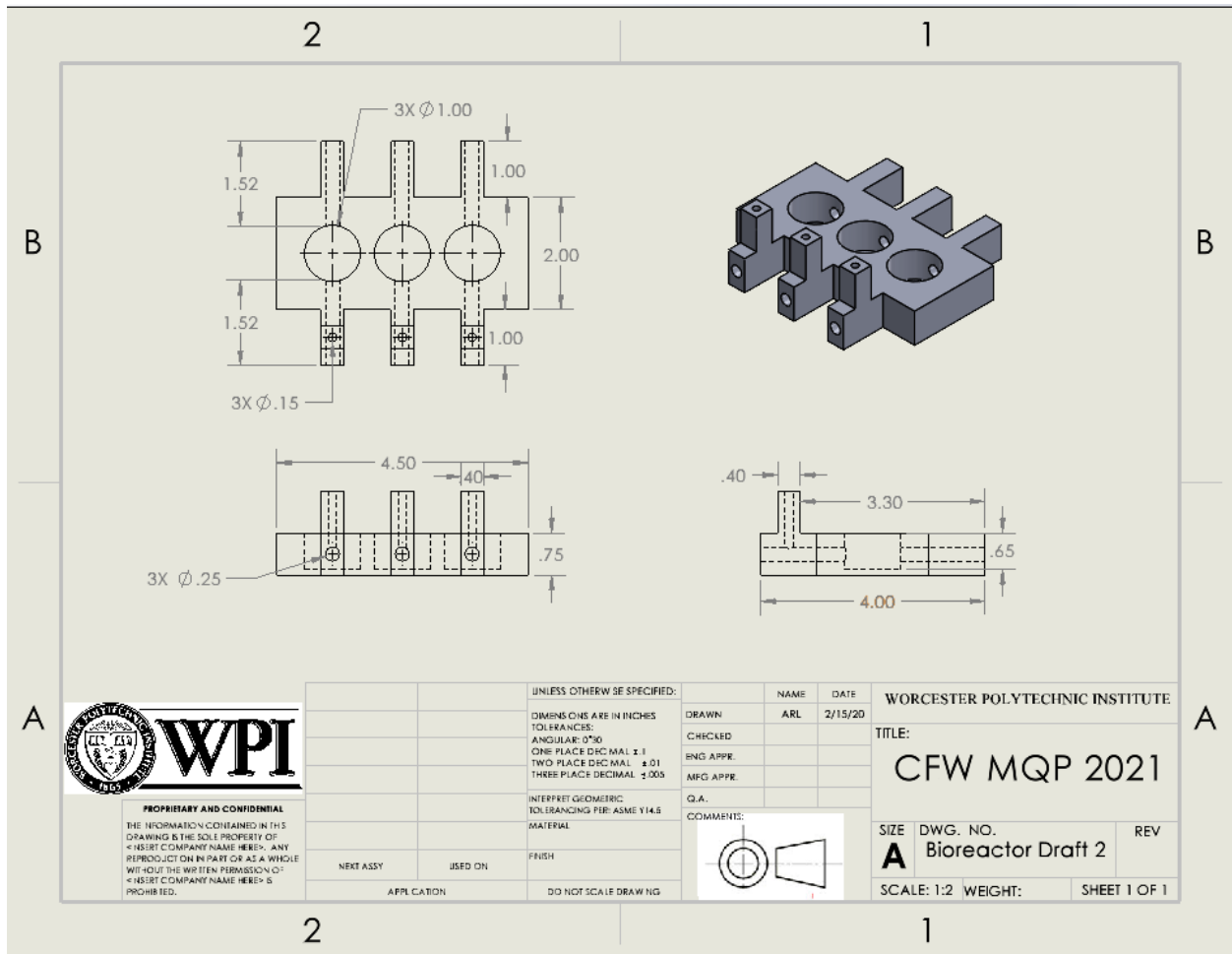
2 **1**

UNLESS OTHERWISE SPECIFIED:		NAME	DATE
DIMENSIONS ARE IN INCHES		ARL	11/23/20
TOLERANCES:			
ANGULAR: 0°30'			
ONE PLACE DECIMAL: ± 0.1			
TWO PLACE DECIMAL: ± 0.01			
THREE PLACE DECIMAL: ± 0.001			
INTERPRET GEOMETRIC TOLERANCING PER: ASME Y14.5	Q.A.		
MATERIAL	COMMENTS:		
FINISH			
NEXT ASSY	USED ON		
APPLICATION			
DO NOT SCALE DRAWING			

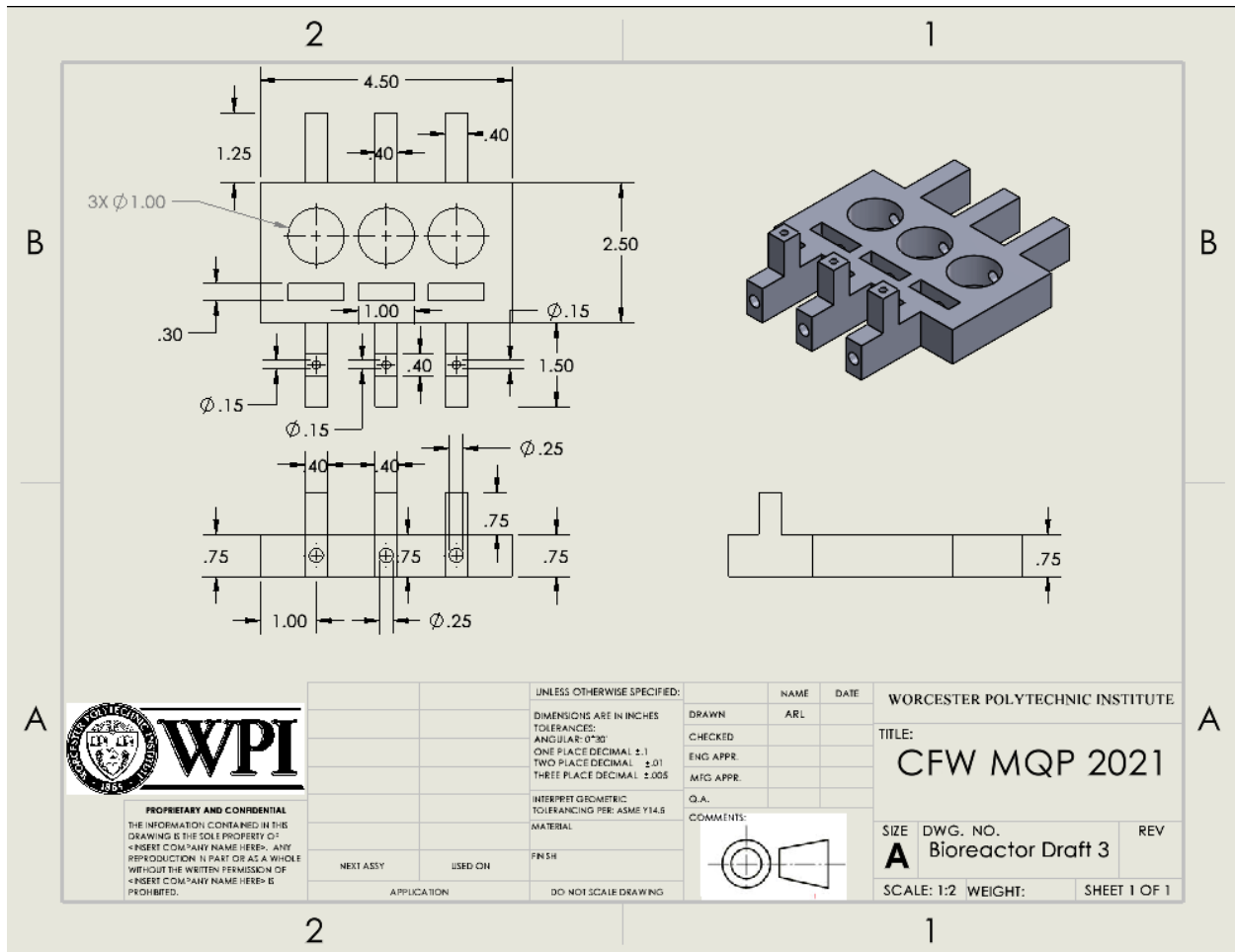
WPI
 PROPRIETARY AND CONFIDENTIAL
 THE INFORMATION CONTAINED IN THIS DRAWING IS THE SOLE PROPERTY OF WPI. ANY REPRODUCTION IN PART OR AS A WHOLE WITHOUT THE WRITTEN PERMISSION OF WPI IS PROHIBITED.

WORCESTER POLYTECHNIC INSTITUTE
 TITLE: **CFW MQP**
 SIZE **A** DWG. NO. **Bioreactor Draft** REV
 SCALE: 1:2 WEIGHT: SHEET 1 OF 1

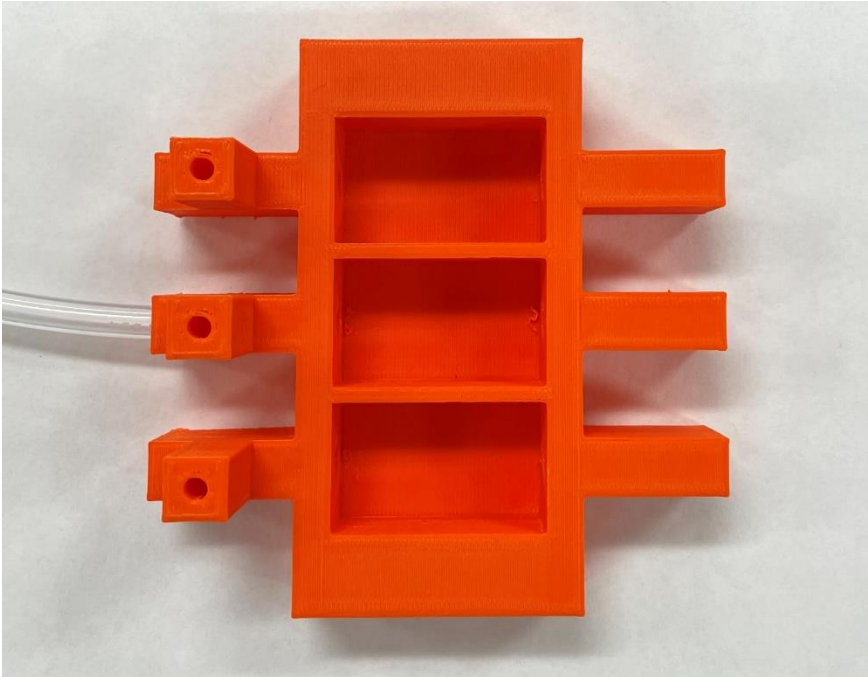
Appendix B: Solidworks Drawing Iteration 2



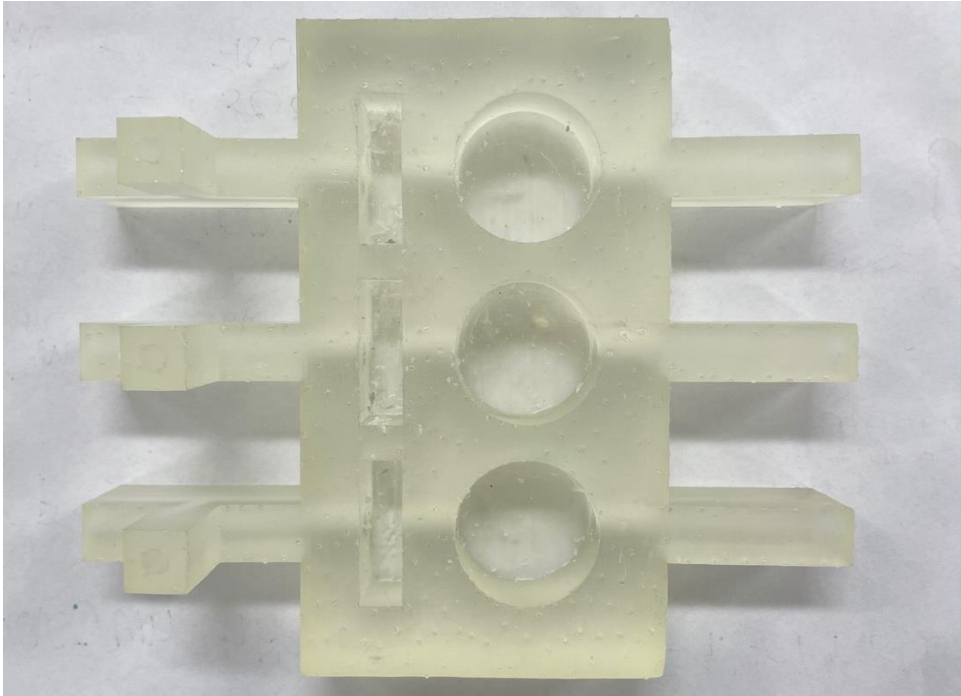
Appendix C: Solidworks Drawing Iteration 2



Appendix D: 3D Printed Iteration 1



Appendix E: 3D Printed Iteration 2



Appendix F: MATLAB® Code for Image Processing

```
%% GUI For Image Processing
function varargout = mqp_gui(varargin)
% MQP_GUI MATLAB code for mqp_gui.fig
%     MQP_GUI, by itself, creates a new MQP_GUI or raises the existing
%     singleton*.
%
%     H = MQP_GUI returns the handle to a new MQP_GUI or the handle to
%     the existing singleton*.
%
%     MQP_GUI('CALLBACK',hObject,eventData,handles,...) calls the local
%     function named CALLBACK in MQP_GUI.M with the given input arguments.
%
%     MQP_GUI('Property','Value',...) creates a new MQP_GUI or raises the
%     existing singleton*. Starting from the left, property value pairs are
%     applied to the GUI before mqp_gui_OpeningFcn gets called. An
%     unrecognized property name or invalid value makes property application
%     stop. All inputs are passed to mqp_gui_OpeningFcn via varargin.
%
%     *See GUI Options on GUIDE's Tools menu. Choose "GUI allows only one
%     instance to run (singleton)".
%
% See also: GUIDE, GUIDATA, GUIHANDLES

% Edit the above text to modify the response to help mqp_gui

% Last Modified by GUIDE v2.5 15-Apr-2020 09:32:15

% Begin initialization code - DO NOT EDIT
gui_Singleton = 1;
gui_State = struct('gui_Name',       mfilename, ...
                  'gui_Singleton',  gui_Singleton, ...
                  'gui_OpeningFcn', @mqp_gui_OpeningFcn, ...
                  'gui_OutputFcn',  @mqp_gui_OutputFcn, ...
                  'gui_LayoutFcn',  [], ...
                  'gui_Callback',   []);
if nargin && ischar(varargin{1})
    gui_State.gui_Callback = str2func(varargin{1});
end

if nargout
    [varargout{1:nargout}] = gui_mainfcn(gui_State, varargin{:});
else
    gui_mainfcn(gui_State, varargin{:});
end
% End initialization code - DO NOT EDIT

% --- Executes just before mqp_gui is made visible.
function mqp_gui_OpeningFcn(hObject, eventdata, handles, varargin)
% This function has no output args, see OutputFcn.
% hObject    handle to figure
% eventdata  reserved - to be defined in a future version of MATLAB
% handles    structure with handles and user data (see GUIDATA)
% varargin   command line arguments to mqp_gui (see VARARGIN)
```

```

% Choose default command line output for mqp_gui
handles.output = hObject;

% Update handles structure
guidata(hObject, handles);

% UIWAIT makes mqp_gui wait for user response (see UIRESUME)
% uiwait(handles.figure1);

% --- Outputs from this function are returned to the command line.
function varargout = mqp_gui_OutputFcn(hObject, eventdata, handles)
% varargout cell array for returning output args (see VARARGOUT);
% hObject handle to figure
% eventdata reserved - to be defined in a future version of MATLAB
% handles structure with handles and user data (see GUIDATA)

% Get default command line output from handles structure
varargout{1} = handles.output;

%Global Variables that are Essential for code function
%These includes saving a copy of uploaded user images, the status of
%distance calibration, and the pixel/micrometer values used for converting
%specific user distances into the appropriate um values
function setGlobalImage(val) %sets the image the user originally uploads
global uploadedImage
uploadedImage= val;

function r = getGlobalImage %returns the image the user originally uploads
global uploadedImage
r = uploadedImage;

function setGlobalCalibrateStatus(val) %sets the calibration status
global calibrateStatus
calibrateStatus = val;

function r = getGlobalCalibrateStatus %returns the calibration status
global calibrateStatus
r = calibrateStatus;

function setGlobalPixelLength(val) %sets the pixel length
global pixelLength
pixelLength = val;

function r = getGlobalPixelLength %returns the pixel length
global pixelLength
r = pixelLength;

function setGlobalumLength(val) %sets the umLength
global umLength
umLength = val;

function r = getGlobalumLength %returns the umLength
global umLength
r = umLength;

% --- Executes on button press in pushbutton1.

```

```

% This button will provide the user with an overlay of cell boundaries and
% a count of the cells in the image.

function pushbutton1_Callback(hObject, eventdata, handles)
    % hObject    handle to pushbutton1 (see GCBO)
    % eventdata  reserved - to be defined in a future version of MATLAB
    % handles    structure with handles and user data (see GUIDATA)

    %reset the appropriate text fields and axis before creating the overlay
    %of cell images and determining the cell count
    set(handles.checkbox1, 'Value',0); %unchecks grid on checkbox
    set(handles.text8, 'String', ' '); %x-axis textbox reset
    set(handles.text11, 'String', ' '); %y-axis textbox reset
    set(handles.text15, 'String', 'N/A'); %specific distance measurement
number textbox
    set(handles.text4, 'String', 'N/A'); %cell count textbox
    cla('reset');

    %gets the jpg image from the user
    [path,filter] = uigetfile('*.jpg');
    uploadedImage= imread(fullfile(filter,path));

    %converts the image to black and white, thresholds the image, and
    %isolates the boundaries of each of the cells.
    grayscaleImage = rgb2gray(uploadedImage); %converts to grayscale
    contrastEnhancedImage = adapthisteq(grayscaleImage); %enhances image
contrast
    borderClearedImage = imclearborder(contrastEnhancedImage); %eliminates
image border
    filteredImage = wiener2(borderClearedImage, [5,5]); %applies wiener
filter to image
    binaryBwImage = im2bw(filteredImage,graythresh(filteredImage)); %binary
image with ostu threshold
    filledImage = imfill(binaryBwImage, 'holes'); %fills holes
    openedImage = imopen(filledImage, strel('disk',2)); %open image to reduce
error
    areaOpenedImage = bwareaopen(openedImage, 60); %area opens image to break
up cells in clumps
    [~,numCells] = bwlabel(areaOpenedImage); %gets the number of cells by
counting objects in areaOpenedImage
    numDisp = int2str(numCells); %converts the number of cells to a string
for display
    perimCellsImage = bwperim(areaOpenedImage); %gets cell perimeters
    se = strel('line',11,90);
    boldPerim = imdilate(perimCellsImage,se); %increases line thickness of
cell borders
    overlay = imoverlay(uploadedImage, boldPerim, [1 .3 .3]);

    imshow(overlay) %shows the image with the cell boundary overlay.
    setGlobalImage(overlay); %sets that image as the global variable
    set(handles.text4, 'String', numDisp) %displays the number of cells counted

% --- Executes on button press in pushbutton7.
%This pushbutton allows the user to calibrate distance
function pushbutton7_Callback(hObject, eventdata, handles)
    %ensures the checkbox is unchecked and the appropriate fields on the
    %image are reset

```

```

set(handles.checkbox1, 'Value',0); %grid on checkbox
set(handles.text8, 'String', ' '); %x-axis textbox
set(handles.text11, 'String', ' '); %y-axis textbox
set(handles.text15, 'String', 'N/A'); %specific distance measurement
number textbox
set(handles.text4, 'String', 'N/A'); %cell count textbox
cla('reset');

[path,filter] = uigetfile('*.jpg');

%resets the old image/axis and displays the choosen image
uploadedImage= imread(fullfile(filter,path));
imshow(uploadedImage)
setGlobalImage(uploadedImage);

%Allows the user to draw a line on the screen across their reference
%distance and calculates that distance in pixels.
[~,~,~, xi,yi] = improfile(1000);
lineLengthPixels = round(sqrt((xi(1)-xi(2))^2 + (yi(1)-yi(2))^2));

%If the line length is greater than 0, it will set the calibrated
%status to true (1) and indicate the pixel length to the user. If the
%length is less than 0, it will set the pixel length to
N/uploadedImageand set the
%calibration status to false (0)
if(lineLengthPixels > 0)
    setGlobalCalibrateStatus(1);
    setGlobalPixelLength(lineLengthPixels);
    prompt = {'Enter the size of the line drawn in um:'};
    dlgtitle = 'Actual Distance Measured';
    dims = [1 35];
    definput = {' '};
    answer = inputdlg(prompt,dlgtitle,dims,definput);
    setGlobalumLength(str2num(answer{1}));
    str = sprintf('%d pixels per %d um', lineLengthPixels,
getGlobalumLength);
    set(handles.text17, 'String', str);
else
    setGlobalCalibrateStatus(0);
    set(handles.text17, 'String', 'N/A'); %text box in results for
'distance calibrated'
end

% hObject    handle to pushbutton7 (see GCBO)
% eventdata  reserved - to be defined in a future version of MATLAB
% handles    structure with handles and user data (see GUIDATA)

% --- Executes on button press in checkbox1.
% This check box is responsible for the addition of an appropriately scaled
% grid overlay on the user's uploaded image.
function checkbox1_Callback(hObject, eventdata, handles)
    % hObject    handle to checkbox1 (see GCBO)
    % eventdata  reserved - to be defined in a future version of MATLAB
    % handles    structure with handles and user data (see GUIDATA)

    % Hint: get(hObject,'Value') returns toggle state of checkbox1

```

```

uploadedImage= getGlobalImage;
value = get(hObject, 'Value');
status = getGlobalCalibrateStatus();
%ensures that the distance has been calibrated by the user
if(status == 1)
    if(value == 0)
        axis off;
        cla('reset');
        imshow(uploadedImage);
        set(handles.text8, 'String', ' ');
        set(handles.text11, 'String', ' ');
    else
        axis on;
        [rows, columns, ~] = size(uploadedImage);
        %Scaling for the pixel and um length determined from
        %calibration is the
        pixel_length = getGlobalPixelLength;
        um_length = getGlobalumLength;

        %Sets the scale and number of x and y ticks for the axis
        set(gca, 'xtick', 0: pixel_length:columns); %creates a verticle
line every pixel_length
        set(gca, 'ytick', 0: pixel_length:rows); %creates a horixontal line
every pixel_length
        ylabel = [0:(rows/pixel_length)];
        xlabel = [0:(columns/pixel_length)];
        yticklabels({ylabel*um_length});
        xticklabels({xlabel*um_length});
        set(handles.text8, 'String', 'x-plane invasion distance (um)');
        set(handles.text11, 'String', 'y-plane invasion distance (um)');

        %draws the grid lines
        hold on;
        for row = 1 : pixel_length : rows
            line([1, columns], [row, row], 'Color', 'b', 'LineWidth', 1);
        end
        for col = 1 : pixel_length : columns
            line([col, col], [1, rows], 'Color', 'b', 'LineWidth', 1);
        end

    end
else
    f = msgbox('First, you must calibrate distance with an image
including a scale bar');
    set(hObject, 'Value', 0);
end

% --- Executes on button press in pushbutton8.
%Allows the user to measure specific distances on their images after
%calibrating their reference image.
function pushbutton8_Callback(hObject, eventdata, handles)
% hObject    handle to pushbutton8 (see GCBO)
% eventdata reserved - to be defined in a future version of MATLAB
% handles    structure with handles and user data (see GUIDATA)
status = getGlobalCalibrateStatus();

%If the user has already calibrated distance, measure and convert the

```

```

%specific distance they measure into micrometers. Otherwise, display a
%popup asking them to calibrate.
if(status == 1)
    %determines start and end points on user's drawn line
    [~,~,~, xi,yi] = improfile(1000);

    %uses the distance equation to determine the length of the user's line
    %in pixels
    distanceMeasured = round(sqrt((xi(1)-xi(2))^2 + (yi(1)-yi(2))^2));
    pixel_length_ref = getGlobalPixelLength; %gets the calibrated pixel
length
    um_length_ref = getGlobalumLength; %gets the calibrated um length

    %performs a unit conversion from pixels to um based on the calibrated
    %values
    distanceUm = (um_length_ref/pixel_length_ref)*distanceMeasured;

    %displays results next to 'specific distance measured'
    set(handles.text15, 'String', num2str(distanceUm));
else
    f = msgbox('First, you must calibrate distance with an image including a
scale bar');
end

% --- Executes on button press in pushbutton10.
%This is the 'Density Profile of Combined Images' function. It takes in a
%set of jpg images from the user, binarizes them, and compresses them all
%so the user can see the density of cells throughout the z-plane/thickness
%of their scaffold.
function pushbutton10_Callback(hObject, eventdata, handles)
% hObject    handle to pushbutton10 (see GCBO)
% eventdata  reserved - to be defined in a future version of MATLAB
% handles    structure with handles and user data (see GUIDATA)
% Get a list of all txt files in the current folder, or subfolders of it.

%reset the appropriate text fields
set(handles.checkbox1, 'Value',0); %grid on checkbox
set(handles.text8, 'String', ' '); %x-axis textbox
set(handles.text11, 'String', ' '); %y-axis textbox
set(handles.text15, 'String', 'N/A'); %specific distance measurement number
textbox
set(handles.text4, 'String', 'N/A'); %cell count textbox
cla('reset');
%the user chooses the folder to import (can only be jpgs)
userLocation = uigetdir(path);

%imports the file paths to the images we want to grab and gets the number
%of images in that folder
ds = imageDatastore(userLocation);
fullFileNames = ds.Files;
numFiles = length(fullFileNames);

%creates a cell array of the size numFiles to hold the processed images
images = cell(1,numFiles,1);

for k = 1 : numFiles

```

```

%extracts the files and converts and thresholds each one, storing them
%into a cell array for further processing
uploadedImage= imread(fullFileNames{k});
if(k > 1)
    %resizes all images to the size of the first image in dataset
    uploadedImage= imresize(uploadedImage, size(images{1}));
end
%processes the image and creates a binary mask of the cell objects in
%the user's uploaded image
grayscaleImage = rgb2gray(uploadedImage);
enhancedContrastImage = adapthisteq(grayscaleImage);
clearedBorderImage = imclearborder(enhancedContrastImage );
filteredImage = wiener2(clearedBorderImage, [5,5]);
binaryBwImage = im2bw(filteredImage,graythresh(filteredImage));
filledImage = imfill(binaryBwImage,'holes');
openedImage = imopen(filledImage, strel('disk',2));
areaOpenedImage = bwareaopen(openedImage, 60);
images{k} = uint8(areaOpenedImage);
end

for k = 1 : numFiles
    if(k == 1)
        totalImageSet = uint8(images{k});
    else
        totalImageSet = imadd(totalImageSet,images{k});
    end
end

%sets the global image to the overlays
setGlobalImage(mat2gray(totalImageSet));
%displays on the axis the combined image overlays
imshow(mat2gray(totalImageSet))

% --- Executes on button press in pushbutton11.
function pushbutton11_Callback(hObject, eventdata, handles)
% hObject    handle to pushbutton11 (see GCBO)
% eventdata  reserved - to be defined in a future version of MATLAB
% handles    structure with handles and user data (see GUIDATA)

%reset the appropriate text fields
set(handles.checkbox1, 'Value',0); %grid on checkbox
set(handles.text8,'String',' ');%x-axis textbox
set(handles.text11,'String',' '); %y-axis textbox
set(handles.text15, 'String','N/A'); %specific distance measurement number
textbox
set(handles.text4, 'String','N/A'); %cell count textbox
cla('reset');
userLocation = uigetdir(path);

%imports the file paths to the images we want to grab and gets the number
%of images in that folder
ds = imageDatastore(userLocation) ;
fullFileNames = ds.Files;
numFiles = length(fullFileNames);

%creates a cell array of the size numFiles to hold the processed images

```

```

images = cell(1,numFiles,1);
overlays = cell(1,numFiles,1);
cellCount = [1:numFiles];
colorChange = [{'yellow'}, {'blue'}, {'red'}, {'cyan'},
{'magenta'},{'green'}];
colorindex = 1;
for k = 1 : numFiles
    %extracts the files and converts and thresholds each one, storing them
    %into a cell array for further processing
    uploadedImage= imread(fullFileNames{k});
    if(k > 1)
        uploadedImage= imresize(uploadedImage, size(images{1}));
    end
    I = rgb2gray(uploadedImage);
    I = adapthisteq(I);
    I = imclearborder(I);
    I = wiener2(I, [5,5]);
    bw = imbinarize(I,graythresh(I));
    bw2 = imfill(bw,'holes');
    bw3 = imopen(bw2, strel('disk',2));
    bw4 = bwareaopen(bw3, 60);
    [~,Num] = bwlabel(bw4);
    bw_perim = bwperim(bw4);
    se = strel('line',11,90);
    bw_bold = imdilate(bw_perim,se);
    overlayFinal = imoverlay(bw4, bw_bold, colorChange{colorindex});
    images{k} = uint8(bw4);
    overlays{k} = overlayFinal;
    cellCount(k) = Num;
    if(colorindex < 6)
        colorindex = colorindex+1;
    else
        colorindex = 1;
    end
end
end

for k = 1 : numFiles
    if(k == 1)
        totalOverlay = uint8(overlays{k});
    else
        totalOverlay = imadd(totalOverlay, overlays{k});
    end
end
end
%get the size of the 2D image array (matrix size)
imshow(totalOverlay)
setGlobalImage(totalOverlay);
totalCount = num2str(sum(cellCount));
set(handles.text4,'String',totalCount) %displays the total number of cells
counted

```

Appendix G: CellProfiler Pipeline

<input checked="" type="checkbox"/>	Images
<input checked="" type="checkbox"/>	Metadata
<input checked="" type="checkbox"/>	NamesAndTypes
<input checked="" type="checkbox"/>	Groups

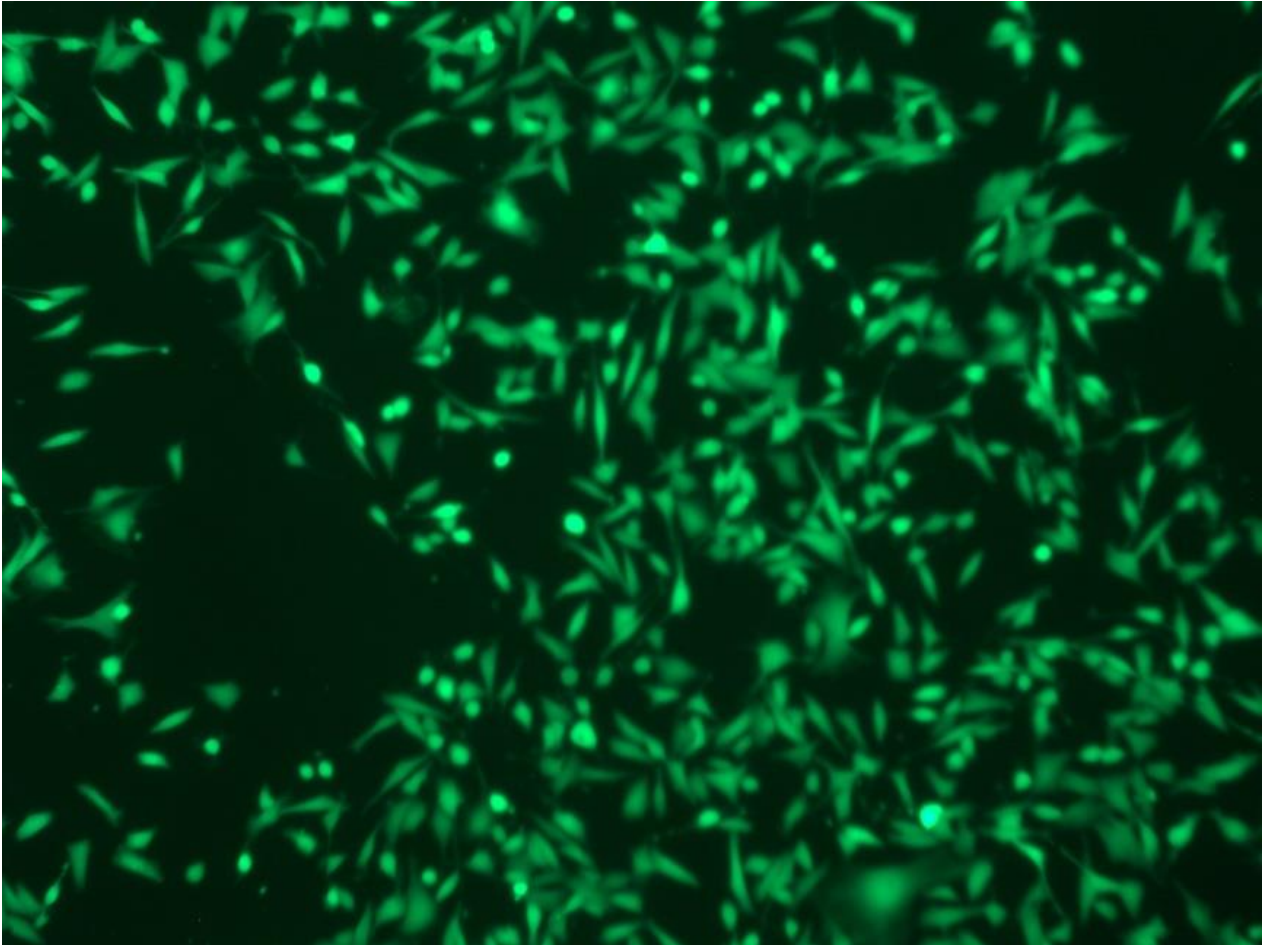
<input type="checkbox"/>	<input checked="" type="checkbox"/> IdentifyPrimaryObjects
<input type="checkbox"/>	<input checked="" type="checkbox"/> CalculateMath
<input type="checkbox"/>	<input checked="" type="checkbox"/> ExportToSpreadsheet

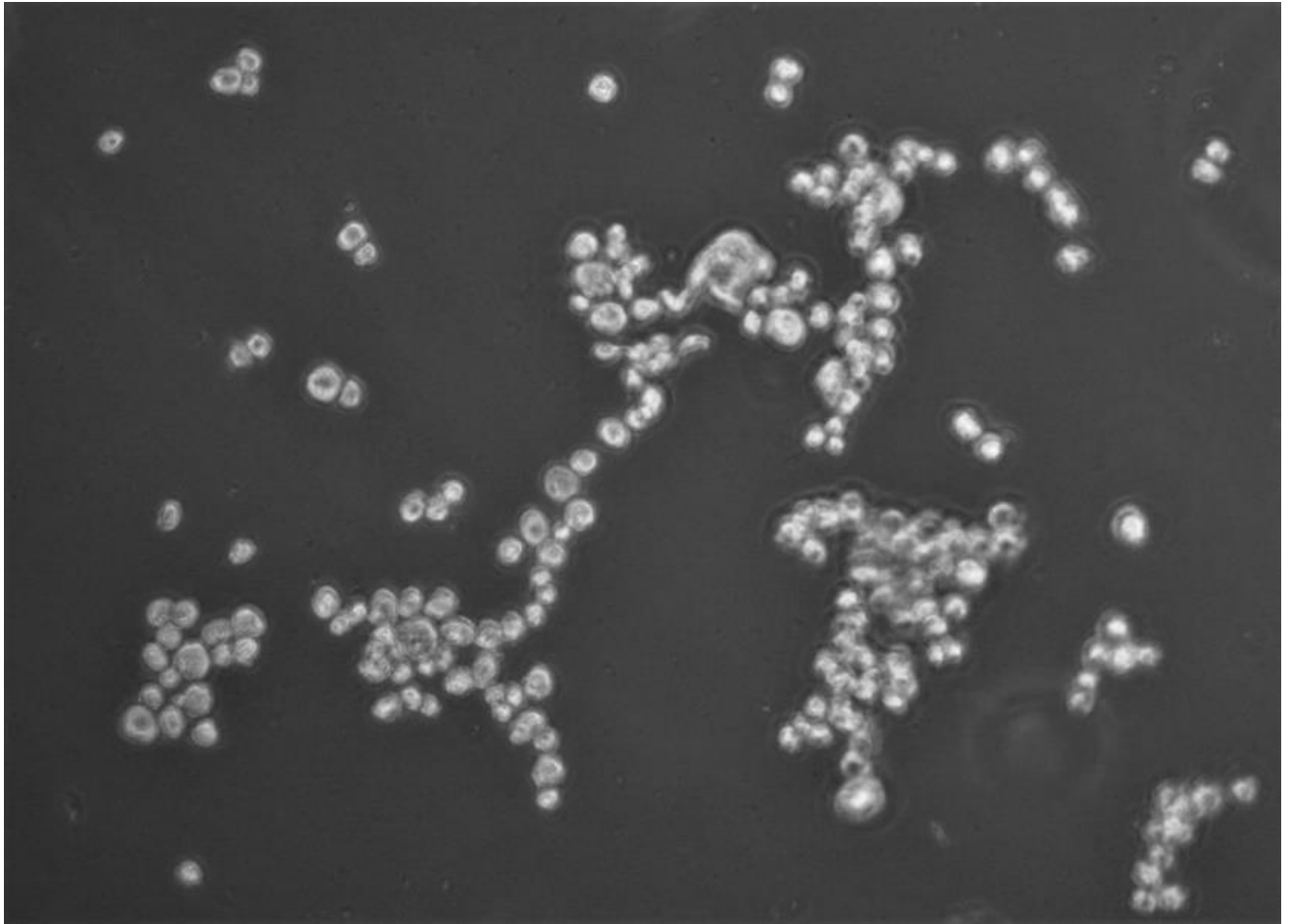
Extra work:

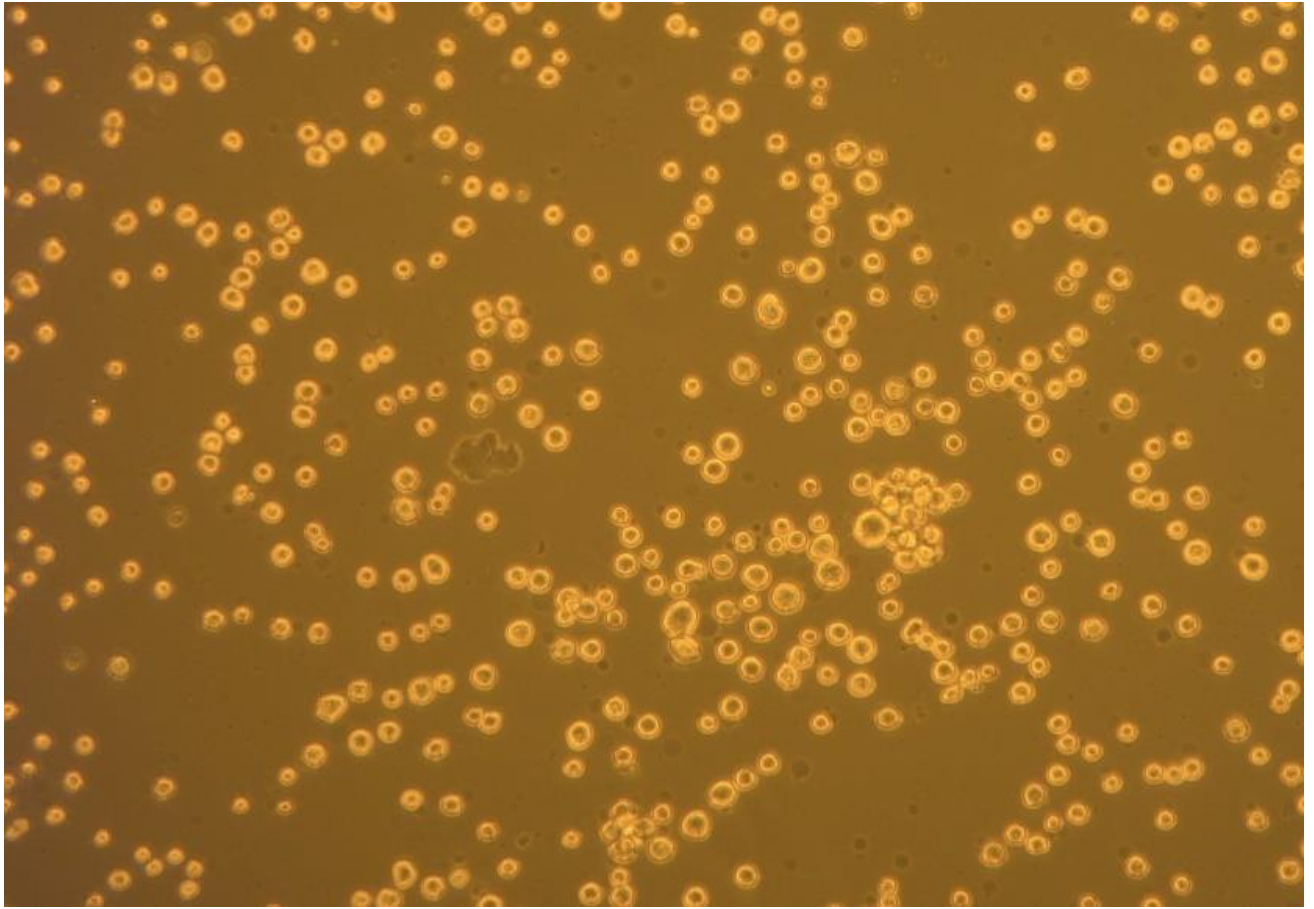
<input checked="" type="checkbox"/>	Images
<input checked="" type="checkbox"/>	Metadata
<input checked="" type="checkbox"/>	NamesAndTypes
<input checked="" type="checkbox"/>	Groups

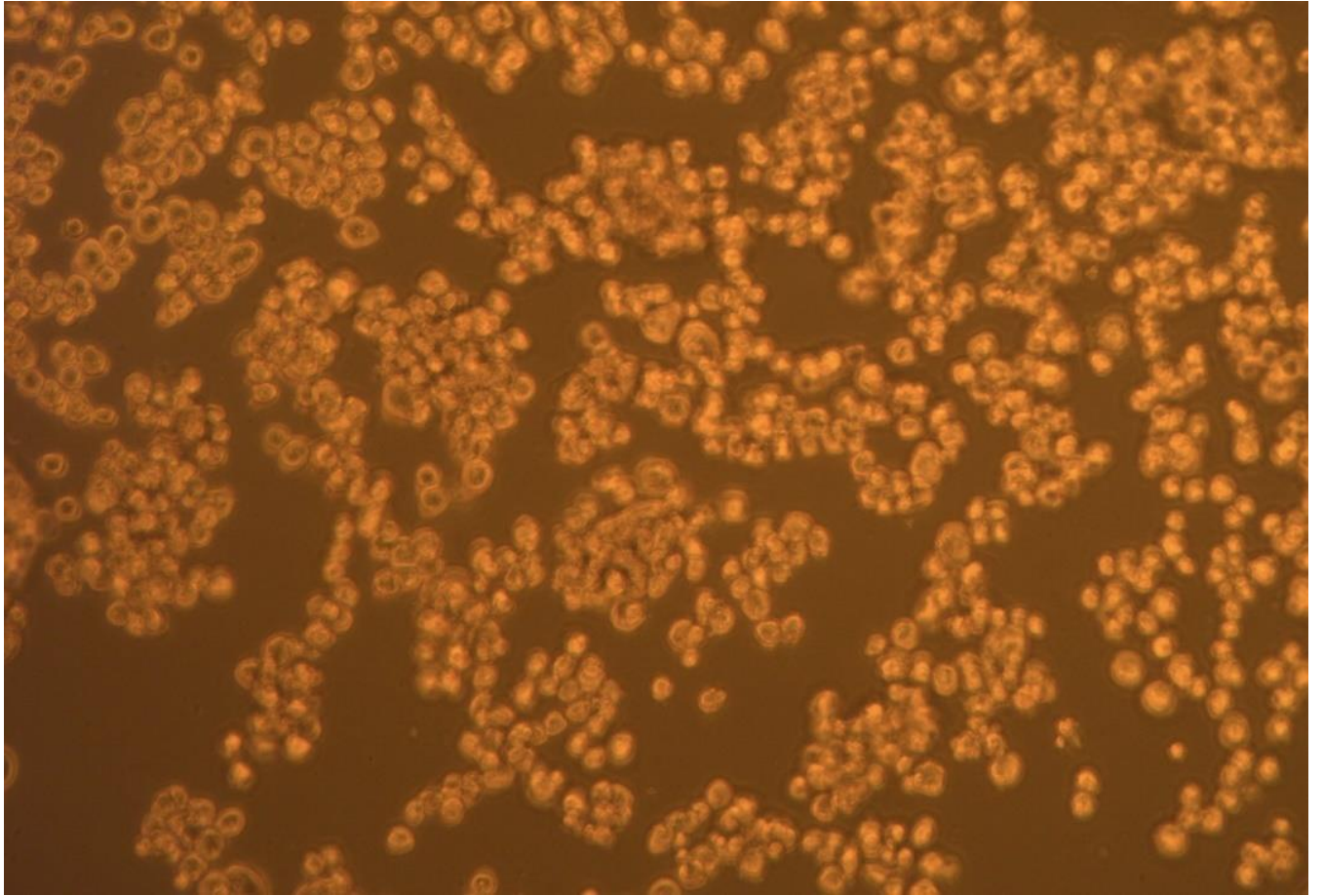
<input type="checkbox"/>	<input checked="" type="checkbox"/> EnhanceEdges
<input type="checkbox"/>	<input checked="" type="checkbox"/> IdentifyPrimaryObjects
<input type="checkbox"/>	<input checked="" type="checkbox"/> OverlayOutlines
<input type="checkbox"/>	<input checked="" type="checkbox"/> DefineGrid
<input type="checkbox"/>	<input checked="" type="checkbox"/> MeasureImageAreaOccupied
<input type="checkbox"/>	<input checked="" type="checkbox"/> IdentifyObjectsInGrid
<input type="checkbox"/>	<input checked="" type="checkbox"/> MeasureImageAreaOccupied
<input type="checkbox"/>	<input checked="" type="checkbox"/> DefineGrid
<input type="checkbox"/>	<input checked="" type="checkbox"/> IdentifyObjectsInGrid
<input type="checkbox"/>	<input checked="" type="checkbox"/> MeasureImageAreaOccupied
<input type="checkbox"/>	<input checked="" type="checkbox"/> ExportToSpreadsheet

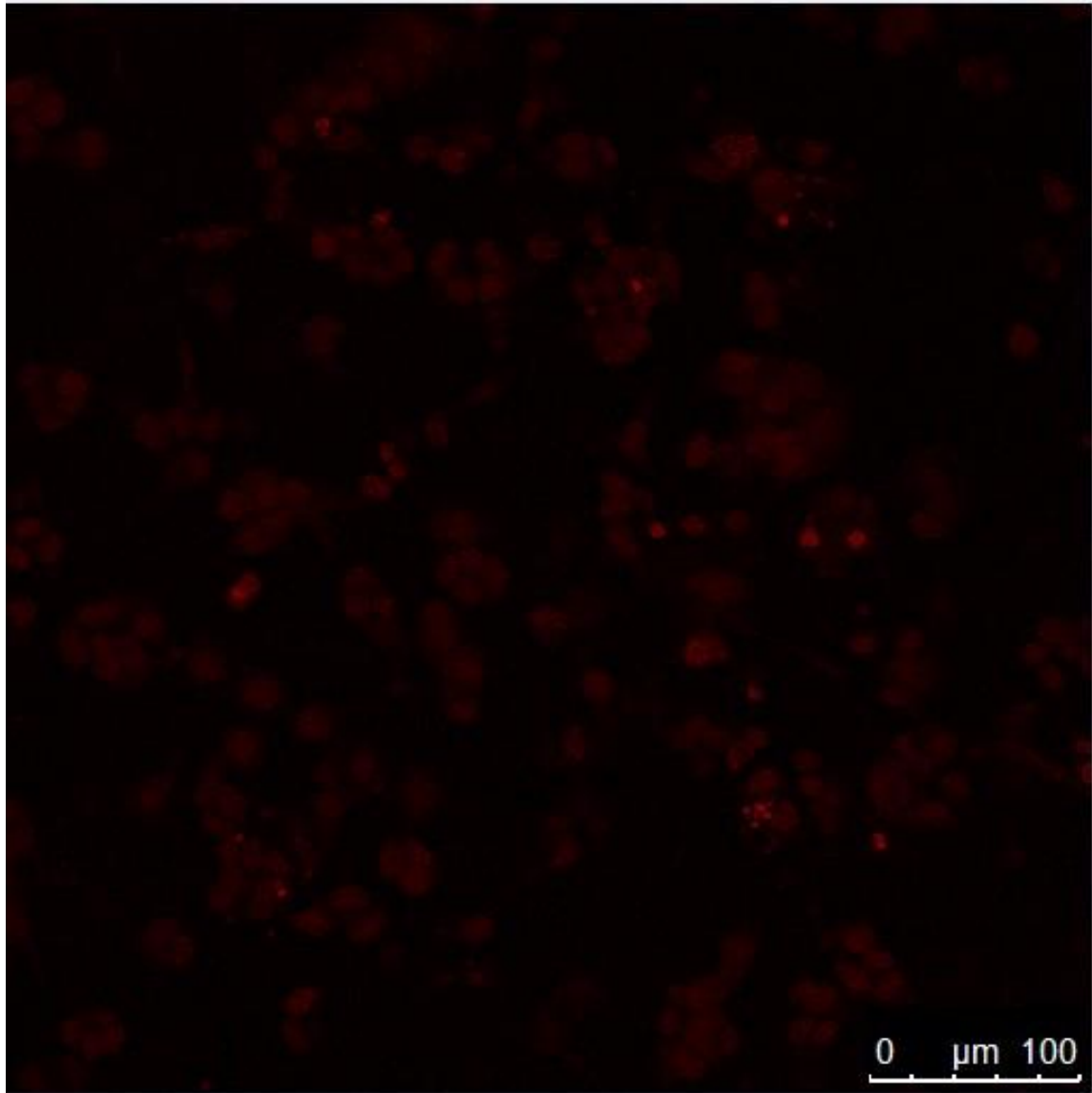
Appendix H: Test Images for Cell Image Analysis











Appendix I: Rheometer Setup/Procedure

Rheometer Quick Guide
Whittington, Updated: 9/9/19

Rheometer Start up Instructions

1. Sign-in on the record sheet
 - User Type: Undergraduate (UG) or Graduate
 - Research Type: Unfunded
 - Project Name: "ECM properties"
2. Check the air gauge to make sure that the pressure is 80-100 psi.
3. Sign into the computer with your own log-in credentials.
4. Turn on the circulator – make sure the wheel turns continuously before moving to the next step.
5. Make sure the lower platform is securely attached to the rheometer.
 - NOTE: The platform is interchangeable between the metal and glass bases.
6. Turn on the rheometer using the switch on the left hand side of the machine.
7. Open the software (Anton Paar RheoCompass1.22).
 - NOTE: The database software has the same icon. Pay attention to the name associated with the icon.
 - Select No new backup (if window pops up)
8. Remove (unscrew) the black cap covering the geometry/tool attachment point (upper portion of the machine).
9. Initialize the machine.
 - In the software window, look along the right hand side for the Control Panel ribbon (right hand side; gray vertical ribbon; click the double arrowheads to expand).
 - Click on the "Initialize" button.
 - NOTE: A window may pop-up regarding the "Measuring Set". If it does, find and click on the "Measuring Set" tab at the top of the window (toward the left of the window), then select the default option.
10. Attach the geometry/tool to the machine and wait for the machine to recognize the geometry/tool.
 - NOTE: Do not overtighten the geometry/tool.
 - Current geometry: 25 mm, cone plate (CP25-1TG)
11. Set the zero gap by clicking on the "Zero Gap" button in the Control Panel window.
12. Raise the geometer after the zero gap by clicking on the  (Control Panel)
 - NOTE: Located to the right of the rheometer icon on the control panel
13. Open project using "RheoFinder" and make any necessary project adjustments.
 - To access project/test steps for editing, first select the "Test" tab.
14. Begin the test
 - Click "Start" button  and enter sample name (Include your initials and the date, along relevant with sample information).
15. Proceed through the program prompts to run the test.
16. **Between tests:**
 - Clean the platform 70% ethanol
 - REMOVE the geometry/tool to clean with 70% ethanol

Rheometer Quick Guide
Whittington, Updated: 9/9/19

Rheometer Shutdown Instructions

1. Remove geometry/tool and clean with 70% ethanol prior to placing in storage container.
2. Clean platform with 70% ethanol.
3. Close software (Do not save Project unless it is your own. We want to keep the default projects.)
 - Tests are saved/archived automatically
4. Turn off the rheometer and cover the geometry/tool attachment point with the black cap.
5. Turn off the circulator.
6. Sign-out on the record sheet.

Test definition 1

Start

Measurement of viscoelastic liquids:
 - Measurement of complex viscosity, G' or G'' at different frequencies
 - Short term (high frequencies) or long term (low frequencies) viscoelastic behavior - Time dependent relaxation behavior

Test name:

Operator:

Sample:

Description:

Test

Test definition 1

Shear rheological measurement

1 9 Points

γ %

f Hz

Control Panel - Default MCR 302 SN81810444

Temperature (P-PTD200):	21.41 °C
Gap:	204.990 mm
Sensor Force:	-0.02 N

TruGap™
 TReady™

MS: <None>
 Cell: P-PTD200 SN82721299

MCR 302 SN81810444

Initialize

Reset force



mm

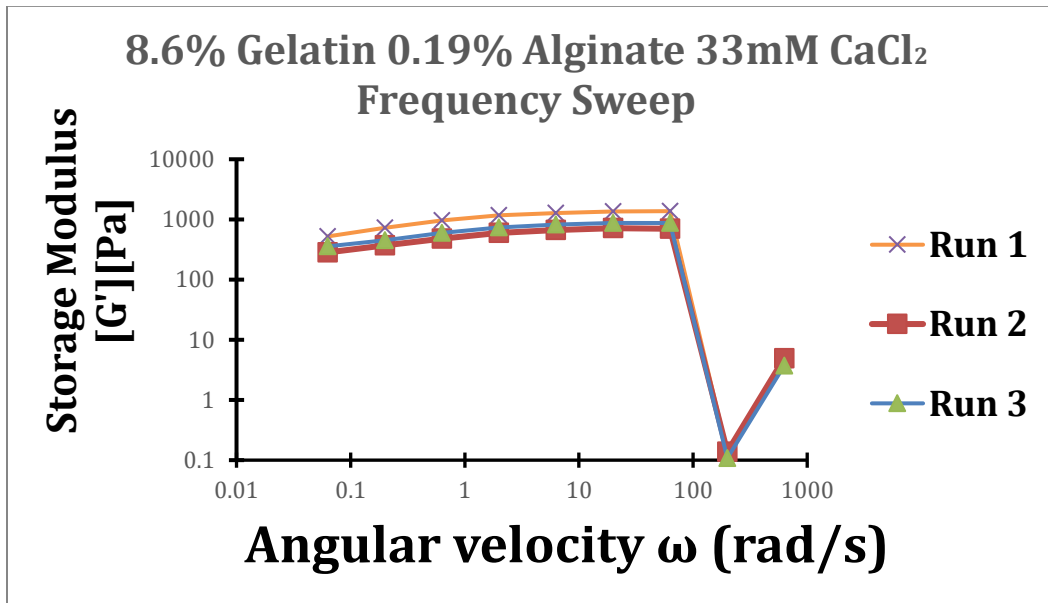
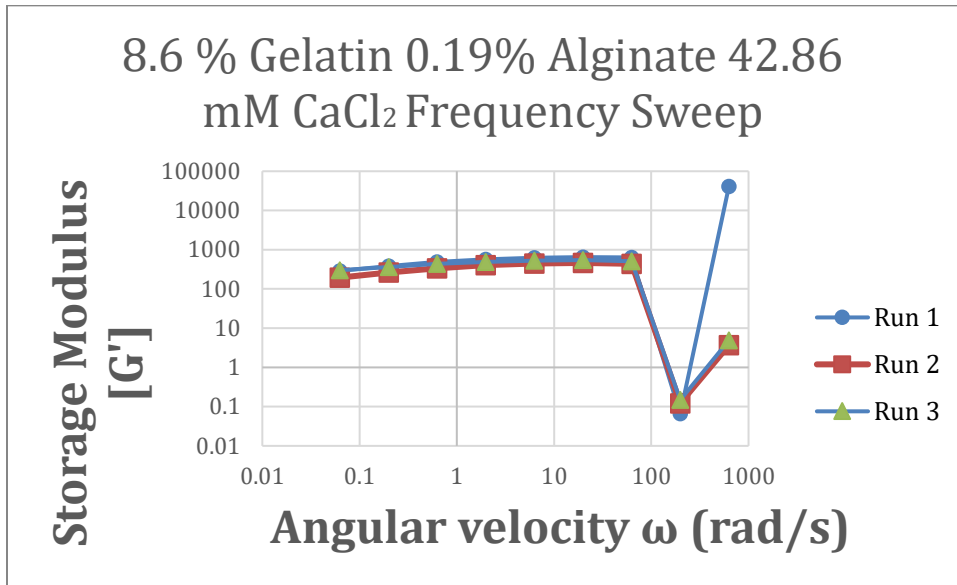
 mm

Moving profile: Viscoelastic

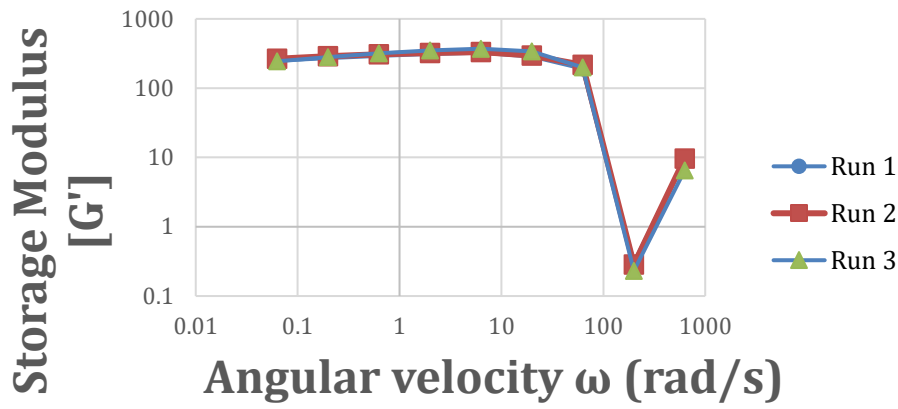
Temperature (P-PTD200): °C

P-PTD200

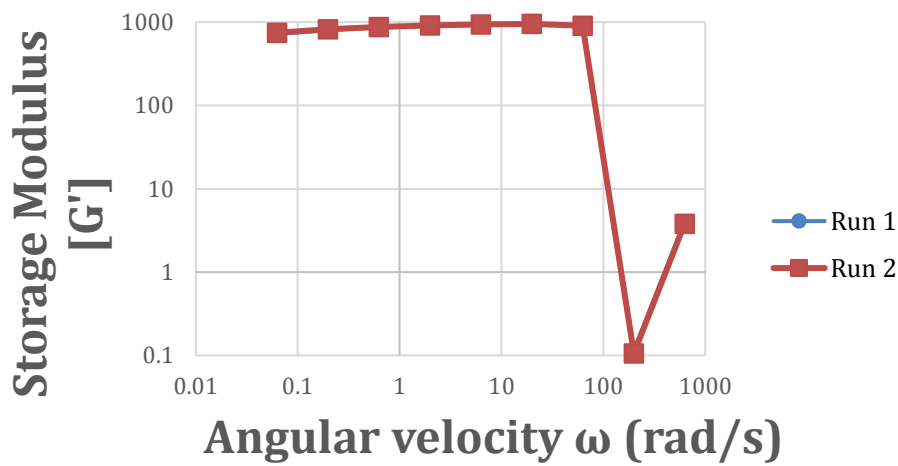
Appendix J: Rheometer Testing Results

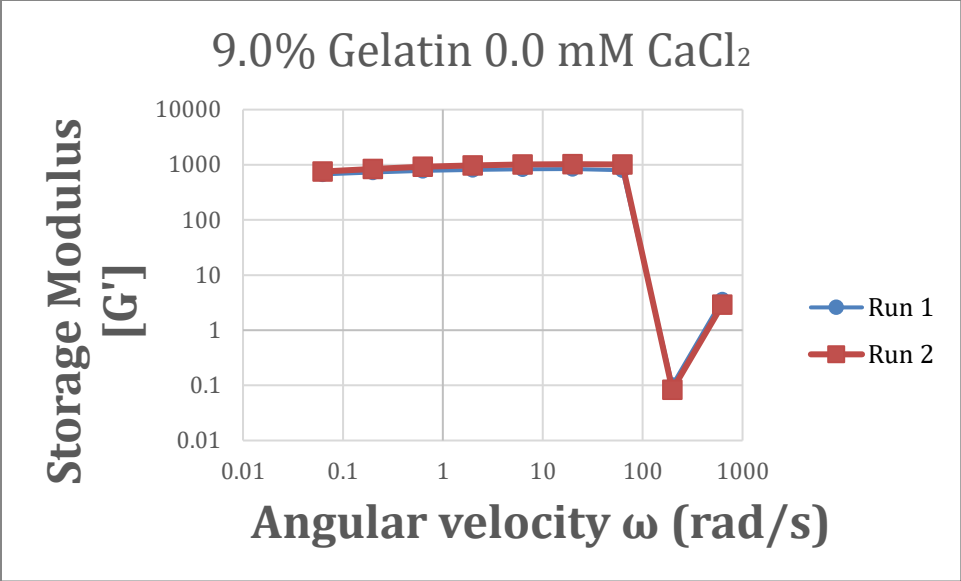


8.6 % Gelatin 0.19% Alginate 31.03 mM CaCl₂ Frequency Sweep



9.0% Gelatin 4.76 mM CaCl₂





Appendix K: Leakage Testing Procedure

Materials:

- CCH unit
- 0.25-inch tubing
- Blue Dyed Water
- Paper towel
- 30 mL syringe

Procedure:

1. Attach 0.25-inch tubing to inlet and outlet channels of the CCH unit
2. Fill tubing and CCH unit chambers with blue dyed water using the 30 mL syringe
3. Place setup on a white paper towel for 24 hours.
4. After 24 hours, report any leaks on paper towel and potential cracks in the tubing or CCH unit

Appendix L: Flow Verification Testing Procedure

Blocked Scaffold Chambers are filled with taped together tissues to fit the scaffold chambers

Materials:

- Syringe Pump
- 3 15 mL syringes
- CCH unit
- 0.25-inch tubing
- 3 15 mL conical tubes
- Blue Dye (Water)

Procedure:

1. Gather materials
2. Connect 0.25-inch tubing to inlet and outlet channels of CCH unit
3. Fill the 3 mL syringes with 10mL of blue dyed water
4. Load syringes into the syringe pump
5. Attach inlet channel tubing to the syringes
6. Place 3 conical tubes at the end of the outlet flow tubing (1 conical tube per outlet flow channel)
7. Program syringe pump to deliver 10 mL of fluid at 5 mL/minute
8. Press 'RUN' on the syringe pump.
9. After syringe pump is finished delivering fluid, power off the syringe pump.
10. Remove conical tubes from set-up and determine the output volume between each chamber/channel.
11. Record data and repeat steps 3-10 for three trials.
12. Same steps are done for both the empty scaffold chambers and blocked scaffold chambers

Appendix M: Procedures for Scaffold Formation

1. The procedure is conducted in a sterile environment.
2. Mix 10 g of powder gelatin (Sigma Aldrich, Type B 250 Bloom) in 100 mL of DPBS (-). Stir constantly at 60°C for one hour
3. After one hour, decrease the temperature to 40°C.
4. Autoclave the gelatin solution for approximately 90 minutes.
5. Put 2 mL of the gelatin solution into the desired container
6. Add the desired concentration of glutaraldehyde to the 2 mL of gelatin. Stir constantly for 30 seconds.
7. Allow solution to gel and sit for 5 minutes in the biosafety cabinet.
8. Transfer the gel in its container into the incubator for 24 hours.
9. After 24 hours., wash the gel in 2 mL of DPBS (+) for 2 minutes.

Procedure for Alginate Solution Formation

1. Mix 4 grams of powder Alginic acid in DPBS (-), stir constantly at 60°C for 3 hours or until all the powder has completely dissolved

Procedure for Calcium Chloride Solution:

1. Mix 100mL of Distilled water with 1.4701 grams of Calcium Chloride Stock solution (0.1 M)

Procedure for Gelatin and Alginate Scaffold formation:

1. Add 100mL of DPBS (-) into a graduated cylinder and put it on the stir plate
2. Mix 5mL of Alginate solution into the DPBS (-)
3. Mix 9 g of powder gelatin (Sigma Aldrich, Type B 250 Bloom) into the 100 mL of DPBS (-) solution. Stir for one hour on heat
4. After one hour, decrease the temperature to 40°C and continue stirring until completely mixed

Appendix N: Scaffold Diffusion Testing Procedure

Testing diffusion of liquid through the scaffold.

Materials

- Glucometer
- Glucose test strips
- Glass Capillary
- Rubber Membrane
- Clamp
- Stir bar
- Stir plate
- 50mL plastic containers
- Syringe and disposable needles
- Volumetric pipette and pipette tips
- Glucose solution (9g/20mL)
- DPBS (-)
- Water

Procedure:

1. Hydrogel formed according to protocol.
2. Segment of scaffold inserted into the glass capillary
3. A mixture of glucose solution is prepared at a concentration of 9g/20mL
4. Glucose solution is tested using the glucometer before passing through the hydrogel
5. Glass capillary fitted through rubber membrane and inserted into each of the plastic containers
6. Containers clamped together and stir bars placed in each one
7. 50mL water added to each plastic container
8. 500uL glucose solution added to donor chamber and 500uL water added to receptor chamber
9. Plastic container caps tightened
10. Stir plate turned on
11. Sample taken from each chamber
12. Equal amount of DPBS added to each sample
13. Reading taken using glucose test strip and glucometer
14. Output multiplied by 2
15. Glucose readings will be taken sporadically for 24 hours as the experiment runs

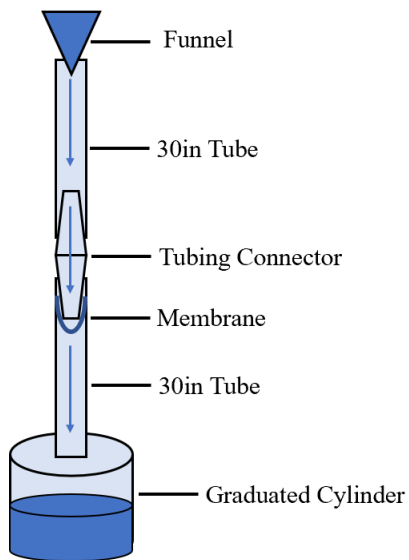
Appendix O: Membrane Fluid Flow Procedure

Materials:

- Funnel
- 2 pieces of 30cm tubing
- Tubing connector
- Graduated cylinder
- Water
- Cell culture medium
- Polycarbonate membrane
- Stopwatch

Procedure:

1. Assemble the apparatus as shown. The membrane should be clamped between the tubing connector and the inner wall of the bottom tube.



2. Once apparatus is assembled, measure out 50mL of water.
3. Begin a stopwatch as the water is poured into the funnel.
4. Continue timing until all of the water has emptied into the graduated cylinder from the bottom tube.
5. Record and repeat two more times, making no changes.
6. Exchange the used membrane for a new one and repeat the experiment three more times.
7. Repeat step 6.
8. Remove the membrane and repeat steps 2-5 with no membrane in the apparatus. This is the control group.
9. Repeat 2-8, but this time using cell culture medium instead of water.
10. Record all results.

Appendix P: Cellular Adhesion Testing

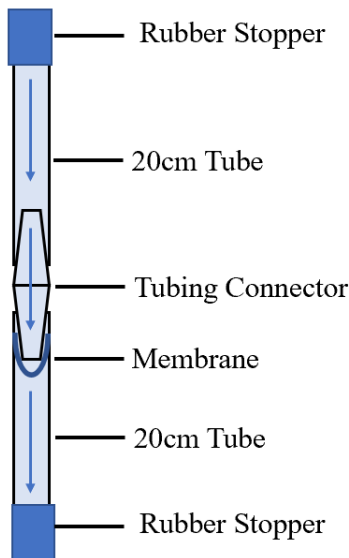
Cellular Adhesion Procedure

Materials:

- 3T3 cells
- 2 20cm tubes
- Tubing connector
- Polycarbonate membrane
- Rubber Stoppers
- Syringe and needle
- Petri dishes
- Microscope

Procedure:

1. Start by assembling the apparatus as shown. The membrane should be clamped between the tubing connector and the inner wall of the bottom tube.



2. Fill both tubes with cell culture medium.
3. Measure out 500,000 cells.
4. Inject cells into the top tube. Place top rubber stopper very lightly to avoid forming a vacuum.
5. Allow 48 hours for cell movement to occur.
6. After 48 hours, empty the contents of the bottom tube into a petri dish.
7. Remove the membrane and put on a petri dish.
8. Analyze and image both the contents of the bottom tube and the membrane with a microscope.
9. Record the presence of cells and their location and density.

Appendix Q: Cell Seeding Procedure

Cell seeding

1. Lay scaffold in 24-well plate, leaving room for controls, 1ml thickness
2. Once scaffold has gelled, lay 100,000 cells in each well, some wells will not have scaffold so that cells can adhere to plate to test controls
3. Incubate for 2 days in order to give time for cells to invade
4. Stain and image, using proper staining procedure
5. **Note:** This procedure can be used in a drug screening further into the project

EQUIPMENT SOLUTIONS

2 mL microcentrifuge tubes or 5 and 15 ml centrifuge tubes

Sterile matrix solution and reagents

Micropipette with tips (sterile)

Sterile Incubator

Parafilm

Well plate

Gilson Microman M1000 positive displacement pipet with tips (CP1000ST tip pack)

Note: Materials may be viscous and there is some loss when pipetting. Neutralize extra material as needed and also allow extra wells when calculating how much to add to the cells.

PROCEDURE

1. All work is done in a biological safety cabinet.
2. Harvest cells (resuspend in volume for counting). Do a cell count and pipette the desired number of cells into the appropriate size tube. Your cell number depends on cell type.
3. Once the desired cell number is determined do one of the following:
 1. If the final desired volume is greater than the volume from Step 3 used for counting, pipet the volume containing the desired cell number into a new tube and add medium to bring up to total volume to achieve the desired cell concentration (and cell number).
 2. If final desired volume is less than the volume from Step 3 used for counting, pipet the volume containing the desired cell number into a new tube, centrifuge 1000 rpm for 5 minutes at room temperature, very carefully remove the media from the cell pellet, rack the pellet a few times (to loosen pellet) and resuspend pellet in appropriate final volume of cell culture medium to achieve the desired cell concentration (and cell number).
4. While the cells are centrifuging, prepare matrix solutions according to datasheets. Be aware, especially with the higher stiffnesses that too much vigorous shaking will result in air bubbles. Keep the tube deep in the ice so the entire amount of material is below the ice surface.
5. Using a wide orifice pipette tip and pipetman (or positive displacement pipette), pipette appropriate volume of matrix **WITHOUT CELLS** into each well of the designated well plate.

6. Place the lid on the well plate. Stretch parafilm around the edge of the plate to keep out air.
7. Place the plate in a 37°C incubator for 30 minutes.
8. Remove the plate from the incubator. Using a pipette, slowly add appropriate volume of cell culture media WITH CELLS to each well (to achieve desired cell number per well). Dispense along the side of the well, not on the construct.
9. Replace lid on plate and place in CO₂ incubator.

References

- [1] T. N. Seyfried and L. C. Huysentruyt, “On the Origin of Cancer Metastasis,” 2013.
- [2] “What is the Tumor Microenvironment?” <https://www.news-medical.net/life-sciences/What-is-the-Tumor-Microenvironment.aspx> (accessed Dec. 07, 2020).
- [3] “The Genetics of Cancer - National Cancer Institute.” <https://www.cancer.gov/about-cancer/causes-prevention/genetics> (accessed May 01, 2021).
- [4] G. M. Cooper, “The Development and Causes of Cancer,” 2000, Accessed: Oct. 12, 2020. [Online]. Available: <https://www.ncbi.nlm.nih.gov/books/NBK9963/>.
- [5] “Cancer Development | CancerQuest.” <https://www.cancerquest.org/cancer-biology/cancer-development#toc-stages-of--KheLAfS5> (accessed Oct. 12, 2020).
- [6] N. I. of H. (US) and B. S. C. Study, “Understanding Cancer,” 2007, Accessed: Oct. 12, 2020. [Online]. Available: <https://www.ncbi.nlm.nih.gov/books/NBK20362/>.
- [7] T. L. Whiteside, “The tumor microenvironment and its role in promoting tumor growth,” doi: 10.1038/onc.2008.271.
- [8] C. Walker, E. Mojares, and A. Del Río Hernández, “Molecular Sciences Role of Extracellular Matrix in Development and Cancer Progression,” doi: 10.3390/ijms19103028.
- [9] “Biopsy: Types of biopsy procedures used to diagnose cancer - Mayo Clinic.” <https://www.mayoclinic.org/diseases-conditions/cancer/in-depth/biopsy/art-20043922> (accessed May 05, 2021).
- [10] “Understanding Your Diagnosis,” *American Cancer Society*. <https://www.cancer.org/treatment/understanding-your-diagnosis/staging.html>.
- [11] “Cancer Basics | Cancer.Net.” <https://www.cancer.net/navigating-cancer-care/cancer-basics/understanding-statistics-used-guide-prognosis-and-evaluate-treatment>. (accessed May 05, 2021).
- [12] “Types of Pancreatic Cancer – Pancreatic Cancer Action Network.” <https://www.pancan.org/facing-pancreatic-cancer/about-pancreatic-cancer/types-of-pancreatic-cancer/> (accessed Oct. 15, 2020).
- [13] “Pancreatic Cancer Prognosis | Johns Hopkins Medicine.” <https://www.hopkinsmedicine.org/health/conditions-and-diseases/pancreatic-cancer/pancreatic-cancer-prognosis> (accessed Oct. 15, 2020).
- [14] B. Uzunparmak and I. H. Sahin, “Pancreatic cancer microenvironment: a current dilemma,” *Clin. Transl. Med.*, vol. 8, no. 1, p. 2, Dec. 2019, doi: 10.1186/s40169-019-0221-1.
- [15] M. Waghray, M. Yalamanchili, M. P. Di Magliano, and D. M. Simeone, “Deciphering the role of stroma in pancreatic cancer,” *Current Opinion in Gastroenterology*, vol. 29, no. 5. NIH Public Access, pp. 537–543, Sep. 2013, doi: 10.1097/MOG.0b013e328363affe.
- [16] V. Lorian and G. Satta, “Differences between in vitro and in vivo studies,” *Antimicrobial Agents and Chemotherapy*, vol. 32, no. 10. American Society for Microbiology (ASM), pp. 1600–1601, 1988, doi: 10.1128/AAC.32.10.1600.
- [17] “In vivo models for cancer stem cell research: a practical guide for frequently used animal models and available biomarkers - PubMed.” <https://pubmed.ncbi.nlm.nih.gov/24781726/> (accessed Dec. 11, 2020).
- [18] A. Akhtar, “The Flaws and Human Harms of Animal Experimentation,” *Cambridge Q.*

- Healthc. Ethics*, vol. 24, no. 4, pp. 407–419, Sep. 2015, doi: 10.1017/S0963180115000079.
- [19] “Pharmaceutical production in developing countries | UNIDO.” <https://www.unido.org/our-focus-advancing-economic-competitiveness-investing-technology-and-innovation-competitiveness-business-environment-and-upgrading/pharmaceutical-production-developing-countries> (accessed Oct. 15, 2020).
- [20] S. Chikhladze *et al.*, “Adjuvant chemotherapy after surgery for pancreatic ductal adenocarcinoma: Retrospective real-life data,” *World J. Surg. Oncol.*, vol. 17, no. 1, Nov. 2019, doi: 10.1186/s12957-019-1732-3.
- [21] M. Kapałczyńska *et al.*, “2D and 3D cell cultures – a comparison of different types of cancer cell cultures,” *Arch. Med. Sci.*, vol. 14, no. 4, pp. 910–919, 2018, doi: 10.5114/aoms.2016.63743.
- [22] K. Duval *et al.*, “Modeling physiological events in 2D vs. 3D cell culture,” *Physiology*, vol. 32, no. 4. American Physiological Society, pp. 266–277, Jun. 14, 2017, doi: 10.1152/physiol.00036.2016.
- [23] R. Edmondson, J. J. Broglie, A. F. Adcock, and L. Yang, “Three-dimensional cell culture systems and their applications in drug discovery and cell-based biosensors,” *Assay and Drug Development Technologies*, vol. 12, no. 4. Mary Ann Liebert Inc., pp. 207–218, May 01, 2014, doi: 10.1089/adt.2014.573.
- [24] P. Mirabelli, L. Coppola, and M. Salvatore, “Cancer cell lines are useful model systems for medical research,” *Cancers*, vol. 11, no. 8. MDPI AG, Aug. 01, 2019, doi: 10.3390/cancers11081098.
- [25] E. L. Deer *et al.*, “Phenotype and genotype of pancreatic cancer cell lines,” *Pancreas*, vol. 39, no. 4. Lippincott Williams and Wilkins, pp. 425–435, 2010, doi: 10.1097/MPA.0b013e3181c15963.
- [26] C. Ferguson, C. Waskowicz, E. Callahan, and L. Steigerwald, “Perfused Tumor-Tissue Model for In Vitro Invasion Analysis,” *Major Qualif. Proj. (All Years)*, May 2020, Accessed: Oct. 13, 2020. [Online]. Available: <https://digitalcommons.wpi.edu/mqp-all/7432>.
- [27] F. J. O’Brien, “Biomaterials & scaffolds for tissue engineering,” *Materials Today*, vol. 14, no. 3. Elsevier B.V., pp. 88–95, Mar. 01, 2011, doi: 10.1016/S1369-7021(11)70058-X.
- [28] Z. Liu and G. Vunjak-Novakovic, “Modeling tumor microenvironments using custom-designed biomaterial scaffolds,” *Current Opinion in Chemical Engineering*, vol. 11. Elsevier Ltd, pp. 94–105, Feb. 01, 2016, doi: 10.1016/j.coche.2016.01.012.
- [29] E. M. Ahmed, “Hydrogel: Preparation, characterization, and applications: A review,” *Journal of Advanced Research*, vol. 6, no. 2. Elsevier B.V., pp. 105–121, Mar. 01, 2015, doi: 10.1016/j.jare.2013.07.006.
- [30] M. H. Kim and W. H. Park, “Chemically cross-linked silk fibroin hydrogel with enhanced elastic properties, Biodegradability, and biocompatibility,” *Int. J. Nanomedicine*, vol. 11, pp. 2967–2978, Jun. 2016, doi: 10.2147/IJN.S106467.
- [31] X. Guan *et al.*, “Development of hydrogels for regenerative engineering,” *Biotechnology Journal*, vol. 12, no. 5. Wiley-VCH Verlag, May 01, 2017, doi: 10.1002/biot.201600394.
- [32] W. Asghar, R. El Assal, H. Shafiee, S. Pitteri, R. Paulmurugan, and U. Demirci, “Engineering cancer microenvironments for in vitro 3-D tumor models,” *Materials Today*, vol. 18, no. 10. Elsevier, pp. 539–553, Dec. 01, 2015, doi: 10.1016/j.mattod.2015.05.002.

- [33] S. M. Ong *et al.*, “Engineering a scaffold-free 3D tumor model for in vitro drug penetration studies,” *Biomaterials*, vol. 31, no. 6, pp. 1180–1190, Feb. 2010, doi: 10.1016/j.biomaterials.2009.10.049.
- [34] “Introduction to 3D Cell Culture.” <https://www.promega.com/resources/guides/cell-biology/3d-cell-culture-guide/> (accessed Dec. 11, 2020).
- [35] M. Millard, I. Yakavets, V. Zorin, A. Kulmukhamedova, S. Marchal, and L. Bezdetsnaya, “Drug delivery to solid tumors: The predictive value of the multicellular tumor spheroid model for nanomedicine screening,” *International Journal of Nanomedicine*, vol. 12, Dove Medical Press Ltd., pp. 7993–8007, Oct. 31, 2017, doi: 10.2147/IJN.S146927.
- [36] C. C. Liang, A. Y. Park, and J. L. Guan, “In vitro scratch assay: A convenient and inexpensive method for analysis of cell migration in vitro,” *Nat. Protoc.*, vol. 2, no. 2, pp. 329–333, Mar. 2007, doi: 10.1038/nprot.2007.30.
- [37] K. I. Hulkower and R. L. Herber, “Cell Migration and Invasion Assays as Tools for Drug Discovery,” *Pharmaceutics*, vol. 3, no. 1, pp. 107–124, Mar. 2011, doi: 10.3390/pharmaceutics3010107.
- [38] “Cell Exclusion Zone Assay - Creative Proteomics.” <https://www.creative-proteomics.com/cell/services/cell-exclusion-zone-assay.htm> (accessed Oct. 15, 2020).
- [39] “Boyden Chamber Technique | Life Science Research | MilliporeSigma.” <https://www.emdmillipore.com/US/en/life-science-research/antibodies-assays/assays-overview/cell-invasion-migration-assays/boyden-chamber-technique/I0qb.qB.KSMAAAFANtY.1ZcQ,nav> (accessed Oct. 15, 2020).
- [40] “Transwell Migration Assay - US,” Accessed: Oct. 15, 2020. [Online]. Available: [//www.thermofisher.com/us/en/home/references/protocols/cell-and-tissue-analysis/cell-profiler-assay-protocols/angiogenesis-protocols/transwell-migration-assay.html](http://www.thermofisher.com/us/en/home/references/protocols/cell-and-tissue-analysis/cell-profiler-assay-protocols/angiogenesis-protocols/transwell-migration-assay.html).
- [41] T. J. Puls, X. Tan, M. Husain, C. F. Whittington, M. L. Fishel, and S. L. Voytik-Harbin, “Development of a Novel 3D Tumor-tissue Invasion Model for High-throughput, High-content Phenotypic Drug Screening OPEN,” *Sci. RePoRTS* /, vol. 8, p. 13039, 2018, doi: 10.1038/s41598-018-31138-6.
- [42] “Fluorescence Microscopy vs. Light Microscopy.” <https://www.news-medical.net/life-sciences/Fluorescence-Microscopy-vs-Light-Microscopy.aspx> (accessed May 01, 2021).
- [43] T. Furuno *et al.*, “In vitro Cell Migration, Invasion, and Adhesion Assays: From Cell Imaging to Data Analysis,” *Front. Cell Dev. Biol.* / www.frontiersin.org, vol. 1, p. 107, 2019, doi: 10.3389/fcell.2019.00107.
- [44] “TPC - Perfusion.” http://www.turkupetcentre.net/petanalysis/model_perfusion.html (accessed Oct. 15, 2020).
- [45] P. L. Ricketts *et al.*, “Non-invasive blood perfusion measurements using a combined temperature and heat flux surface probe,” *Int. J. Heat Mass Transf.*, vol. 51, no. 23–24, pp. 5740–5748, Nov. 2008, doi: 10.1016/j.ijheatmasstransfer.2008.04.051.
- [46] T. W. Miller, J. S. Isenberg, and D. D. Roberts, “Molecular Regulation of Tumor Angiogenesis and Perfusion via Redox Signaling,” doi: 10.1021/cr8005125.
- [47] J. M. Munson and A. C. Shieh, “Interstitial fluid flow in cancer: Implications for disease progression and treatment,” *Cancer Management and Research*, vol. 6, no. 1. Dove Press, pp. 317–318, Aug. 19, 2014, doi: 10.2147/CMAR.S65444.
- [48] W. Yao, Y. Li, and G. Ding, “Interstitial fluid flow: The mechanical environment of cells

- and foundation of meridians,” *Evidence-based Complement. Altern. Med.*, vol. 2012, 2012, doi: 10.1155/2012/853516.
- [49] A. E. Guller, P. N. Grebenyuk, A. B. Shekhter, A. V Zvyagin, and S. M. Deyev, “Bioreactor-Based Tumor Tissue Engineering,” 2016.
- [50] J. M. Munson and A. C. Shieh, “Cancer Management and Research Dovepress Interstitial fluid flow in cancer: implications for disease progression and treatment,” *Cancer Manag. Res.*, pp. 6–317, 2014, doi: 10.2147/CMAR.S65444.
- [51] “Darcy Law - an overview | ScienceDirect Topics.”
<https://www.sciencedirect.com/topics/physics-and-astronomy/darcy-law> (accessed Dec. 07, 2020).
- [52] Z. Zhang and S. Nagrath, “Microfluidics and cancer: Are we there yet?,” *Biomed. Microdevices*, vol. 15, no. 4, pp. 595–609, Aug. 2013, doi: 10.1007/s10544-012-9734-8.
- [53] L. Avraham-Chakim, D. Elad, U. Zaretsky, Y. Kloog, A. Jaffa, and D. Grisaru, “Fluid-Flow Induced Wall Shear Stress and Epithelial Ovarian Cancer Peritoneal Spreading,” *PLoS One*, vol. 8, no. 4, Apr. 2013, doi: 10.1371/journal.pone.0060965.
- [54] W. J. Polacheck, A. E. German, A. Mammoto, D. E. Ingber, and R. D. Kamm, “Mechanotransduction of fluid stresses governs 3D cell migration,” *Proc. Natl. Acad. Sci. U. S. A.*, vol. 111, no. 7, pp. 2447–2452, Feb. 2014, doi: 10.1073/pnas.1316848111.
- [55] B. S. Wong *et al.*, “A microfluidic cell-migration assay for the prediction of progression-free survival and recurrence time of patients with glioblastoma,” *Nat. Biomed. Eng.*, pp. 1–15, Sep. 2020, doi: 10.1038/s41551-020-00621-9.
- [56] L. E. Marshall, K. F. Goliwas, L. M. Miller, A. D. Penman, A. R. Frost, and J. L. Berry, “Flow-perfusion bioreactor system for engineered breast cancer surrogates to be used in preclinical testing HHS Public Access,” *J Tissue Eng Regen Med*, vol. 11, no. 4, pp. 1242–1250, 2017, doi: 10.1002/term.2026
- [57] B. Zohar *et al.*, “Multi-flow channel bioreactor enables real-time monitoring of cellular dynamics in 3D engineered tissue,” *Commun. Biol.*, vol. 2, no. 1, pp. 1–10, Dec. 2019, doi: 10.1038/s42003-019-0400-z.
- [58] “MATLAB - MathWorks - MATLAB & Simulink.”
<https://www.mathworks.com/products/matlab.html> (accessed May 01, 2021).
- [59] “CellProfiler.” <https://cellprofiler.org/> (accessed May 01, 2021).
- [60] McQuin C, Goodman A, Chernyshev V, Kamensky L, Cimini BA, Karhohs KW, Doan M, Ding L, Rafelski SM, Thirstrup D, Wiegraebe W, Singh S, Becker T, Caicedo JC, Carpenter AE (2018). CellProfiler 3.0: Next-generation image processing for biology. *PLoS Biol.* 16(7):e2005970 / doi. PMID: 29969450 (Research article)
- [61] “File Processing — CellProfiler 3.0.0 documentation.” <http://cellprofiler-manual.s3.amazonaws.com/CellProfiler-3.0.0/modules/fileprocessing.html#exporttospreadsheet> (accessed May 01, 2021).
- [62] “Gelatin - an overview | ScienceDirect Topics.”
<https://www.sciencedirect.com/topics/chemistry/gelatin> (accessed May 01, 2021).
- [63] Q. Xing, K. Yates, C. Vogt, Z. Qian, M. C. Frost, and F. Zhao, “Increasing Mechanical Strength of Gelatin Hydrogels by Divalent Metal Ion Removal,” doi: 10.1038/srep04706.
- [64] “Gelatin Type B, powder, BioReagent, cell culture | mammalian | 9000-70-8 | Sigma-Aldrich.”
https://www.sigmaaldrich.com/catalog/product/sigma/g9391?lang=en®ion=US&cm_s

- p=Insite_-caContent_prodMerch_gruCrossEntropy_-_prodMerch10-3 (accessed May 01, 2021).
- [65] K. Y. Lee and D. J. Mooney, “Alginate: properties and biomedical applications,” 2011, doi: 10.1016/j.progpolymsci.2011.06.003.
- [66] “Alginic acid powder | 9005-38-3 | Sigma-Aldrich.”
https://www.sigmaaldrich.com/catalog/product/aldrich/180947?lang=en®ion=US&cm_sp=Insite_-caContent_prodMerch_gruCrossEntropy_-_prodMerch10-2 (accessed May 01, 2021).
- [67] “COLLAGEN TYPE I (NATIVE): Overview, Uses, Side Effects, Precautions, Interactions, Dosing and Reviews.” <https://www.webmd.com/vitamins/ai/ingredientmono-1610/collagen-type-i-native> (accessed May 05, 2021).
- [68] E. E. Antoine, P. P. Vlachos, and M. N. Rylander, “Review of collagen i hydrogels for bioengineered tissue microenvironments: Characterization of mechanics, structure, and transport,” *Tissue Engineering - Part B: Reviews*, vol. 20, no. 6. Mary Ann Liebert Inc., pp. 683–696, Dec. 01, 2014, doi: 10.1089/ten.teb.2014.0086.
- [69] “Collagen Type 3 - an overview | ScienceDirect Topics.”
<https://www.sciencedirect.com/topics/neuroscience/collagen-type-3> (accessed May 05, 2021).
- [70] “Type IV Collagen - an overview | ScienceDirect Topics.”
<https://www.sciencedirect.com/topics/biochemistry-genetics-and-molecular-biology/type-iv-collagen> (accessed May 05, 2021).
- [71] “Collagen I, bovine.”
<https://www.thermofisher.com/order/catalog/product/A1064401#/A1064401> (accessed May 05, 2021).
- [72] “Glutaraldehyde | NIOSH | CDC.”
<https://www.cdc.gov/niosh/topics/glutaraldehyde/default.html> (accessed May 01, 2021).
- [73] Y. You, X. Sun, Q. Cui, B. Wang, and J. Ma, “The retention and drainage behavior of cross-linked gelatin with glutaraldehyde in a papermaking system,” *BioResources*, vol. 11, no. 3, pp. 6162–6173, 2016, doi: 10.15376/biores.11.3.6162-6173.
- [74] “Glutaraldehyde 50wt. % water | 111-30-8 | Sigma-Aldrich.”
<https://www.sigmaaldrich.com/catalog/product/sial/340855?lang=en®ion=US> (accessed May 01, 2021).
- [75] K. Y. Lee and D. J. Mooney, “Alginate: properties and biomedical applications,” 2011, doi: 10.1016/j.progpolymsci.2011.06.003.
- [76] “Lab Grade Anhydrous Calcium Chloride, 500g for sale. Buy from The Science Company.” <https://www.sciencecompany.com/Calcium-Chloride-Lab-Grade-500g-P6381.aspx> (accessed May 01, 2021).
- [77] W. F. Quirós-Solano *et al.*, “Microfabricated tuneable and transferable porous PDMS membranes for Organs-on-Chips,” *Sci. Rep.*, vol. 8, no. 1, pp. 1–11, Dec. 2018, doi: 10.1038/s41598-018-31912-6.
- [78] A. V. Nguyen *et al.*, “Stiffness of pancreatic cancer cells is associated with increased invasive potential,” *Integr. Biol. (United Kingdom)*, vol. 8, no. 12, pp. 1232–1245, Dec. 2016, doi: 10.1039/c6ib00135a.

- [79] H. Hydrogel, X. Chen, and S. Thibeault, “Effect of DMSO Concentration, Cell Density and Needle Gauge on the Viability of Cryopreserved Cells in Three Dimensional,” doi: 10.1109/EMBC.2013.6610976.
- [80] Z. Zhang, W. Zhang, Z. J. Zhai, and Q. Y. Chen, “Evaluation of various turbulence models in predicting airflow and turbulence in enclosed environments by CFD: Part 2— comparison with experimental data from literature,” *HVAC R Res.*, vol. 13, no. 6, pp. 871–886, 2007, doi: 10.1080/10789669.2007.10391460.
- [81] E. Tomás-Bort, M. Kieler, S. Sharma, J. B. Candido, and D. Loessner, “3D approaches to model the tumor microenvironment of pancreatic cancer,” *Theranostics*, vol. 10, no. 11. Ivyspring International Publisher, pp. 5074–5089, 2020, doi: 10.7150/thno.42441.
- [82] G. Vozzi *et al.*, “Cell Seeding Process Experiment and Simulation on Three-Dimensional Polyhedron and Cross-Link Design Scaffolds,” *Front. Bioeng. Biotechnol*, vol. 8, p. 104, 2020, doi: 10.3389/fbioe.2020.00104.